Stochastic expression of the *hecRE* module controls *Pseudomonas aeruginosa* surface colonization and phage sensitivity

Inauguraldissertation
zur
Erlangung der Würde eines Doktors der Philosophie
vorgelegt der
Philosophisch-Naturwissenschaftlichen Fakultät
der Universität Basel

von

Christina Maria Manner

2023

Genehmigt von der Philosophisch-Naturwissenschaftlichen Fakultät

auf Antrag von

Erstbetreuer: Prof. Dr. Urs Jenal

Zweitbetreuer: Prof. Dr. Marek Basler

Externer Experte: Prof. Dr. Jan-Willem Veening

Basel, den 14.12.2021

Prof. Dr. Marcel Mayor

Dekan

The first 3 years of my PhD were funded by the 'Biozentrum PhD Fellowships Program' of the University of Basel, formerly known as 'Fellowships For Excellence' (FFE). The following months were funded by the Swiss National Science Foundation (SNSF).

"This is ten percent luck, twenty percent skill
Fifteen percent concentrated power of will
Five percent pleasure, fifty percent pain
And a hundred percent reason to remember the ~~name~~ main findings"

Adapted Lyrics from "Remember the Name"

by Fort Minor, 2005

SUMMARY

The ubiquitous opportunistic human pathogen *Pseudomonas aeruginosa* can cause life-threatening acute and chronic infections, with chronic pulmonary infections being the leading cause of morbidity and mortality in patients with cystic fibrosis (CF). These long-term *P. aeruginosa* lung infections are characterized by the transition from an acute to a chronic stage with attenuated virulence, emergence of biofilms, and the diversification into different phenotypes. Among the phenotypes frequently isolated from the sputum of CF patients are small colony variants (SCVs), whose appearance correlates with increased antibiotic tolerance and poor clinical outcomes. SCVs are characterized by slow growth, autoaggregation, and increased exopolysaccharide production and their morphotype has been linked to the signaling molecule cyclic di-GMP (c-di-GMP). In this work, the role of the *hecRE* module in *P. aeruginosa* SCV formation and c-di-GMP regulation is described.

In the first part of this work, I address the effects of HecR and HecE on SCV formation, cellular c-di-GMP levels, and c-di-GMP-regulated phenotypes including biofilm formation and motility. Together with my collaborators, I demonstrate that HecE increases c-di-GMP levels by directly inhibiting the phosphodiesterase BifA and by modulating the activity of the diguanylate cyclase WspR. This results in elevated c-di-GMP levels and subsequently enhanced production of the Pel and Psl exopolysaccharides, an increase in surface attachment, cellular aggregation, and reduced motility. Furthermore, the HecE-mediated increase in c-di-GMP levels and Psl production sensitizes *P. aeruginosa* for infection with the newly identified bacteriophage Knedl. Our findings provide a new direct link between the c-di-GMP network and sensitivity to phage predation while also showing for the first time that exopolysaccharides of *P. aeruginosa* can be exploited as phage receptors.

In the second part, I investigate the factors regulating expression of the *hec* module. I developed reporter tools to show that the *hec* genes are expressed stochastically in stationary phase due to the autoregulatory action of HecR. With the assistance of my collaborators, I confirmed the regulatory role of RsmA on *hec* expression, connecting the *hecRE* module to the global Gac/Rsm signaling cascade. We demonstrate that *hecRE* expression is growth phase dependent and responds to environmental changes by mechanisms beyond the regulation by the Gac/Rsm cascade.

Together, this work provides a new connection between the Gac/Rsm and c-di-GMP networks, strengthening the findings that signaling via the cascade promotes high c-di-GMP levels and increased exopolysaccharide production promoting chronic infection. The additional heterogeneity in HecE expression and thereby c-di-GMP levels is probably used as bet-hedging strategy to increase fitness during infections.

ACKNOWLEDGEMENTS

"Nobody said it was easy
No one ever said it would be this hard
Oh, take me back to the start

I was just guessing at numbers and figures
Pulling the puzzles apart
Questions of science, science and progress"

Lyrics from "The Scientist"
by Coldplay, 2002

Music had originally brought me into science, so I think it is only fitting that I quote a song to reflect on my time as PhD student.

While in the beginning I was really just guessing at numbers and figures, I grew a lot as scientist and person throughout this adventure. Clearly, this did not happen in isolation, so I want to thank everyone who was involved in the process.

First and foremost, I would like to thank Prof. Urs Jenal. When I heard a talk of his in Vienna in 2017, I was so amazed by the research of the Jenal lab and by his passion for science and microbiology that I decided to give it a try and apply for a PhD in his group. Luckily, he agreed, and I want to thank him for giving me this opportunity and for his continuous support throughout the last 4+ years. The close mentoring and frequent group seminars together with numerous discussions on science in general and my project in particular helped me to develop as person and scientist.

I would also like to thank Prof. Marek Basler and Prof. Jan-Willem Veening for taking over the roles of second supervisor and external expert in my PhD committee and for their valuable input.

When I first started in the Jenal lab, I was taken under the wings of Dr. Benoît-Joseph Laventie, who was an immense support in starting my journey as microbiologist. Though after a while I decided to "spread my wings" and run my project more independently, I always knew I could come back to him for support if needed and I would like to thank him for all of that.

Before I continue with all other lab members that have supported me in my journey, I want to thank Raphaela Zemp for her immense contribution to this project. Her time as a master student resulted in many interesting findings and I really enjoyed working with her. Special thanks also go to Fabienne Hamburger, who was a great support both in and outside the lab. Without her help, the creation of so many strains and plasmids would not have been possible.

Academia is a dynamic environment; therefore, I have seen several members of the Jenal group come and go. I would like to thank them collectively for the nice working atmosphere, numerous fantastic social events, and the immense support throughout my time in the group.

In particular, I want to thank Dr. Alexander Klotz for sharing his insights and views on microbiology, thesis writing, rock music, and the world, and for always answering my manifold

questions. I also want to thank Dr. Pablo Manfredi for many exciting discussions about this project, microbiology, science, and society while working in the lab or swimming in the Rhine.

Even though, the phage hunters have only affected the course of my project in the last year, their presence close to the Jenal lab led to many stimulating discussions and a nice atmosphere throughout. I want to thank Dr. Alexander Harms for his support in the last years, especially during my own phage hunt, subsequent phage experiments and my many questions. In addition, I want to thank Enea Maffei who generously shared his time to explain me how to work with phages and without whom my phage hunting enterprise would not have been possible. Furthermore, I want to thank Dr. Raphael Dias Teixeira for taking over most of the biochemistry work and Dr. Simon van Vliet for the valuable discussions about science and his help with writing.

While science is the focus of a PhD, social interactions are key to make life beyond the lab interesting. Numerous social events with PostDocs, PhDs, and master students enriched my time in Basel and led to a roommate, long lasting connections and friendships. Thank you Aisylu, Beni, Do (also for your priceless support with Theresa), Fabian, Fabienne, Hector, Julia, Maartje, Marco, Margo, Maya, Nicole, Noemi, Roman, Ruta, Shannon, and Vanja for these great memories.

With the group members being the key interaction partners in such an undertaking, I also relied on the work and effort of many others in the Biozentrum. Having amazing administrative assistants like Claudia Erbel-Sieler, Sarah Thomforde, and Manuela Holzer, who take/took over most administrative work does really make life easier as PhD student. Thank you all for your work, open ears, and support. Similarly, I want to thank, our floor managers, Marina Kuhn Rüfenacht and Patric Hänni, who are doing a fantastic job in making sure that we get our equipment, consumables and that everything is running, as it should.

Over the last years, I started hundreds of bacterial cultures, restreaked strains on an uncountable amount of agar plates and created a lot of waste, all of this while never running an autoclave or preparing my own media on a regular basis. It is a very fortunate situation for a microbiologist to have a media and washing kitchen taking over this tasks and I want to give them my earnest gratitude for their work. I would also like to thank all past and present members of the “infection biology” floors for creating a nice, open, and supportive research community.

Beyond the borders of the microbiology realm, I have to mention a few more people. When I applied to the PhD Fellowship, I had the pleasure to meet Đorđe Relić who luckily also started his PhD at the Biozentrum. Over the last years, he has become a close friend. I want to thank him for all the supportive discussions and I am looking forward to future discussions with him and Enea.

I want to thank the people from the Flow Cytometry, Proteomics, and Biophysics core facilities as well as SciCore for their support in my project and the administration, PhD office, events team, shop, and IT services for their work.

Obviously, support during the last years was not just coming from within the Biozentrum, but also from friends and family. I want to thank my parents, aunts, and grandparents for their financial and personal support throughout my studies and PhD.

Furthermore, I would like to thank my siblings, Elli and Andi, as well as my friends Verena, Katja, Judith, Ramona, Eva, Andi, Lisa, Sarah, Kathi, Ju, Julia, Pau, and all others for their invaluable friendship and support in the last years.

TABLE OF CONTENT

ABBREVIATIONS

AHLs	N-Acyl homoserine lactones
ASM	Artificial sputum medium
a.u.	Arbitrary units
BifA	Biofilm formation
bp	Base pairs
cAMP	cyclic AMP
c-di-GMP	bis-(3′-5′)-cyclic dimeric guanosine monophosphate
CF	Cystic fibrosis
ChIP-Seq	Chromatin Immunoprecipitation Sequencing
Co-IP	Co-immunoprecipitation
Csr	Carbon Storage Regulator
CV	Crystal violet
DGC	Diguanylate cyclase
eDNA	Extracellular DNA
EMSA	Electromobility Shift Assay
EPS	Exopolysaccharide
EV	Empty vector
Gac	Global activation of antibiotic and cyanide synthesis
Hec	Heterogeneous, environment-responsive, c-di-GMP controlling
HK	Histidine kinase
Hpt	Histidine phosphotransfer
IPTG	Isopropyl-β-D-thiogalactopyranosid
LadS	Lost adherence sensor
Las	Elastase controlling QS system
LB	Lysogeny broth
LPS	Lipopolysaccharide
OD	Optical density
Pch	Phosphodiesterase determinant of c-di-GMP heterogeneity
PDE	Phosphodiesterase
PQS	*Pseudomonas* quinolone signal
Psl	Polysaccharide synthesis locus
QS	Quorum sensing
REC	Receiver domain
RetS	Regulator of exopolysaccharide and type III secretion
Rhl	Rhamnolipid controlling QS system
RR	Response regulator
Rsm	Regulator of secondary metabolites
SadC	Surface attachment defective
SCFM	Synthetic cystic fibrosis medium

SCV	Small colony variants
sRNA	small regulatory RNA
T3SS	Type III secretion system
T4P	Type IV pili
T6SS	Type IV secretion system
TCS	Two-component systems
Transposon	Tn
Wsp	Wrinkly spreader
Y2H	Yeast two-hybrid
WT	Wild type

1 INTRODUCTION

1.1 *Pseudomonas aeruginosa*: Easy to encounter – tough to treat

"Uniformity is not nature's way; diversity is nature's way" says environmental activist Vandana Shiva. A statement true for many aspects of life, certainly for the microbial one. With an estimated 10^{11}-10^{12} microbial species and ~10^{30} prokaryotic cells on earth, microbial life, though mostly invisible to the eye, should definitely not be belittled (Locey and Lennon, 2016; Whitman *et al*., 1998). Microbes can be found nearly everywhere on our planet, including hot springs, permafrost, deserts, or acidic lakes (Merino *et al*., 2019). While extremophiles specialized to populate extremely harsh environments (at least from a human perspective), other microbes are generalists, able to thrive in many (not too extreme) environments (Merino *et al*., 2019; Monard *et al*., 2016).

One of the most diverse bacterial genera is the genus *Pseudomonas*, a diverse group of bacteria with more than 100 species. Pseudomonads are γ-Proteobacteria, able to colonize various habitats including distilled, fresh, and ocean water and terrestrial environments such as hot deserts, cold alpine environments, and even heavy metal-contaminated sites. Moreover, many *Pseudomonas* species interact with plants, animals, and humans with effects ranging from beneficial or neutral to harmful, including the plant-pathogen *Pseudomonas syringae* or the opportunistic human pathogen *Pseudomonas aeruginosa* (Selvakumar *et al*., 2015).

P. aeruginosa is a ubiquitous Gram-negative rod shaped bacterium, able to cause a variety of life-threatening acute and chronic diseases. Infections with this bacterium can be community- or hospital-acquired and affect both healthy and immunocompromised patients, including patients with cystic fibrosis (CF). CF is a genetic disorder causing a dysregulation of the chloride and bicarbonate ion transport channel CFTR in epithelial cells, leading to increased mucus viscosity, which ultimately facilitates bacterial colonization. *P. aeruginosa* can cause chronic pulmonary infections in patients with CF, thereby becoming the leading cause of morbidity and mortality in these patients (Malhotra *et al*., 2019).

Besides chronic infections in CF patients, common infections caused by *P. aeruginosa* include ulcerative keratitis, otitis externa, skin and soft tissue infections, chronic obstructive pulmonary disease, pneumonia as well as urinary tract, bloodstream, and burn wound infections (Driscoll *et al*., 2007; Murphy, 2008).

1.1.1 P. aeruginosa acute and chronic infections

P. aeruginosa can establish infections in a multitude of hosts, raising the question: What makes *P. aeruginosa* such a versatile and successful pathogen? The answer to this question is likely the grand arsenal of virulence factors *P. aeruginosa* employs during infection combined with numerous strategies to adapt to the host environment and evade host defense mechanisms. Long term lung infections of *P. aeruginosa* are characterized by the transition from an acute stage (<6 months) to a chronic infection with attenuated virulence and reduced stimulation of the immune system (>6 months) (Sousa and Pereira, 2014).

To initiate infection, bacterial cells need to colonize host tissue, which often relies on a rupture of cutaneous or mucosal barriers, or on a compromised immune defense (Strateva and Mitov, 2011). Motility and adherence are key steps in initial colonization and these processes are mediated by type IV pili (T4P), flagella, and lectins (Haiko and Westerlund-Wikström, 2013; Strateva and Mitov, 2011). To adhere to host cells, *P. aeruginosa* employs several other strategies besides the use of pili as anchors. *P. aeruginosa* secrets two sugar binding proteins, the lectins LecA and LecB, that support binding to carbohydrates at the host and a neuraminidase, which facilitates attachment by exposing additional adherence receptors (Strateva and Mitov, 2011).

Following adherence, *P. aeruginosa* must both invade host tissues and resist the host immune response to establish infection. To degrade tissue components *P. aeruginosa* secrets several virulence factors including two elastases LasA and LasB, an alkaline protease, the two hemolysins, PlcH and rhamnolipid, and a cytotoxin which promotes pore formation in the membranes of host cells (Strateva and Mitov, 2011). Furthermore, *P. aeruginosa* secrets small molecules that can interfere with a range of host cell functions. Secretion of phenazines (redox-active pigments) can lead to formation of reactive oxygen species, hindering respiration, calcium homeostasis, and parts of the immune response (Pierson and Pierson, 2010). The secretion of siderophores (iron-chelating compounds) circumvents the limiting availability of iron during infection by “stripping” iron from host iron-sequestering factors (Smith *et al*., 2013). Additionally, colonization, invasion, and immunosuppression are supported by the production of Exotoxin A (blocking elongation factor 2), and various cytotoxic effector proteins (ExoS, ExoT, ExoU and ExoY) that are translocated to the cytosol of host cells via the type III secretion system (T3SS) (Strateva and Mitov, 2011).

The transition from acute to chronic infections is marked by a phenotypic and genotypic diversification of the population. Some isolates from CF sputum exhibit changes in colony morphology including the mucoid morphotype, resulting from alginate overproduction, and the small colony variant (SCV) morphotype, characterized by slow growth and autoaggregation. The presence of these morphotypes was linked to increased antibiotic resistance and reduced susceptibility to host immune defenses, thus contributing to diminished eradication of chronic *P. aeruginosa* infections (Sousa and Pereira, 2014).

Another adaptive mechanism leading to persistent chronic infection is the formation of biofilms, microbial communities surrounded by an extracellular matrix composed of exopolysaccharides, proteins, and DNA. Biofilms exhibit high antibiotic tolerance, in part due to limited penetration of antimicrobials and slow growth of cells within the biofilm (Sousa and Pereira, 2014). Chronic *P. aeruginosa* infections are hard to eradicate, leading to persistent infections that can last for years. To fight *P. aeruginosa* infections, it is crucial to understand the mechanisms underlying colonization, infection progress, and adaption.

1.2 Stress factors impacting *P. aeruginosa*

Versatile bacteria like *Pseudomonas aeruginosa* that can thrive in various environments, are unavoidably confronted with changing conditions including differences in temperature, pH, osmolarity, radiation, availability of nutrients or concentration of toxins (Marles-Wright and Lewis, 2007). Since bacteria often live in dense, multispecies communities they must compete for resources with other bacteria but also resist chemical and mechanical attacks of their companions (Granato *et al.*, 2019). Besides the attacks of their competitors, bacteria are also confronted by predation from bacteriophages, protists, and predatory bacteria *(Hampton et al*., 2020; Johnke *et al*., 2017).

Pathogenic bacteria face stress accompanied by infecting their hosts, for example respiratory pathogens typically encounter bactericidal peptides produced by epithelial cells, nitrosative stress, hyper osmolarity, and oxygen limitation (Fang *et al*., 2016). In addition to the immune response, pathogens are also targeted by therapeutic approaches, such as antibiotics, antimicrobial peptides (AMPs) and enzymes, or bacteriophages (Kalelkar *et al*., 2021). Due to their importance during *P. aeruginosa* infections, the impact of temperature, antibiotics and bacteriophages will now be discussed in more detail.

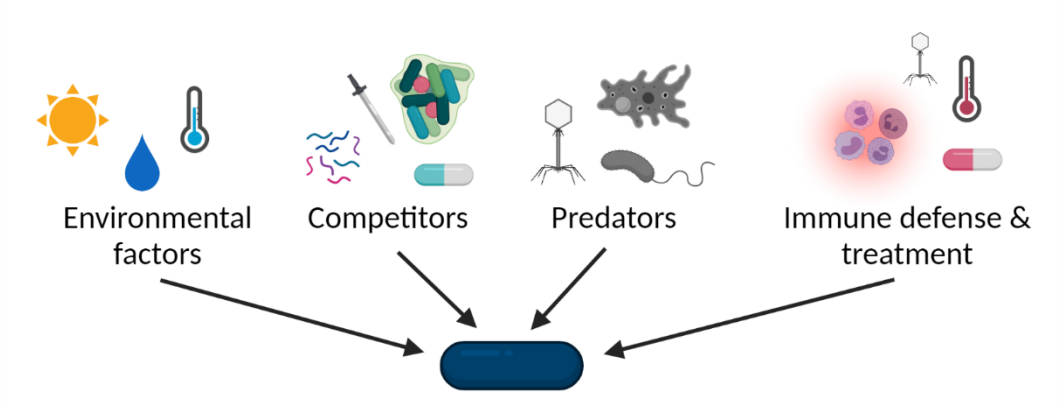

P. aeruginosa is constantly exposed to changes in environmental factors like UV radiation, osmolarity or temperature. Furthermore, life in multispecies communities comes along with competition for nutrients enforced by chemical and mechanical attacks as well as predation. During host infections, *P. aeruginosa* must face the adverse effects of the immune system and therapeutics.

1.2.1 Temperature

Being both a ubiquitous environmental bacterium and a successful pathogen, *P. aeruginosa* is exposed to a broad range of temperatures and it must adopt to a change in temperature once it encounters a warm-blooded host. *P. aeruginosa* grows readily between 25°C and 40°C in planktonic culture, and survives temperatures ranging from 4°C to 50°C for a certain time (Kim *et al*., 2020; Tsuji *et al*., 1982). Growth at 20°C was also observed, but seems to favor growth in biofilms rather than planktonic cultures and comes along with a change in gene expression levels and concentration of intracellular signaling molecules (Kim *et al*., 2020). A total of 6.4% of the genome was found to be differentially regulated when comparing growth at 22°C and 37°C. Differentially expressed genes linked to metabolism, replication, nutrient acquisition, quorum-sensing (QS, a mechanism for bacterial cell-to-cell communication), and factors involved in host infection were identified, showing how crucial an appropriate response to temperature is (Barbier *et al*., 2014).

1.2.2 Antibiotics

Due to high levels of intrinsic and acquired resistance to a wide range of antibiotics, treatment of *P. aeruginosa* has become increasingly challenging (Pang *et al*., 2019). Therefore, the WHO listed carbapenem resistant *P. aeruginosa* as one of three highest priority targets with critical

need for research and development of new antibiotics (Tacconelli *et al*., 2018). *P. aeruginosa* is naturally exposed to antibiotics produced by bacteria and fungi (e.g. *Bacillus* spp., *Streptomyces* spp., *Penicillium* spp., *Cephalosprium* spp.,) because of its presence in soil and water habitats (Neves *et al*., 2014). This likely promoted the development of resistance mechanism against certain antibiotics. Intrinsic resistance mechanisms of *P. aeruginosa* are linked to its low outer-membrane permeability combined with antibiotic efflux and degradation (Hancock and Speert, 2000). Additionally, mutations causing reduced uptake of antibiotics, increased expression of efflux pumps, and antibiotic-inactivating enzymes or modification of the antibiotic targets have been observed. *P. aeruginosa* can also acquire genes conferring antibiotic resistance through horizontal gene transfer (Pang *et al*., 2019).

1.2.3 Bacteriophages

Since in some cases *P. aeruginosa* infections are barely treatable with currently available antibiotics, hope is put on new strategies like bacteriophage therapy (Krylov, 2014). Bacteriophages, literally meaning "bacteria eaters" are bacteria-infecting viruses. There is an estimated 10^{31} bacteriophages (phages, in short) in the biosphere, outnumbering prokaryotes by a factor of 10 for many environments (Hendrix *et al*., 1999; Bar-On *et al.*, 2018; Cobián Güemes *et al*. 2016).

To date it remains difficult to grasp the diversity of phages, with predictions of about 10^8 phage species and estimates of total numbers of phage open-reading-frames (ORFs) ranging between 10^6 and 10^9 (Cobián Güemes *et al*., 2016). What is clear however, is that phages play a key role in biogeochemical cycles and microbial evolution due to the continuous infection and lysis of bacterial cells (Hampton *et al*., 2020).

Phages come in many shapes and sizes. Most known phages have dsDNA genomes and capsids connected to tails (*Caudovirales*). Morphologically, the order of *Caudovirales* is divided into three groups (*Siphoviridae*: long non-contractile tail, *Myoviridae*: long contractile tail, *Podoviridae*: short contractile tail) (Dion *et al*., 2020). Phages of these families vary in the structure of their tails and subsequently also in the ways they interact with the bacterial host cell. Proteins responsible for interaction with receptors on the host cell surface are found in the tail fibres and spikes (Nobrega *et al*., 2018). The lateral tail fibers are often used to bind reversibly to so-called primary receptors on the surface of bacterial cells. Irreversible

attachment to the secondary receptor is mediated by structures at the end of the tail, that vary between the phage families (Maffei *et al*., 2021). The primary and secondary host cell receptors differ in their location and structure; examples include peptide sequences and polysaccharides in cell walls, capsules, and cellular appendages like pili and flagella in both Gram-positive and –negative bacteria (Bertozzi Silva *et al*., 2016). Known phage receptors of *Pseudomonas aeruginosa* include the lipopolysaccharide (LPS), type IV pili (T4P) and outer membrane proteins such as OprM (Bertozzi Silva *et al*., 2016; Chan *et al*., 2016; Harvey *et al*., 2018).

1.3 Responses to Unfavorable Environments

The diversity of microbial stress factors is immense and so is the bacterial response to them. So how exactly do bacteria endure unfavorable environments? The stress response usually comes with a concerted regulation of transcription, translation, proteolysis, or additional modifications. For example, bacteria possess heat shock and cold shock proteins that mediate the response to sudden changes in temperature (Keto-Timonen *et al*., 2016; Roncarati and Scarlato, 2017). The reaction to nutrient starvation is mediated by the stringent stress response, resulting in the production of alarmones that affect DNA replication, nucleotide synthesis, transcription, translation, and metabolism (Irving *et al*., 2021). Bacteria can also reversibly transition into a state of reduced metabolic activity. This state of dormancy allows them to be in “stand-by mode” until conditions become more supportive again (Lennon and Jones, 2011).

Additionally, bacteria can escape certain adversities by moving to environments that are more favorable, which is mediated by a wide range of motility mechanisms (Wadhwa and Berg, 2021). On the contrary, creation of a spatial barrier can also protect bacteria from certain stress factors, especially when they are short-ranged like bactericidal peptides, phages or antibiotics. Bacteria form so called biofilms that often exhibit tolerance to antibiotic treatment and a reduced response to host defense systems, thereby causing persistent infections (Römling and Balsalobre, 2012).

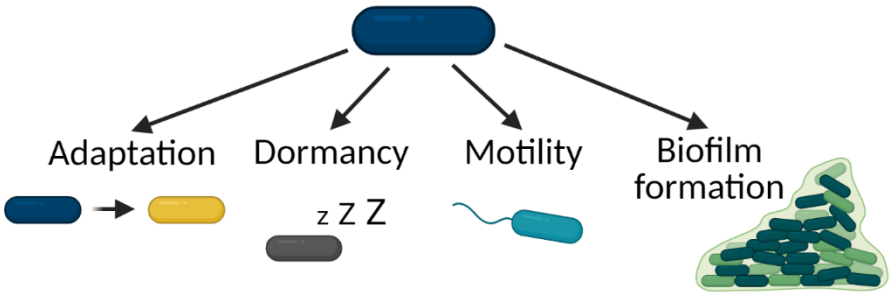

Figure II: *P. aeruginosa* responds to changes in the environment in different ways.
P. aeruginosa can react to changes in the environment by the adaptation to the new surroundings or the transition into a state of reduced metabolic activity (dormancy). Furthermore, various motility mechanisms or the formation of multicellular structures can be employed to generate spatial separation from stress factors.

1.3.1 Motility Mechanisms of *P. aeruginosa*

P. aeruginosa possesses several motility mechanisms, including swimming, swarming, twitching, sliding, and surfing (Harshey, 2003; Kazmierczak *et al*., 2015; Murray and Kazmierczak, 2008; Sun *et al*., 2018).

Swimming motility in aqueous environments is driven by rotation of a single polar flagellum (Kazmierczak *et al*., 2015). The flagellum is a multiprotein complex, whose gene expression is transcriptionally regulated in a four-class hierarchy, including the regulatory protein FleQ (Dasgupta *et al*., 2003). FleQ activity itself is controlled by the second messenger cyclic di-GMP (c-di-GMP), which inhibits flagella biosynthesis (Baraquet and Harwood, 2013; Hickman and Harwood, 2009).

In addition to swimming motility in aqueous environments, *P. aeruginosa* possesses several additional mechanisms to move on surfaces. One type of movement on semisolid surfaces is swarming motility, a multicellular flagella-mediated movement (Köhler *et al*., 2000; Rashid and Kornberg, 2000). Swarmer cells of *P. aeruginosa* express a second flagellum and an alternative motor to move on surfaces and in viscous environments. Additional factors facilitating swarming motility are type IV pili (T4P) and the production of rhamnolipids as surfactants. Since swarming is a population based phenomenon, functional cell-to-cell communication (quorum-sensing, QS) is required (Kearns, 2010; Köhler *et al*., 2000).

P. aeruginosa exhibits also twitching motility on various surfaces, which is driven by the retraction of surface-attached pili. Type IV pili are long thin protein fibers on the surface of bacteria that can repeatedly extend, adhere, and retract, thereby bringing the bacterial cell

closer to the attachment point. T4P function is a complex process, regulated by more than 40 genes as well as the signaling molecules cyclic-AMP and c-di-GMP (Leighton *et al*., 2015). Besides mediating motility, T4P play roles in virulence, DNA uptake, surface attachment, biofilm formation and phage infection (Harvey *et al*., 2018; Leighton *et al*., 2015).

In the lung *P. aeruginosa* will encounter environments containing the glycoprotein mucin (Ridley and Thornton, 2018), a protein that allows for an additional motility mechanism called surfing. Surfing motility depends on QS and flagella, but not T4P, and is more rapid than swimming or swarming motility (Sun *et al*., 2018). Furthermore, flagella and T4P mutants were found to display sliding motility on semisolid surfaces, which is dependent on rhamnolipid surfactants similar to swarming (Murray and Kazmierczak 2008).
The multitude of motility mechanisms exhibited by *P. aeruginosa* suggests the importance of movement to survive and thrive in different environments.

1.3.2 Biofilm Formation

Biofilms are multicellular structures in which bacteria are surrounded by an extracellular matrix consisting of exopolysaccharides, extracellular DNA, and proteins and are believed to cause up to 80% of human bacterial infections (Römling and Balsalobre, 2012). To form such multicellular structures, bacteria periodically switch from the planktonic to the sessile lifestyle by transitioning through the consecutive stages of initial attachment, biofilm maturation, and dispersion (O'Toole *et al*., 2000).

Initial attachment is reversible, thus giving cells the opportunity to decide against a long-term sessile lifestyle in the case of unfavorable conditions (O'Toole *et al*., 2000). Interestingly, the creation of phenotypic heterogeneity following cell division after surface attachment, leads to both a surface-committed and a motile cell (Laventie *et al*., 2019), which allows cells to find appropriate locations for initiation of infection or biofilm formation.

After cells encounter a surface, the intracellular levels of the second messenger c-di-GMP and the expression of type IV pili (T4P) increase, helping with attachment and supporting twitching motility. Twitching then guides surface exploration and eventually results in the formation of aggregates and microcolonies (Kazmierczak *et al*., 2015). The increase in c-di-GMP levels after surface attachment also regulates the formation of the extracellular matrix by positively regulating the production of the adhesin CdrA and the exopolysaccharides Pel,

Psl, and alginate. Psl (polysaccharide synthesis locus) is a key component during initiation and maintenance of biofilms by facilitating surface attachment and cell-to-cell interactions and providing structural support together with extracellular DNA (eDNA). The role of Pel is similar, as it aids biofilm structure in non-mucoid strains. Alginate overproduction leads to slimy, mucoid phenotypes, often observed in strains isolated from CF patients (Lee and Yoon, 2017).

As the biofilm grows in size, gradients of nutrient resources, oxygen, and waste products arise within the biofilm. This leads to the formation of subpopulations that initiate dispersion upon cue sensing (nutrient availability, nitric oxide, iron, and oxygen depletion), reduction of c-di-GMP levels and degradation of the polymeric matrix. The low c-di-GMP levels of dispersed cells support motility and thereby allow these cells to spread and initiate biofilm formation at a new site (Rumbaugh and Sauer, 2020).

1.3.3 Heterogeneity

Living in populations offers cells additional mechanisms to deal with stress by creating the opportunity for heterogeneity within the population. The creation of phenotypically distinct subpopulations increases the chance that a part of the population shows an appropriate response to whatever stress is encountered, thereby allowing for survival and subsequent re-population of the changed environment (Booth, 2002).

The mechanisms leading to phenotypic heterogeneity are manifold, including amplification of signals generated by noise in gene expression, feedback loops leading to two stable steady states (bistability), phase variation, epigenetic inheritance, or the spatial segregation of enzymes during cell division (Jenal *et al*., 2017; Norman *et al*., 2015; Veening *et al*., 2008). In *P. aeruginosa* phenotypic heterogeneity has been observed in several contexts. During tissue colonization, asymmetric cell division leads to one surface-committed and one flagellated, motile daughter cell, thereby increasing infection spread and tissue damage (Laventie *et al*., 2019). Heterogeneity in quorum-sensing initiation results in distinct growth rates in single cells (Boedicker *et al*., 2009) and might enable cells to engage in distinct biological functions. In addition, physiological heterogeneity in biofilms was linked to antibiotic tolerance and persistence (Soares *et al*., 2020).

1.4 Sensing and Responding to the Environment

To react to changes in the environment bacteria need to sense their surroundings, transmit the signal internally and potentially also communicate with other bacteria for an appropriate response. *P. aeruginosa* possesses several interconnected signaling networks for both extracellular and intracellular signaling. Chemosensory pathways and two-component systems are the key constituents of signaling networks used for sensing external signals beyond cell-to-cell communication. Cell-to-cell communication, called quorum sensing (QS), is crucial for population-based behavior and it is mediated by several diffusible molecules and their respective autoinduced regulatory networks. Nucleotide-based signals play an important role in intracellular signaling networks, coordinating the response to sensed signals.

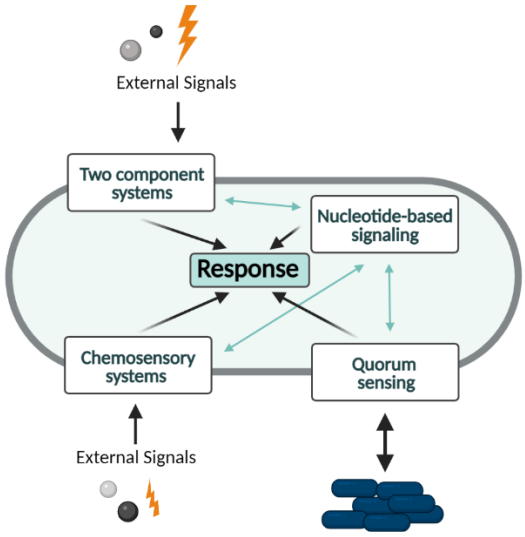

Figure III*:* Schematic representation of signaling networks in *P. aeruginosa*.
P. aeruginosa encodes two-component and chemosensory systems to sense external signals and coordinate appropriate responses. Cell-to-cell communication is mediated by diffusible signals and their autoinduced regulatory networks (quorum sensing). Nucleotide-based signaling molecules are an important part of intracellular signaling networks that are often intertwined with other signaling systems.

1.4.1 Chemosensory Pathways

Chemosensory pathways are widespread signal transduction systems used to respond to external stimuli. These pathways are highly complex and involve the concerted action of at least six proteins. Canonically, detection of the stimulus leads to a conformational change of the chemoreceptor. The sensitivity of the chemoreceptor to temporal changes of the stimulus is modulated by methylation and demethylation, exerted by a methyltransferase and

methylesterase, respectively. Activation of the chemoreceptor causes the phosphorylation of a kinase, which in turn phosphorylates the receiver (REC) domain of a response regulator (RR). The RR then generates a specific output, depending on its domain composition. RRs possessing only a REC domain often control flagellar motility directly, while RRs with additional domains can create an interplay with other signaling pathways (Matilla *et al*., 2021).

P. aeruginosa possesses four chemosensory pathways that belong to different classes of chemosensory systems. A total of 26 chemoreceptors respond to environmental cues like O2, amino acids, inorganic phosphate, or proximity to surfaces. Of these 26 chemoreceptors, 23 feed into the chemotaxis controlling Che pathway, highlighting again the importance of motility as response to environmental cues. The three remaining chemoreceptors are specific to the Che2 (unknown output), Wsp (c-di-GMP mediated motility and biofilm formation) and Chp (T4P synthesis, cAMP mediated virulence, and motility) pathways (Matilla *et al*., 2021).

1.4.2 Two-component Systems

Besides chemosensory systems, bacteria also use two component systems (TCS) to sense and respond to environmental signals. TCS consist of histidine kinases (HKs, also called sensor kinases) and response regulators (RRs). Briefly, the HK senses a specific signal, which leads to autophosphorylation of a conserved histidine in its transmitter domain. The phosphoryl group is subsequently transferred to a conserved aspartic residue in the receiver (REC) domain of an RR, which mediates the output, like in chemosensory systems. The HKs can be classified into three groups, based on their mode of transferring the phosphoryl group. Classical HKs show a two-step phosphorelay mechanism, like the one described above. Unorthodox HKs possess an additional receiver and histidine phosphotransfer (Hpt) domain, which eventually transfers the phosphoryl group to the receiver domain of the RR, creating a four-step phosphorelay. Hybrid HKs, like unorthodox HKs, also mediate a four-step phosphorelay, but the second transmitter domain of the HK is substituted by an external protein possessing the Hpt domain that transfers the phosphoryl group to the RR (Liu *et al*., 2019). *P. aeruginosa* possesses 64 HKs, 72 RRs and 3 Hpt proteins, of which a substantial amount have been connected to virulence-associated behaviors. TCSs are often considered to be stand-alone systems, sensing a narrow range of stimuli to avoid crosstalk and propagate defined responses, though more and more multikinase networks are being described (Francis *et al*., 2017).

1.4.2.1 The Gac/Rsm Cascade

One of the most studied multikinase networks of *P. aeruginosa* is the GacS/GacA (global activation of antibiotic and cyanide synthesis) TCS, a network involved in regulating the switch between acute and chronic infections. The key kinase of the network is GacS, an unorthodox HK, whose activity is controlled by three other HKs, LadS, RetS, and PA1611 (Francis *et al.*, 2017). LadS (lost adherence sensor) is a calcium-responsive HK, which can phosphorylate GacS, thereby upregulating GacS signaling (Broder *et al.*, 2016; Chambonnier *et al.*, 2016; Ventre *et al.*, 2006). RetS (regulator of exopolysaccharide and type III secretion), a HK with two REC domains, inhibits GacS via three specific mechanisms. Two are dephosphorylation mechanisms and the third one is inhibition of autophosphorylation by formation of RetS-GacS heterodimers (Francis *et al.*, 2018; Goodman *et al.*, 2004; Goodman *et al.*, 2009; Laskowski *et al.*, 2004; Laskowski *et al.*, 2006; Ryan Kaler *et al.*, 2021; Ventre *et al.*, 2006). In turn, RetS is activated by mucins, glycosylated proteins which are key components of mucus (Ridley and Thornton, 2018) and inhibited by the HK PA1611, which can bind to RetS, subsequently preventing the interaction of RetS and GacS (Bhagirath *et al.*, 2017; Kong *et al.*, 2013).

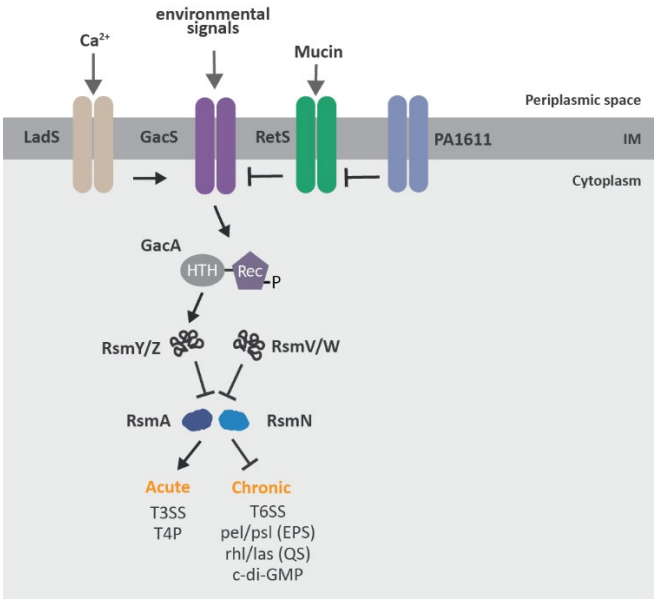

Figure IV: The Gac/Rsm cascade controls the switch between acute and chronic infections in *P. aeruginosa*.
Activity of the central kinase GacS is inversely controlled by the kinases LadS, RetS and PA1611. Activation of GacS leads to phosphorylation and activation of the transcription factor GacA, who in turn regulates expression of the small regulatory RNAs *rsmY* and *rsmZ*. Together with two additional sRNAs, RsmV and RsmW, RsmY and RsmZ sequester the RNA-binding proteins RsmA and RsmN away from their target mRNAs, thereby inhibiting the post-transcriptional control of RsmA/N. Activation of the cascade leads to a switch from acute to chronic infection by regulating type III (T3SS) secretion system, type IV pili (T4P), type IV secretion systems (T6SS), exopolysaccharide production (EPS), quorum sensing (QS) and cyclic di-GMP (c-di-GMP) levels.

GacS itself is activated by molecule(s) present after kin cell lysis and produced in high density cultures, though the chemical nature of these molecule(s) remains unknown (Heeb *et al*., 2002; Le Roux *et al*., 2015). When GacS signaling is active, it activates the transcription factor and RR GacA through phosphorylation (Heeb and Haas, 2001). GacA in turn regulates expression of the two small regulatory RNAs *rsmY* and *rsmZ* (repressor of stationary phase metabolism) (Brencic *et al*., 2009), forming the so-called Gac/Rsm cascade. Together with two additional small RNAs, *rsmV* and *rsmW*, they bind to the RNA-binding proteins RsmA and RsmN/RsmF (Heurlier *et al*., 2004; Janssen *et al*., 2018; Marden *et al*., 2013; Miller *et al*., 2016; Morris *et al*., 2013; Valverde *et al*., 2003).

RsmA and RsmN are homologues of CsrA (carbon storage regulator), a small, highly conserved protein exerting posttranscriptional control that functions as homodimer. Although RsmN also forms a homodimer, its secondary structure is distinct from other RsmA/CsrA homologues (Dubey *et al*., 2003; Marden *et al*., 2013; Morris *et al*., 2013; Rife *et al*., 2005). Typically, RsmA-like proteins inhibit translation by binding conserved GGA sequence motifs in their target mRNAs. Several target mRNAs possess more than one GGA motif which can be found in the 5' leader sequence, overlapping with the Shine-Dalgarno sequence, the start codon or the beginning of the translated region (Pourciau *et al*., 2020). While RsmN requires two binding sites, RsmA binding requirements seem less stringent (Schulmeyer *et al*., 2016). Binding of the sRNAs to RsmA and RsmF sequesters the proteins away from their mRNA targets, thus relieving the post-transcriptional control (Pourciau *et al*., 2020).

In *P. aeruginosa* PAK around 9% of all genes show altered transcript levels when *rsmA* was mutated (Brencic and Lory, 2009). In *P. aeruginosa* PAO1-L almost 400 transcripts linked to mRNAs or sRNAs interact with RsmN (Romero *et al*., 2018). Moreover, a recent study detected 411 and 186 binding sites for RsmA and RsmN, respectively, of which 75 were overlapping (Chihara *et al*., 2021), demonstrating the extent of the Gac/Rsm network. RsmA promotes expression of factors important for acute infections (type IV pili, type III secretion system) while inhibiting factors for chronic disease progression (type IV secretion system, Pel/Psl exopolysaccharides, quorum sensing) (Brencic and Lory, 2009; Goodman *et al*., 2004; Pessi *et al*., 2001). The extended Gac/Rsm network also regulates the second messenger c-di-GMP, by controlling the translation and activity of c-di-GMP synthesizing diguanylate cyclases (Moscoso *et al*., 2014; Valentini *et al*., 2016). On top of that, the Gac/Rsm cascade regulates quorum sensing by inhibiting synthesis of the signaling molecules (Pessi *et al*., 2001).

1.4.3 Quorum Sensing

Quorum sensing is a cell density-dependent mechanism mediated by several distinct molecules and pathways. Most prominent in Gram-negative bacteria are N-Acyl homoserine lactones (AHLs) which signal through the interconnected Las and Rhl systems in *P. aeruginosa*. Once a certain threshold of AHLs is produced, corresponding to the density of bacterial cells, the AHLs bind their corresponding transcriptional regulators. This leads to a change in expression of multiple genes, including those responsible for the synthesis of the respective AHL, creating an autoinduction feedback loop (Nadal Jimenez *et al*., 2012). In addition, *P. aeruginosa* produces cyclic dipeptides, called diketopiperazines, which interfere with AHL signaling. The *Pseudomonas* quinolone signal (PQS) provides another cell-to-cell signaling pathway that is intertwined with the AHL signaling systems. Together these QS systems regulate virulence factors including elastases, exotoxin A, T3SS or pyocyanin. In addition to interspecies signaling, *P. aeruginosa* also produces diffusible signal factors used for interkingdom interactions, for example it can inhibit *Candida albicans* virulence factor production (Nadal Jimenez *et al*., 2012).

1.4.4 Nucleotide-based messengers

While diffusible signals are used for cell-to-cell communication, bacteria use nucleotide-based messenger molecules for intracellular signaling. Well known second messengers include the signaling molecules cyclic di-GMP (c-di-GMP), cyclic AMP and (p)ppGpp, though more and more molecules including cyclic di-AMP and cyclic GMP-AMP have been identified in recent years (Camilli and Bassler, 2006; Jenal *et al*., 2017). These second messengers play crucial roles in bacterial lifestyle regulating metabolism, gene expression or antibiotic resistance (Jenal *et al*., 2017).

1.4.4.1 The Second Messenger cyclic di-GMP

C-di-GMP is the most studied second messenger in *P. aeruginosa.* The second messenger was initially found in Moshe Benzimans lab as activator of the cellulose synthesis in Komagataeibacter xylinus (formerly Acetobacter xylinum) (Ross *et al.* 1986). Since then c-di-GMP has been shown to influence a wide variety of bacterial behaviors such as cell division,

virulence, motility, and biofilm formation (Jenal *et al*., 2017). C-di-GMP is formed from two molecules of GTP by diguanylate cyclases (DGCs) (Ross *et al*., 1986). DGCs contain GGDEF domains, with the eponymous amino acid motif GGDEF that catalyzes the production of c-di-GMP (Ryjenkov *et al*., 2005). Hydrolysis is catalyzed by the EAL or HD-GYP domain of phosphodiesterase (PDEs), cleaving c-di-GMP into pGpG or two GMP molecules, respectively (Bellini *et al*., 2014; Schmidt, Ryjenkov *et al*., 2005).

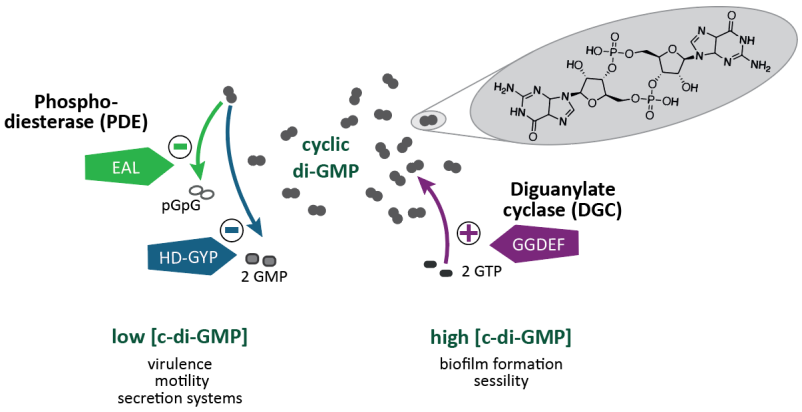

Figure IV: Levels of the second messenger cyclic di-GMP are inversely controlled by the action of diguanylate cyclases and phosphodiesterases. Diguanylate cyclases, containing GGDEF domains, catalyze the formation of cyclic di-GMP from two molecules of GTP. Degradation of cyclic di-GMP is mediated by phosphodiesterases containing either an EAL or HD-GYP domain, cleaving cyclic di-GMP into pGpG or two molecules of GMP, respectively.

DGCs and PDEs are present in members of all major bacterial phyla indicating the importance of c-di-GMP as a signaling molecule (Jenal *et al*., 2017). In the annotated genome of *P. aeruginosa* strain PAO1, 43 proteins that contain a DGC (18), PDE (9) or both domains (16) have been found (Kulasakara *et al*., 2006). In addition to the extensive number of c-di-GMP-modulating enzymes, there are at least nine more proteins binding c-di-GMP and mediating downstream signaling in *P. aeruginosa*. Eight of them possess a PilZ domain, though the eponymous PilZ itself does not bind c-di-GMP (Laventie *et al*., 2019; Merighi *et al*., 2007). The ninth is FleQ, a transcriptional regulator and AAA+ ATPase, whose Walker A motif is bound by c-di-GMP (Baraquet and Harwood, 2013; Hickman and Harwood, 2009). Except for PA2771 and PA2818, all DGCs and PDEs are found in the core genome of *P. aeruginosa* strains (Kulasakara *et al*., 2006), suggesting that these enzymes fulfill specific, non-redundant roles.

Indeed, many DGCs and PDEs of *P. aeruginosa* have been shown to control specific behaviors. A good example are the effects of distinct PDEs during biofilm formation. Current results indicate that BifA, Pch, and MorA mediate the early stages of biofilm development

(Choy *et al*., 2004; Kuchma *et al*., 2007; Roy *et al*., 2012) while RmcA and MorA are needed for biofilm maintenance *(Choy et al., 2004;* Katharios-Lanwermeyer *et al*., 2021). Dispersion in response to glutamate, ammonium chloride and nitric oxide is regulated by RbdA and Pch, but not BifA (An *et al*., 2010; Roy *et al*., 2012) and the PDE PA4781 affects eDNA levels, which seems not to be the case for BifA, MucR, and FcsR (Ueda and Wood, 2010). Similarly, DGCs such as SadC, RoeA, and WspR have distinct functions in swarming motility and biofilm development (Hickman *et al*., 2005; Merritt *et al.,* 2010; Zhu *et al*., 2016).

Phylogenetic analysis of *P. aeruginosa* genes containing GGDEF domain across multiple Pseudomonad genomes indicates that five DGCs and PDEs control the basal levels of c-di-GMP (DGCs: DgcH and PA0290, PDEs: BifA, RbdA, and Pch). Together, with the diverse roles in biofilm formation and motility, these findings underline the key importance of phosphodiesterases in *P. aeruginosa*.

1.4.4.2 Regulation and function of the phosphodiesterase BifA

BifA (PA4367, *bi*ofilm *f*ormation) contains both a GGDEF and an EAL domain of which the conserved motif of the GGDEF domain is mutated to GGDQF but the EAL motif is unaltered. BifA shows c-di-GMP phosphodiesterase activity, but no DGC activity, likely due to the mutation of the GGDEF core motif, though interestingly, the GGDEF domain is needed for the PDE activity of BifA (Kuchma *et al*., 2007). Similar to other PDEs like Pch or RbdA, BifA localizes to the inner membrane (Roy *et al*., 2012; Liu *et al*., 2018).

Expression of BifA is downregulated by SuhB, a regulator of virulence factors during acute infections (Li *et al*., 2013; Li *et al*., 2017), but positively regulated by FliA, a factor controlling flagellin synthesis (Lo *et al*., 2016; Starnbach and Lory, 1992). Furthermore, BifA protein levels are upregulated by AmpR, a transcriptional regulator known for its role in the acute-chronic infection switch (Kumari *et al*. 2014; Balasubramanian *et al*., 2015).

A transposon mutant in *bifA* shows increased biofilm formation while overexpression of the gene reduces biofilm formation and cell toxicity (Kulasakara *et al*., 2006). In parallel, *bifA* was also identified in a transposon screen studying SadC-mediated biofilm formation (Kuchma *et al*., 2007). Moreover, loss of BifA activity resultes in swarming defects in both PAO1 and PA14 and increased production of the exopolysaccharide Pel in PA14 (Kuchma *et al*.

2007; Roy *et al*., 2012). BifA seems to regulate these phenotypes together with the DGC SadC in a SadB dependent manner (Kuchma *et al*., 2007; Merritt *et al*., 2007).

Recently, a small molecule (H6-335-P1) that increases BifA activity and subsequently leads to biofilm dispersion has been identified. These results suggest new treatment strategies for biofilm infections by externally triggering a decrease in c-di-GMP levels and demonstrate the importance of understanding the c-di-GMP network.

1.4.4.3 Regulation and function of the diguanylate cyclase WspR

Upregulation of c-di-GMP levels is also a key factor for the induction of small colony variants (SCVs) during persistent lung infections. One well-studied player involved in SCV formation is the diguanylate cyclase WspR. WspR was initially identified in *Pseudomonas fluorescens* as wrinkly spreader phenotype regulator. Wrinkly spreaders are a diverse group of *P. fluorescens* strains that form wrinkled colonies on solid surfaces and colonize the air-broth interface by adhering strongly to other cells and surfaces (Rainey and Travisano, 1998). Analysis of mutants that lost the wrinkled colony morphology revealed *wspR*, a gene with sequence similarity to the response regulator PleD of *Caulobacter crescentus* (Spiers *et al*., 2002; Hecht and Newton, 1995). WspR is the terminal gene of the seven-gene *wsp* encoding a chemosensory system (D'Argenio *et al*. 2002; Bantinaki *et al*., 2007). The *wsp* locus, comprised of *wspABCDEFR*, encodes for a membrane-associated methyl-accepting chemotaxis protein (WspA), two scaffold proteins (WspB and WspD), a methyltransferase (WspC), a protein with a histidine kinase and a response regulator domain (WspE), a methylesterase with a response regulator domain (WspF) and a protein with GGDEF and response regulator domains (WspR) (Bantinaki *et al*., 2007). The Wsp chemosensory system was subsequently studied in *P. aeruginosa* and *P. fluorescens* and revealed WspR to be a cytoplasmic diguanylate cyclase and response regulator (Hickman *et al*., 2005; Goymer *et al*., 2006). Activation of WspA on solid surfaces or by ethanol induces WspE-mediated phosphorylation of WspR thereby stimulating WspR activity (Matilla *et al*., 2021). Phosphorylation of WspR results in the formation of protein clusters, which leads to increased c-di-GMP synthesis (Güvener and Harwood, 2007; Huangyutitham *et al*., 2013). Additionally, WspR mediates c-di-GMP heterogeneity in early stages of biofilm formation, leading to a population that starts biofilm formation and one that stays motile on the surface (Armbruster *et al*., 2020).

1.5 Aim Of This Thesis

P. aeruginosa is the leading cause of morbidity and mortality in patients with cystic fibrosis (CF) due to chronic lung infections. During the establishment of persistent infections, *P. aeruginosa* undergoes extensive adaptation to the lung environment leading to diversification into different phenotypes including small colony variants (SCVs). The appearance of SCVs is connected to increased antibiotic resistance and poor clinical outcome and has been linked to high levels of the second messenger cyclic di-GMP.

The aim of this thesis was to obtain a better understanding of the molecular mechanisms underlying SCV formation, by studying the impact of the *hecRE* module, a newly identified mediator of SCV formation in *P. aeruginosa*. This will be achieved by studying the impact of the *hecRE* module on cyclic di-GMP levels and associated phenotypes, and by determining the molecular basis of these effects. Furthermore, the expression of the *hecRE* module and its regulation will be studied on single cell and population level using fluorescent reporters.

2 RESULTS

Stochastic expression of the *hecRE* module controls *Pseudomonas aeruginosa* surface colonization and phage sensitivity

Christina Manner[1], Raphael Dias Teixeira[1], Tina Jaeger[2], Raphaela Zemp[+], Benoît-Joseph Laventie[1], Thomas Bock[3], Urs Jenal[1]

[1] Focal Area Infection Biology, Biozentrum, University of Basel, Basel, Switzerland
[2] Department Biomedizin, University of Basel, Basel, Switzerland
[3] Proteomics Core Facility, Biozentrum, University of Basel, Basel, Switzerland
[+] formerly: Focal Area Infection Biology, Biozentrum, University of Basel, Basel, Switzerland

I performed all experiments shown with the following exceptions: Table 1; Fig. 2A,B; Fig. 3A,B,C,D; Fig. S3A,B; Fig. 4B; Fig. 5A,B,C; Fig. 6B; Fig. 7F,G; Fig. 8D,E,F; Fig S6C,D; Fig.10; Fig. 19.

2.1 Stochastic expression of the *hecRE* module controls *Pseudomonas aeruginosa* surface colonization and phage sensitivity

2.1.1 Transposon insertions in *PA2780* cause SCV formation via altered c-di-GMP levels

To investigate how small colony variant (SCV) formation in *Pseudomonas aeruginosa* is regulated, random transposon insertions in the chromosome of strain PAO1 were screened for mutants leading to the SCV phenotype (Malone *et al*., 2010). This identified twenty different gene targets, most of which have direct links to c-di-GMP **(Table 1)**. The most frequent hit was in *dsbA*, a gene encoding a periplasmic thiol:disulfide oxidoreductase that is predicted to be in an operon with *dgcH*, one of several diguanylate cyclase genes in *P. aeruginosa*. Previous studies had shown that disruption of *dsbA* leads to increased c-di-GMP levels via dysregulation of the *yfiN* diguanylate cyclase (Malone *et al*. 2010, Malone *et al*., 2012). In line with this, our screen also identified the y*fiR* gene itself. Additional transposon insertions mapped to diguanylate cyclase genes *sadC*, *PA0338,* and *PA0847* and to P*A3528,* which encodes a putative c-di-GMP specific phosphodiesterase. Likewise, several other insertions could be linked to c-di-GMP, including *wspF* (Hickman *et al*., 2005) or *PA5294,* which is positioned next to a gene encoding a c-di-GMP specific phosphodiesterase (Kulasakara *et al*., 2006). Of note, the mariner transposon used for this transposon screen contains an outward facing promoter. We presume that insertions can be either disrupting genes or activating their expression.

The second most prominent hit after *dsbA* was *PA2780*, a gene encoding a transcription factor positioned in a bicistronic module together with *PA2781* **(Fig. 1A)** (Wang *et al*., 2014). To test if the *PA2780*::Tn mutant also caused changes in c-di-GMP, we compared overall c-di-GMP levels to the isogenic wild-type strain using a BldD2-eGFP based c-di-GMP sensor (Kaczmarczyk *et al*., unpublished). As shown in **Fig. 1B**, c-di-GMP levels were indeed strongly increased in this background, suggesting that disruption of *PA2780* or increased expression of the downstream gene, *PA2781,* deregulates c-di-GMP levels. Intriguingly, c-di-GMP levels in the *PA2780*::Tn mutant strongly increased in mid-log phase coinciding with a bend of the growth curve and a flattening of optical density increase. Mutants lacking *PA2780* or *PA2781* showed unaltered levels of c-di-GMP, indicating that these genes are either not expressed or their products not active in growing cultures of *P. aeruginosa* (**Fig. S1A**).

Together, this reinforced the notion that c-di-GMP is a primary driver of the SCV morphotype in *P. aeruginosa* and identified novel genes involved in regulating the concentration of the second messenger in this pathogen.

Gene	Name	# Hits	Orientation	Description
0153	*pcaH*	1	-	protocatechuate 3,4-dioxygenase
0171		7	+/-	protein associated with twitching motility in literature
0338		4	-	protein containing a GGDEF, PAS and a PAC domain
0727		1	-	Pf replication initiator protein
0847		7	+/-	diguanylate cyclase, containing a PAS, PAC and a HAMP domain with a transmembrane region
1121	*yfiR*	3	+/-	controller of the diguanylate cyclase YfiN
1485		1	+	amino acid permease
1803	*lon*	1	-	Lon protease
2670		1	-	protein, next to type II secretory system
2780		16	+/-	transcription factor
2966	*acpP*	1	+	Small acyl carrier protein
3159	*wbpA*	1	-	UDP-N-acetyl-d-glucosamine 6-Dehydrogenase
3258		1	-	protein with an EAL, a degenerate GGDEF and two CBS domains
3703	*wspF*	5	+/-	methylesterase of the Wsp chemosensory system
4332	*sadC*	1	+	diguanylate cyclase with a transmembrane domain
4710	*phuR*	1	+	Heme/Hemoglobin uptake outer membrane receptor PhuR precursor
5015	*aceE*	1	+	pyruvate dehydrogenase
5294	*norA*	1	-	multidrug efflux protein, next to GGDEF/EAL protein PA5295
5487	*dgcH*	1	-	protein wih a GGDEF domain
5489	*dsbA*	28	+/-	oxidoreductase

Table 1: List of transposon mutants exhibiting the small colony variant morphology.
The transposon screen was performed by Malone *et al*., 2010. Strains with insertions of the Mariner transposon leading to a small colony variant morphotype were isolated on Congo Red plates and transposons were mapped by semi-random PCR and sequencing.

2.1.2 PA2780 and *PA2781* form a conserved toxin/antitoxin-like module in *P. aeruginosa*

Intrigued by the strong effects on c-di-GMP caused by the transposon insertion in *PA2780*, we set out to functionally characterize *PA2780* and *PA2781*. Based on their chromosomal organization, their small size (*PA2780*: 345 bp, *PA2781*: 342 bp, with an overlap of 4 bp) and probable transcriptional coupling, the two genes were predicted to form a toxin/antitoxin-like module (Sevin and Barloy-Hubler, 2007). Furthermore, *PA2780* and *PA2781* were found to be

co-transcribed in *P. aeruginosa* strain PA14, suggesting that they form an operon (Wurtzel *et al*., 2012). While *PA2780* encodes a transcription factor with an N-terminal HTH-domain and a C-terminal dimerization domain (Wang *et al*., 2014), sequence- or structure-based searches failed to provide functional clues about PA2781. In line with this, PA2781 is only found in *P. aeruginosa* strains, such as PA14, PA7, LESB58 and PAO1, but has no orthologues in other *Pseudomonads* or any other bacterial genus (OMA group Q9I062, https://omabrowser.org/oma/home/). An analysis of more than 7500 sequenced *P. aeruginosa* strains revealed that *PA2780* and *PA2781* are highly conserved with 99.18% (PA2780) and 96.99% (PA2781) of the strains showing identical sequences (**Supp. Table 1**).

Based on this and our in-depth analyses of the *PA2780/81* module (below), we propose to rename the genes *hecR* and *hecE* for heterogeneous, environment-responsive, c-di-GMP controlling regulator and effector.

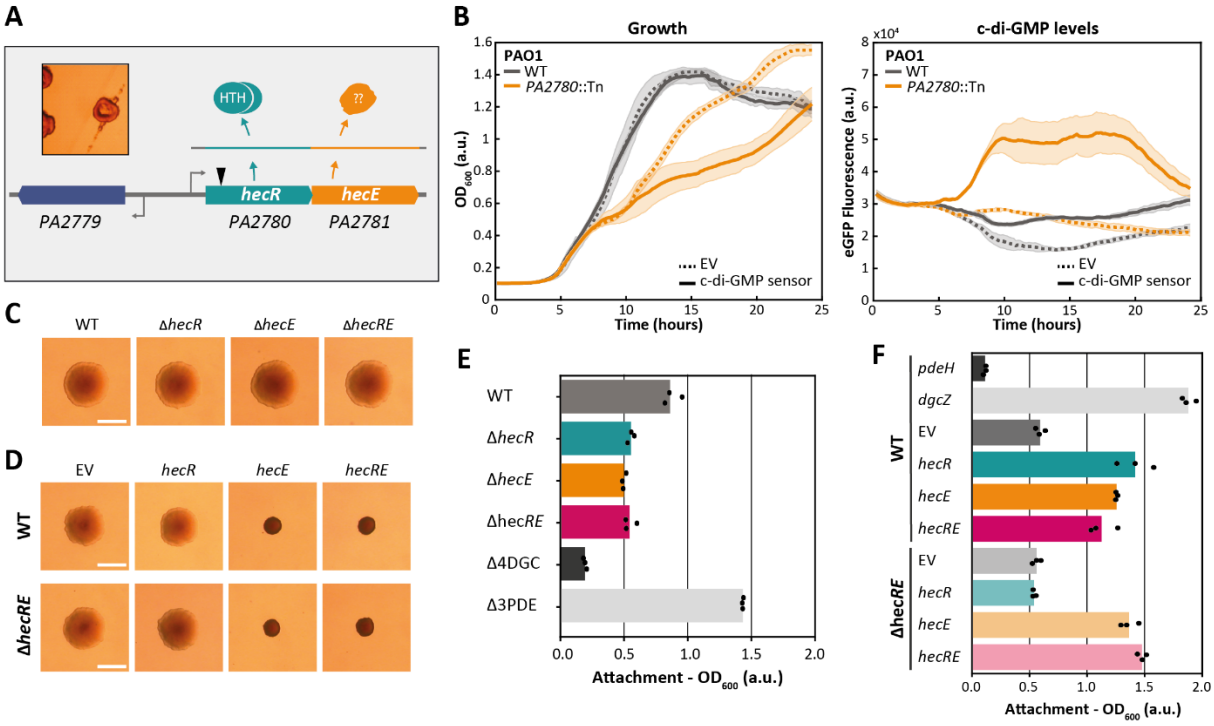

Figure 1: The *hecRE* module regulates SCV formation, c-di-GMP levels, and biofilm formation.
A: Typical example of SCV colonies on Congo red plates as observed in the transposon screen and schematic organization of the *hecR*/*hecE* (*PA2780*/*81*) operon. The location of transposon insertion in *hecR* is marked with a triangle. The *hecR* gene encodes a transcription factor with a classical helix-turn-helix (HTH) DNA binding domain (Wang *et al*., 2014). **B:** The *PA2780*::Tn mutant shows increased c-di-GMP levels. Growth (left) and fluorescence (right) of *P. aeruginosa* wild type (WT) and *PA2780*::Tn mutant carrying a control plasmid (EV) or a plasmid expressing the BldD-eGFP c-di-GMP sensor. Strains were grown in LB and mean values and standard deviations of two biological replicates (with six technical replicates each) are shown. **C:** Deletion of the *hec* genes does not alter colony morphology. Colony morphology of *hecR* and *hecE* single or double mutants grown on LB plates containing Congo Red and Coomassie Brilliant Blue. The scale bar represents 1 mm. Experiments were done in triplicates; one representative image is shown. **D:** Expression of *hecE* induces SCV formation. Colony morphology of *P. aeruginosa* WT or Δ*hecRE* mutant expressing *hecR*, *hecE*, or both genes from an IPTG-inducible promoter grown on LB plates containing Congo Red and Coomassie Brilliant Blue and 100 µM IPTG. Experiments were done in triplicates; one representative image is shown. **E:** HecR and HecE are required for biofilm maturation. Surface attachment of *P. aeruginosa*

WT and *hec* deletion strains after growth in LB for 20 hours was quantified by crystal violet (CV) staining. Control strains with artificially high or low c-di-GMP levels were included. Strain Δ3PDE lacks phosphodiesterases BifA (PA4367), Pch (PA5017) and RbdA (PA0861); strain Δ4DGC lacks the diguanylate cyclases SadC (PA4332), DgcH (PA5487), PA0338 and PA0847. Mean values and standard deviations of three biological replicates (each with six technical replicates) are shown. **F:** Ectopic expression of *hecE* strongly induces biofilm formation. Surface attachment of *P. aeruginosa* wild type (WT) and *hec* deletion strains expressing *hecR*, *hecE* or both genes from a plasmid. Strains expressing *pdeH* (phosphodiesterase) or *dgcZ* (diguanylate cyclase) are show as controls for situations with low or high c-di-GMP, respectively. The attachment was quantified after growth in LB for 10 hours by CV staining. Mean values of one biological and three technical replicates are shown.

2.1.3 HecE mediates SCV formation and regulates biofilm formation

To better understand how the transposon insertion in *hecR* leads to SCV formation, we analyzed strains carrying deletions in *hecR* or *hecE* and strains expressing the *hec* genes from an IPTG inducible promoter on a plasmid. While deleting *hecR*, *hecE* or both did not alter the colony morphology (**Fig. 1C**), expression of *hecE* but not *hecR* from a plasmid induced the classical SCV morphotype. Likewise, co-expression of *hecR* and *hecE* caused an SCV phenotype, indicating that HecR does not counteract the action of HecE (**Fig. 1D**). From this we conclude that HecE alone can induce SCV formation and that Tn-mediated expression of *hecE* is likely responsible for the SCV phenotype in the original *hecR*::Tn isolate.

Because *P. aeruginosa* SCVs are known to strongly adhere to surfaces and to strongly express biofilm matrix components (Déziel *et al*., 2001; Malone *et al*., 2010), we next compared biofilm formation of wild type and *hec* mutants. Although no difference in attachment and biofilm formation was observed at early stages of surface colonization, mutants lacking HecR, HecE or both proteins showed strongly decreased biofilms at later time points **(Fig. 1E, S1B)**. This, together with the observation that these strains did not differ in growth (**Fig. S1C**) argued that the observed differences in late biofilms are caused by different attachment behavior or increased cell dispersal. These results also indicated that *hecR* and *hecE* are expressed during biofilm formation where they may contribute to increasing c-di-GMP levels or maintaining high levels of the second messenger.

Even though *hecR* does not seem to be the driver of SCV formation, expressing *hecR* alone from a plasmid significantly stimulated *P. aeruginosa* surface attachment in a HecE-dependent manner **(Fig. 1F, S1E)**. The observations that ectopic expression of *hecE* and *hecR* led to increased biofilm formation and that the role of HecR depends on HecE, but not *vice versa*, indicted that HecE is the primary effector of the observed c-di-GMP dependent changes, while the main role of HecR is to mediate *hecE* expression.

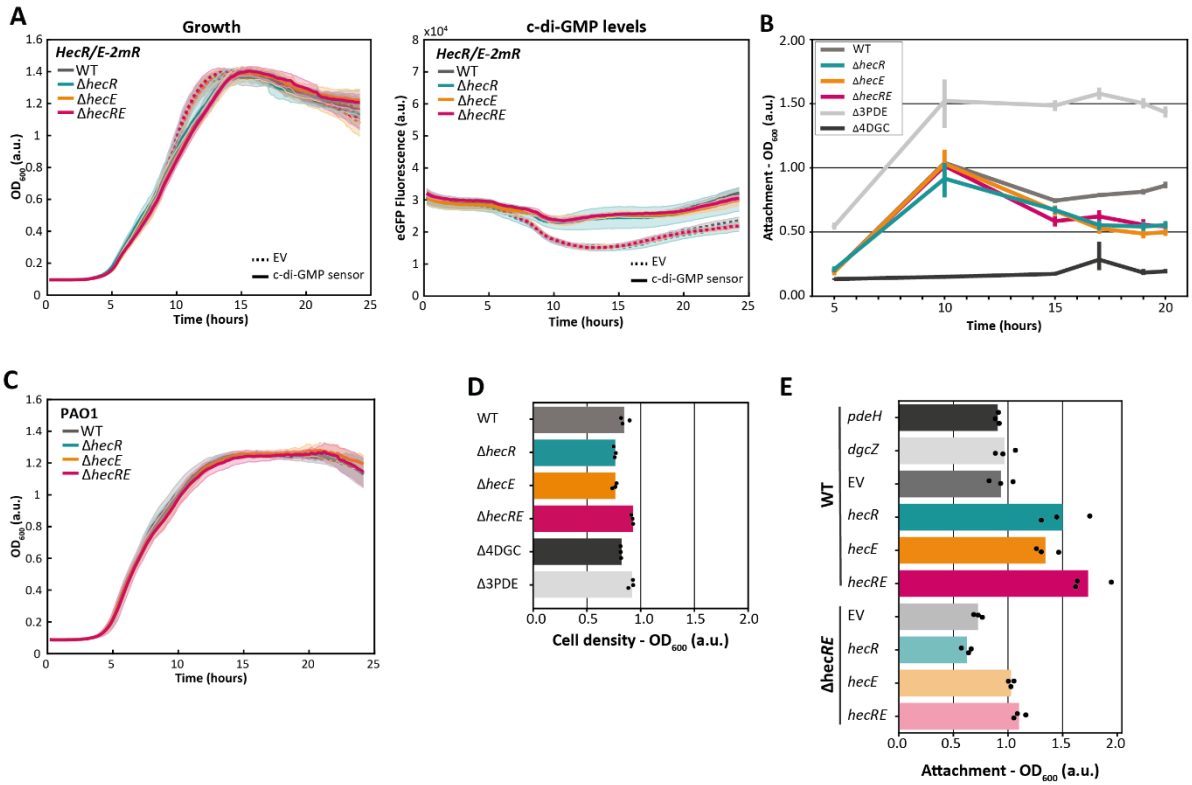

Supplementary Figure 1: The *hecRE* module regulates SCV formation, c-di-GMP levels, and biofilm formation.
A: Growth (left) and fluorescence (right) of *P. aeruginosa* wild type (WT) and mutant strains carrying a control plasmid (EV) (stippled lines) or a plasmid expressing the BldD-eGFP c-di-GMP sensor (solid lines). Mean values and standard deviations of two biological replicates (with six technical replicates) are shown. **B:** HecR and HecE are required for biofilm maturation. Surface attachment of *P. aeruginosa* wild type (WT) and indicated mutants grown in LB. Mean values and standard deviations of three biological technical (with six technical replicates) are shown. **C:** Growth of *P. aeruginosa* wild type (WT) and *hec* deletion strains in LB with mean values and standard deviations of three biological replicates (with six technical replicates each). **D:** Optical density of the strains indicated in (**Fig. 1B**) at time point 20 hours. **E:** Attachment of *P. aeruginosa* wild type (WT) and a Δ*hecR* Δ*hecE* deletion strain harboring an empty control plasmid (EV) or a plasmid with *hecR*, *hecE* or *hecRE* expressed from an IPTG-inducible promoter. Strains were grown in LB for 10 hours before attachment was scored by staining with CV. Mean values of three biological replicates are shown.

2.1.4 The *hecRE* module regulates *P. aeruginosa* motility, cell aggregation, and phage sensitivity

Our findings that HecE influences *P. aeruginosa* morphotype and biofilm formation via c-di-GMP raised the question if other c-di-GMP-dependent behavioral processes are also controlled by the Hec proteins. This includes different forms of motility like swimming in liquid media or swarming and twitching on surfaces (Fazli *et al.*, 2014; Kazmierczak *et al.*, 2015; Malone, 2015). Intriguingly, swarming motility was increased in the Δ*hecR*, Δ*hecE* and Δ*hecRE* mutants, but strongly inhibited when *hecR, hecE* or *hecRE* were expressed from a plasmid (**Fig. 2A**). In contrast, swimming motility was unaltered in *hecR or hecE* deletion strains, but was markedly reduced upon ectopic expression of *hecE* and *hecRE*, but not of *hecR* alone (**Fig. 2B**). Finally, twitching was unaltered in *hec* deletion strains **(Fig. S2A)**, but overexpression of *hecE*

or *hecRE* from a plasmid inhibited twitching motility and led to increased crystal violet (CV) staining inside the twitching zone **(Fig. 2C)**. Expression of *hecR* from a plasmid left the twitching zone unchanged, but led to CV staining inside the twitching zone, indicating an increased tendency of twitching cells to adhere to the plastic surface (**Fig. 2C**). This *hecR*-mediated effect was dependent on the presence of a chromosomal copy of *hecE* **(Fig. 2C)** again emphasizing that HecE and not HecR is the primary effector of this response. Together these experiments demonstrated that HecR and HecE are able to tune *P. aeruginosa* motility behavior and that swarming may represent a particularly sensitive readout for HecE function.

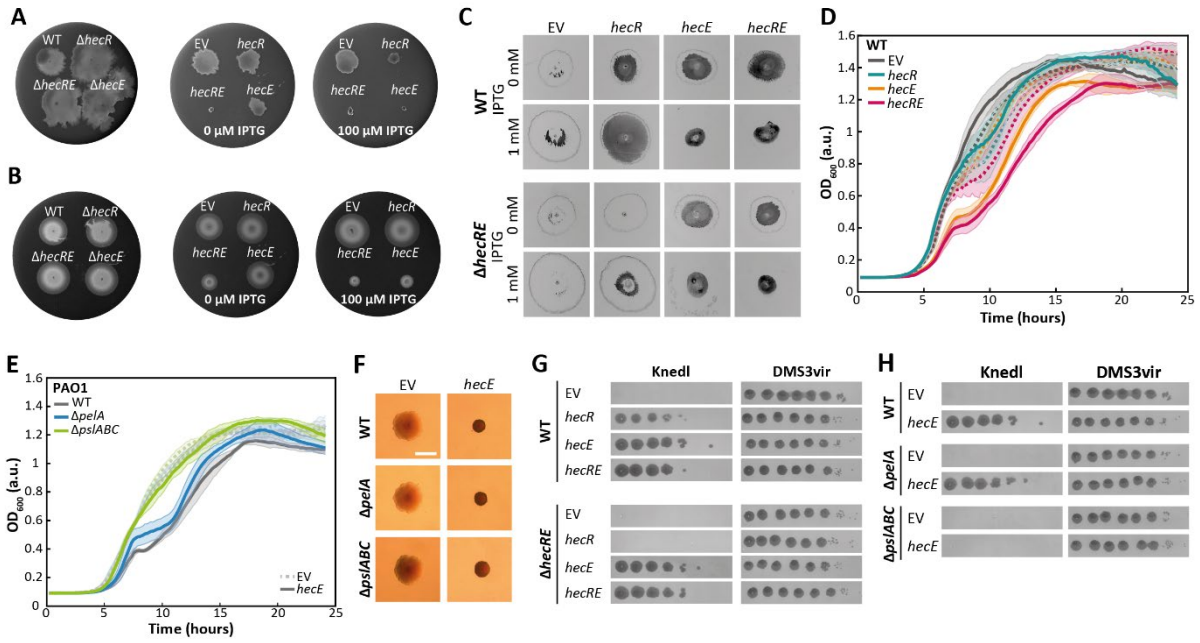

Figure 2: The *hecRE* module regulates *P. aeruginosa* motility, cell aggregation, and phage sensitivity.
A: The *hec* module controls swarming motility. Swarming motility of *P. aeruginosa* wild type (WT), *hec* deletion mutants and strains expressing *hec* genes from an arabinose-inducible promoter. Experiments were done in two biological replicates with one representative image being shown. **B:** Ectopic expression of the *hec* genes inhibits swimming motility. Swimming motility of *P. aeruginosa* wild type, *hec* deletion mutants and strains expressing *hec* genes from an arabinose-inducible promoter. Experiments were done in two biological replicates with one representative image being shown. **C:** HecE expression inhibits twitching motility. Twitching motility of *P. aeruginosa* wild type and a Δ*hecR* Δ*hecE* mutant expressing *hec* genes from an IPTG-inducible promoter. Experiments were done in triplicates with one representative image being shown. **D:** Ectopic expression of the *hec* genes impacts growth. Growth of *P. aeruginosa* wild type containing empty plasmid (EV) or plasmids with *hec* genes expressed form an IPTG-inducible promoter. Growth in LB (dashed lines) or in LB supplemented with 100 µM IPTG (solid lines) was recorded and mean values and standard deviations of three biological replicates (with three technical replicates each) are shown. **E:** The HecE-mediated growth phenotype is Psl dependent. Growth of *P. aeruginosa* wild type (WT) and mutant strains expressing *hecE* from an IPTG-inducible promoter in LB supplemented with 100 µM IPTG. Mean values and standard deviations of three biological replicates (with three technical replicates each) are shown. **F:** HecE stimulates Pel and Psl production. Colony morphology of *P. aeruginosa* wild type and exopolysaccharide mutants expressing *hecE* from a plasmid. Strains were grown on LB plates containing Congo Red, Coomassie Brilliant Blue and 100 µM IPTG. Experiments were done in triplicates; one representative image is shown. **G:** Infection of *P. aeruginosa* by phage KnedI requires *hecE* expression. Ten-fold dilutions of phage stocks (KnedI and DMS3vir) were spotted on LB top agar supplemented with 100 µM IPTG containing indicated seed cultures of the *P. aeruginosa* strains and expressing the *hec* genes from an IPTG-inducible promoter. Experiments were done in triplicates; one representative image is shown. **H:** Infection of *P. aeruginosa* by phage KnedI requires Psl. Experiments were carried out as indicated in **(G)**.

In line with the observed kink in the growth curve of the *hecR*::Tn mutant (**Fig. 1B**), expression of *hecR*, *hecE* or both genes from an IPTG-inducible promoter also led to a temporary reduction in the increase of optical density (OD) during growth in liquid media (**Fig. 2D**). While this effect was observed only when cultures had reached a relatively high optical density in strains expressing *hecR,* expression of *hecE* or both *hecRE* from an IPTG-inducible promoter caused a prolonged lag phase and a strong nick already at a relatively low OD. Also, while ectopic expression of *hecR* affected growth only if a functional copy of *hecE* was present on the chromosome, the phenotype caused by *hecE* expression was not dependent on chromosomal copies of *hecR* or *hecE*. (**Fig. 2D, 2SB**). The observation that the characteristic nicks in the growth curves were abolished if *hecE* was expressed in a mutant unable to secrete the exopolysaccharide Psl (Δ*pslABC*) (**Fig. 2F**) indicated that this phenomenon is likely due to Psl-mediated cell aggregation during growth *(Borlee et al., 2010; Hickman et al., 2005; Irie et al*., 2012). In contrast, ectopic expression of *hecE* induced an SCV morphotype in mutants either lacking Pel (Δ*pelA*) or Psl (Δ*pslABC*), indicating that the HecE pathway upregulates both exopolysaccharides. Together, this indicated that expression of *hecE* in growing cells leads to HecE-mediated upregulation of c-di-GMP and in turn, ectopically stimulates the production of Pel and Psl exopolysaccharides.

Bacterial surface glycans like Pel and Psl can be exploited by bacteriophages as primary receptors (Bertozzi Silva *et al*., 2016). To investigate if HecE is able to sensitize *P. aeruginosa* for phage attack, we screened sewage water samples for phage predators that infect the pathogen in a HecE-dependent manner. This led to the isolation of a new phage called Knedl that infects growing cells of *P. aeruginosa* only when *hecE, hecR* or both genes are ectopically expressed (**Fig. 2G**). While *hecE* was able to sensitize *P. aeruginosa* for Knedl infection irrespective of the chromosomal context, *hecR*-mediated Knedl sensitivity strictly depended on the presence of a functional chromosomal copy of *hecE* (**Fig. 2G**). Importantly, HecE-mediated phage sensitivity was abolished in the Δ*pslABC* mutant, but not in the Δ*pelA* mutant (**Fig. 2H**), arguing that Psl serves as primary receptor for phage Knedl. Based on this and the observations that HecE boosts Psl-dependent cell aggregation and that Psl biogenesis itself depends on c-di-GMP (Hickman and Harwood, 2009; Irie *et al*., 2012), we concluded that phage *Knedl* exploits Psl as primary surface receptor and that HecE activity sensitizes *P. aeruginosa* for phage infection by stimulating Psl biogenesis through a boost of c-di-GMP.

Altogether, these findings strongly indicated that the primary function of HecE activity is to increase the concentration of c-di-GMP in *P. aeruginosa* leading to reduced motility and increased production of both Pel and Psl exopolysaccharides and subsequently SCV formation, cell aggregation, and phage sensitivity.

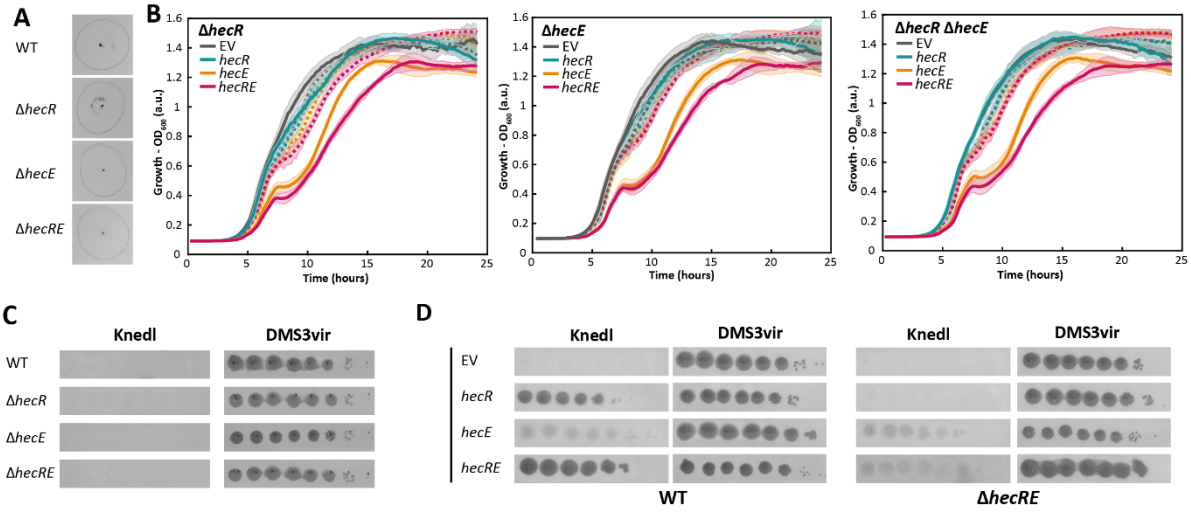

Supplementary Figure 2: The *hecRE* module regulates *P. aeruginosa* motility, cell aggregation, and phage sensitivity.
A: Deletion of *hec* genes does not affect twitching motility. Twitching motility of *P. aeruginosa* wild type (WT) and mutant strains. Twitching experiments were done in triplicates; one representative image is shown. **B:** Growth of *P. aeruginosa* Δ*hecR*, Δ*hecE* or Δ*hecR* Δ*hecE* mutants containing an empty plasmid (EV) or plasmids with *hec* genes expressed from an IPTG-inducible promoter. Growth in LB (dashed lines) or in LB supplemented with 100 µM IPTG (solid lines) was recorded and mean values and standard deviations of three biological replicates (with three technical replicates each) are shown. **C, D:** Infection of *P. aeruginosa* wild type (WT) and different *hec* deletion mutants (**C**) harboring an empty plasmid (EV) or plasmids expressing *hec* genes from an IPTG-inducible promoter (**D**) with phage KnedI or control phage DSM3vir as indicated in **Fig. 2G**. Experiments were done in triplicates; one representative image is shown.

2.1.5 HecE modulates c-di-GMP levels by directy inhibiting the phosphodiesterase BifA

While the above experiments indicated that *hecE* expression boosts c-di-GMP levels, the mechanism(s) responsible for the HecE-mediated activity remained unclear. Homology-modelling of HecE with AlphaFold (Senior *et al.*, 2020) revealed alpha-helical features, but given the large distances between individual helices the predicted structure does not seem to be realistic (**Fig. S3A**). This and the fact that HecE lacks structural motifs or domains known to regulate c-di-GMP (GGDEF, EAL or HD-GYP) or to alter the expression of c-di-GMP related proteins, prompted us to speculate that HecE regulates c-di-GMP indirectly, by interacting with one or several c-di-GMP modulating partners. To identify candidate interactors of HecE, we used HecE as prey to screen a library of *P. aeruginosa* PAO1 clones in a yeast-two-hybrid (Y2H) assay. This revealed 13 possible interaction partners, four of which showed high confidence scores (**Supp. Table 2**). High confidence hits included PA1243, a sensor histidine

kinase involved in *P. aeruginosa* stress response (Aspedon *et al*., 2006; Wood and Ohman 2012) and biofilm formation (Müsken *et al*., 2010); PA5246 a conserved hypothetical protein, containing a thioesterase domain *(Dötsch et al*., 2009); AlkB2 (PA1525), a membrane bound alkane hydroxylase (Marín *et al*., 2003) regulating elastic film formation at oil-water interfaces (Niepa *et al*., 2017); and BifA (PA4367), a membrane bound c-di-GMP specific phosphodiesterase involved in biofilm formation and swarming motility (Kuchma *et al*., 2007).

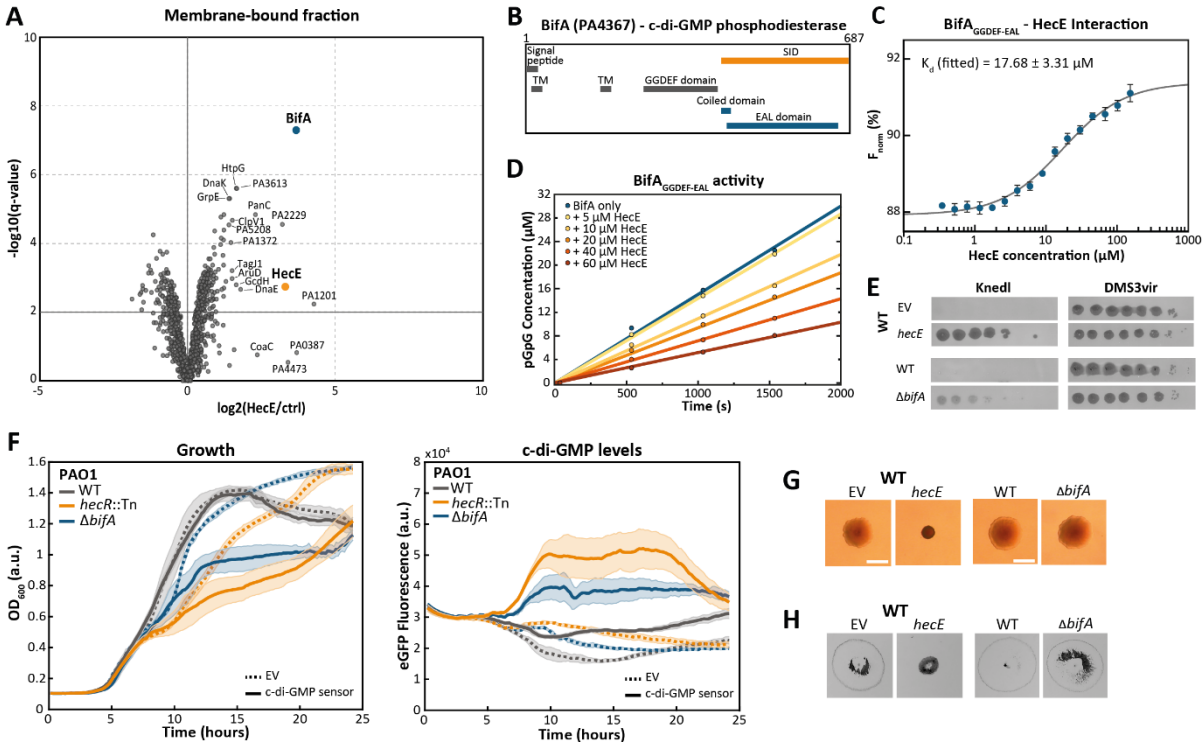

<u>Figure 3:</u> HecE modulates c-di-GMP via inhibition of the phosphodiesterase BifA.
A: CoIP-MS analysis of HecE. Immunoprecipitation experiments were performed using the PAO1 wild type strain or a strain expressing C-terminally FLAG-tagged HecE and anti-M2 antibody-conjugated magnetic beads. Proteins retained on the beads were analyzed using mass spectrometry. Data obtained from three biological replicates are shown as volcano plots. Log2-intensity ratios of detected peptides between HecE-Flag and wild type (ctrl) were calculated and plotted versus values derived from significance analysis (modified t-statistic, empirical Bayes method, Smyth, 2004). Strains were grown in LB to an optical density of 1.5. **B:** Schematic of the BifA domain structure and the BifA fragment identified by Y2H to specifically interact with HecE. **C:** HecE interacts with BifA *in vitro*. Microscale thermophoresis with the purified GGDEF-EAL domain fragment of BifA and HecE. Purified BifA was labelled with RED-tris-NTA dye and used for HecE titration experiments. **D:** HecE inhibits BifA phosphodiesterase activity *in vitro*. Purified BifA (GGDEF-EAL) and increasing amounts of HecE were incubated with c-di-GMP and enzyme turnover was measured over time using online ion exchange chromatography to record the formation of the enzymatic product, pGpG. **E:** BifA protects *P. aeruginosa* against phage infections. Ten-fold dilution series of phage KnedI were applied on LB top agar containing *P. aeruginosa* wild type (WT) or Δ*bifA* mutant strains as indicated. WT containing an empty plasmid (EV) or a plasmid expressing *hecE* from an IPTG-inducible promoter was used as control. Experiments were done in triplicates; one representative image is shown. **F**: A *P. aeruginosa* mutant lacking BifA phenocopies ectopic expression of *hecE*. Growth (left) and fluorescence (c-di-GMP levels, right) of *P. aeruginosa* wild type (WT), *hecR*::Tn and Δ*bifA* strains carrying an empty plasmid (EV) or a plasmid copy of the BldD-eGFP c-di-GMP sensor. Mean values and standard deviations of two biological replicates (with six technical replicates each) are shown. **G**: A Δ*bifA* mutant does not adopt SCV morphotype on Congo Red plates. Colony morphology of a Δ*bifA* mutant and wild type (WT) with ectopic expression of *hecE* are shown. Strains were grown on LB plates containing Congo Red, Coomassie Brilliant Blue and 1mM IPTG. Experiments were done in triplicates; one representative image is shown. **H:** A Δ*bifA* mutant shows unaltered twitching motility. Experiments were done in triplicates; one representative image is shown.

Because BifA provided a direct link to c-di-GMP and because co-immunoprecipitation experiments with epitope-tagged HecE also identified BifA as the main hit in membrane fractions of *P. aeruginosa* (**Fig. 3A**), we focused our analyses on this protein. The Y2H analysis indicated that HecE interacts with the EAL domain of BifA (**Fig. 3B**). This was confirmed by microscale thermophoresis using purified HecE and a soluble part of BifA containing the GGDEF and EAL domains (**Fig. 3C**). Moreover, phosphodiesterase activity assays with the purified GGDEF and EAL domain of BifA and with purified HecE, demonstrated that the BifA phosphodiesterase was inhibited by HecE in a concentration dependent manner (**Fig. 3D**). From this, we concluded that HecE increases c-di-GMP levels *in vivo* by interfering with the activity of the BifA phosphodiesterase. In line with BifA being a target of HecE, a *ΔbifA* mutant was sensitive to phage Knedl, indicating that its inactivation increases the overall level of c-di-GMP (**Fig. 3E**). This was confirmed when assaying c-di-GMP levels directly in *P. aeruginosa* wild type and the Δ*bifA* mutant (**Fig. 3F**). However, both phage sensitivity and the c-di-GMP concentration were lower in the Δ*bifA* mutant as compared to a strain expressing *hecE* from a plasmid (**Fig. 3E, F**). Also, deleting *bifA* failed to induce the SCV morphotype (**Fig. 3G**) and inhibit twitching motility (**Fig. 3H**). Thus, although HecE directly inhibits BifA activity, this interaction alone cannot explain the strong *in vivo* phenotypes observed when *hecE* is ectopically expressed in *P. aeruginosa*.

This raised the possibility that HecE may target additional phosphodiesterases. Using the Washington transposon library, we identified insertions in two additional phosphodiesterase genes, *pch,* and *rbdA*, that showed similar effects like a *bifA* mutant or a strain expressing *hecE* when grown in liquid. Notably, deleting *bifA*, *pch* and *rbdA* in the same strain showed strong additive effects on optical density (**Fig. S3C**), phage sensitivity (**Fig. S3D**) and twitching motility (**Fig. S3E**). However, none of the double or triple mutants generated the strong SCV phenotype that was observed when *hecE* was expressed ectopically (**Fig. 3G, Fig S3F**). From this, we concluded that although Pch and RbdA contribute to keeping c-di-GMP concentrations low during exponential growth in complex media, both enzymes are unlikely to be targets of HecE-mediated control.

Together, this demonstrated that HecE interferes with the cellular c-di-GMP pool by specifically inhibiting the phosphodiesterase BifA. These findings also implied that HecE targets additional components of the c-di-GMP network to mediate its strong *in vivo* response.

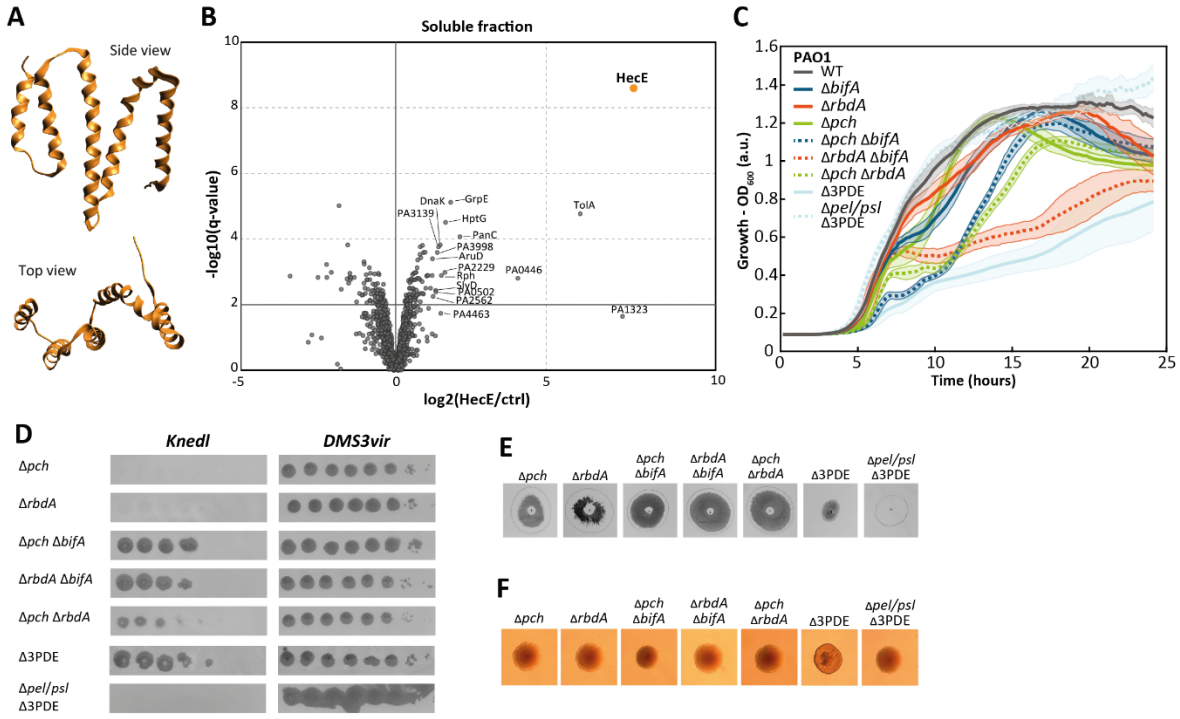

Supplementary Figure 3: HecE modulates c-di-GMP levels via inhibition of the phosphodiesterase BifA.
A: Structure of HecE as predicted by homology-modelling using AlphaFold (Senior *et al.*, 2020). **B:** CoIP-MS analysis of HecE. Immunoprecipitation experiments were performed using the PAO1 wild type strain or a strain expressing C-terminally FLAG-tagged HecE and anti-Flag antibody-conjugated magnetic beads. Proteins retained on the beads were analyzed using mass spectrometry. Data obtained from three biological replicates are shown as volcano plots. Log2-intensity ratios of detected peptides between HecE-Flag and wild type (ctrl) were calculated and plotted versus values derived from significance analysis (modified t-statistic, empirical Bayes method, Smyth, 2004). Strains were grown in LB to an optical density of 1.5. **C:** Growth of *P. aeruginosa* wild type and phosphodiesterase mutant strains. Strains harboring single, double or triple deletions (Δ3PDE) of *bifA*, *rbdA,* and *pch* genes were assayed. Mean values and standard deviations of three biological replicates (with three technical replicates each) are shown. **D:** A gradual loss of phosphodiesterases sensitizes *P. aeruginosa* for phage infection. Ten-fold dilution series of phage KnedI or DMS3vir were applied on LB top agar containing *P. aeruginosa* mutant strains harboring deletions in phosphodiesterase genes as indicated. Experiments were done in triplicates; one representative image is shown. **E:** A gradual loss of phosphodiesterases impacts twitching motility. Mutants with deletions in phosphodiesterase genes are indicated. Experiments were done in triplicates; one representative image is shown. **F:** A gradual loss of phosphodiesterases results in a moderate SCV morphotype. Indicated mutant strains were grown on LB plates containing Congo Red and Coomassie Brilliant Blue. Experiments were done in triplicates; one representative image is shown.

2.1.6 HecE controls c-di-GMP levels by activating the diguanylate cyclase WspR

To identify additional components of the c-di-GMP network that are regulated by HecE, we carried out a genetic screen with the Mariner transposon to identify suppressors of HecE-induced SCVs that regained their smooth morphotype. A total of 51 smooth suppressors were isolated and mapped to 38 individual genes (**Supp. Table 3**). While this identified several hits in genes encoding transcription factors and components of Cup fimbrae or type IV pili, the most frequent hits mapped to genes encoding components of the Wsp chemosensory system. Intriguingly, the Wsp system is a chemotaxis-like sensory system that culminates in the phosphorylation and activation of the diguanylate cyclase WspR (**Fig. 4A**) (Hickman *et al.*,

2005). To test if HecE interferes with WspR activity, we used Phos-tag gel electrophoresis to assay WspR phosphorylation state in strains ectopically expressing *hecE*. As shown in **Fig. 4B**, induction of *hecE* expression in *P. aeruginosa* wild type or Δ*hecRE* mutant significantly increased the phosphorylation of WspR, similar to a Δ*wspF* control strain that lacks the central negative regulator of the Wsp system, WspF. These data suggest that HecE boosts c-di-GMP levels by activating the Wsp system.

To corroborate these findings, we next tested if deleting *wspR* would abolish the HecE-mediated phenotypes. Indeed, deleting *wspR* in a strain expressing *hecE* completely abolished cell aggregation, while deleting two other cyclase genes, *sadC* or *yfiN*, showed no effect (**Fig. 4C**). Thus, HecE-mediated cell aggregation requires WspR activity. The observation that the cell aggregation phenotype observed in mutants lacking phosphodiesterases BifA or RbdA is not reversed when deleting *wspR* (**Fig. 4D**), indicated that WspR is not active in growing *P. aeruginosa* cells, unless it is stimulated by HecR.

Deleting *wspR* also abolished the HecE-mediated SCV morphotype (**Fig. 4E**), HecE-mediated inhibition of twitching motility (**Fig. 4F**) as well as HecE-mediated sensitivity to phage Knedl (**Fig. 4G**). Of note, *hecE* expression altered twitching motility even in absence of WspR (**Fig. 4F**). While the overall twitching diameter was restored in the Δ*wspR* mutant, increased cellular biomass stained by crystal violet was observed inside the twitching zone, similar to the Δ*bifA* mutant (**Fig. 3H**). Thus, HecE likely influences twitching motility by interfering with BifA and with WspR activity.

The above findings indicated that HecE-mediated cell aggregation, SCV formation and phage susceptibility depend primarily on stimulation of WspR, while its effect on twitching motility appears to be a combination of WspR stimulation and BifA inhibition. Because we have shown above that ectopic expression of *hecE* boosts surface colonization at early stages of biofilm formation (**Fig. 1F**) and that deleting *hecE* leads to increased biofilm dispersal at later stages (**Fig. 1D**), we wanted to clarify if these effects are mediated via BifA or WspR. Intriguingly, deleting *bifA* in a strain lacking HecR and HecE restored biofilms at late stages and abolished the HecE-mediated differences observed in a wild type background (**Fig. 4H, I**). This effect was not dependent on WspR, arguing that WspR does not play a major role in biofilm maintenance (**Fig. 4H, I**).

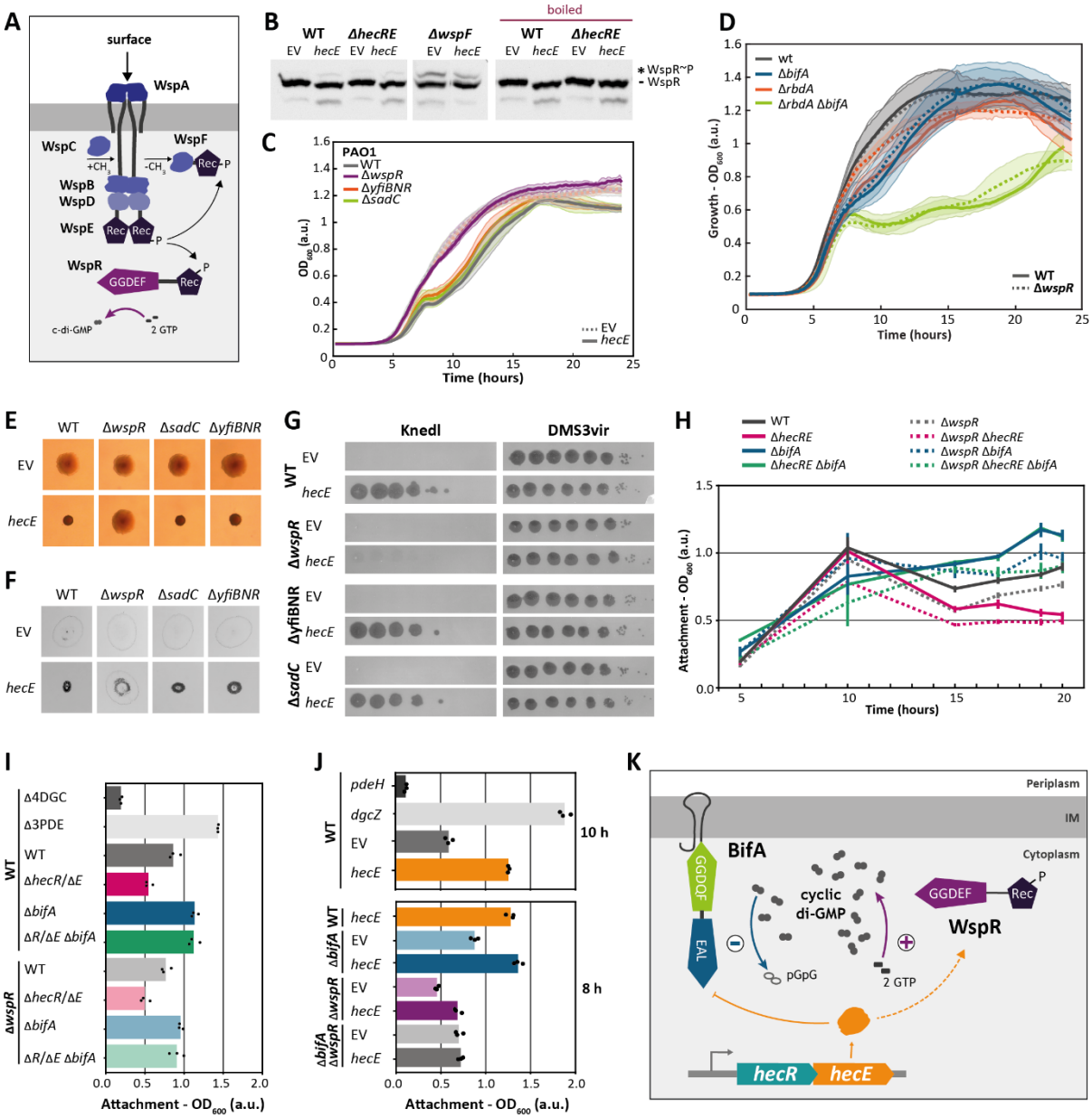

Figure 4: HecE boosts c-di-GMP levels by stimulating the Wsp chemosensory system.

A: Schematic of the Wsp chemosensory system. **B**: Expression of *hecE* leads to increased phosphorylation of WspR *in vivo*. Phos-Tag SDS-PAGE showing WspR-FLAG phosphorylation in wild type (WT) or the Δ*hecR* Δ*hecE* mutant strain carrying a control plasmid (EV) or a plasmid expressing *hecE* from an arabinose-inducible promoter. A Δ*wspF* strain was used as positive control for WspR phosphorylation. Strains were grown on LB plates supplemented with 0.5% arabinose and incubated at 37°C for 6 hours. Samples were scraped from plates, and boiled samples were heated to 95°C for 10 minutes. **C**: Deletion of *wspR*, but not other diguanylate cyclase genes, restores normal growth of strains expressing *hecE*. *P. aeruginosa* wild type (WT) and diguanylate cyclase deletion mutants harboring an empty control plasmid (EV) (dashed lines) or a plasmid with an IPTG-inducible copy of hecE (solid lines) were grown in LB supplemented with 100 µM IPTG as indicated. Mean values and standard deviations of three biological replicates (with three technical replicate) are shown. **D:** Deletion of *wspR* does not restore normal growth of phosphodiesterase deletion mutants. Growth of *P. aeruginosa* wild type and of the indicated phosphodiesterase deletion strains was scored in LB (solid lines) and compared to isogenic strains harboring a deletion in *wspR* (Δ*wspR*). Mean values and standard deviations of two biological replicates (with three technical replicates) are shown. **E:** Deletion of *wspR* restores the smooth colony morphotype of a HecE-mediated SCV. *P. aeruginosa* wild type (WT) and diguanylate cyclase deletion mutants harboring an empty control plasmid (EV) or a plasmid with an IPTG-inducible copy of *hecE* were grown on LB plates containing Congo Red, Coomassie Brilliant Blue and 1 mM IPTG. Experiments were done in triplicates; one representative image is shown. **F:** Deletion of *wspR* restores twitching motility of a strain expressing *hecE*. Strains are as indicated in **(E)** and twitching experiments were carried out as described in **Fig. 2C**. Experiments were done in triplicates; one representative image is shown. **G:** HecE-mediated phage sensitivity depends on WspR. Ten-fold dilutions of phages KnedI or DMS3vir were applied in LB top agar containing 100 µM IPTG and the *P. aeruginosa* strains indicated. Strains contained either an empty control plasmid (EV) or a plasmid expressing *hecE* from an IPTG-inducible promoter. Experiments

were done in triplicates; one representative image is shown. **H, I**: HecE-mediated biofilm maturation requires BifA, but not WspR. *P. aeruginosa* wild type and indicated mutant strains were grown in LB and attachment was determined at indicated times (**H**) and 20 hours (**I**) after inoculation (see Supplementary Figure **1B**). The Δ3PDE strains lacks the phosphodiesterase genes *bifA*, *pch* and *rbdA*, the Δ4DGC strain lacks the diguanylate cyclases *sadC*, *dgcH*, *PA0338* and *PA0847*. Attachment was quantified by crystal violet (CV) staining and mean values and standard deviations of three biological replicates (with six technical replicates each) are shown. **J**: HecE-mediated early biofilm formation requires WspR, but not BifA. Microtiter plate-based attachment assay of Δ*wspR* and Δ*bifA* deletion strains expressing *hecE* from an IPTG inducible promoter in LB supplemented with 100 µM IPTG was scored after 8 or 10 hours. The mean ± standard deviation of one biological replicate, with three technical replicates is shown. **K**: Model of HecE-mediated c-di-GMP control. HecE directly interacts with BifA to inhibit its phosphodiesterase activity (solid line) and stimulates WspR activity by modifying its phosphorylation state (stippled orange line).

These observation align with the role described for BifA in *P. aeruginosa* biofilm formation and dispersal (Andersen *et al*., 2021; Kuchma *et al*., 2007) and argue that HecE plays an important role in biofilm maintenance by restricting BifA activity in mature biofilms. In contrast, the boost in biofilm formation observed upon ectopic expression of *hecE* (**Fig. 1F**) appears to be mediated primarily by its stimulatory effect on WspR (**Fig. 4J**).

Taken together, these findings demonstrated that HecE tunes c-di-GMP levels in *P. aeruginosa* by targeting the activities of both the phosphodiesterase BifA and the diguanylate cyclase WspR. We propose that simultaneous BifA inhibition and WspR activation by HecE leads to a robust increase of c-di-GMP and to subsequent changes in *P. aeruginosa* behavior including motility, cell aggregation as well as biofilm formation (**Fig. 4K**).

2.1.7 Transcription of the *hecRE* module is autoregulated by the transcription factor HecR

The above findings identified HecE as an important cellular effector modulating c-di-GMP levels but left it open how *hecE* expression is regulated. To investigate the role of HecR in *hecE* expression we grafted Flag-tagged copies of the *hec* genes into the *P. aeruginosa* chromosome. This revealed that HecR and HecE levels increased upon ectopic expression of *hecR*, indicating that HecR stimulates *hec* gene expression. In contrast, ectopic expression of *hecE* did not alter HecE or HecR levels (**Fig. 5A**). Thus, *hecR* and *hecE* are co-regulated with HecR imposing positive feedback on *hecE* expression. In line with this, electromobility shift assays with purified HecR demonstrated that HecR directly binds to the *hecR* promoter region (**Fig. 5B**). Chromatin immunoprecipitation (ChIP-Seq) experiments with epitope-tagged HecR confirmed this and revealed the *hecRE* locus as the only region on the *P. aeruginosa* chromosome binding HecR. Two prominent HecR binding sites were detected, one in the *hec* promoter region and the other spanning the entire *hecE* gene (**Fig. 5C**). While binding of HecR

to the promoter likely contributes to transcription control of the module, the significance of the observed HecR binding to the *hecE* coding region remains unclear. These findings confirm that HecR is a highly specific transcription factor controlling expression of *hecE*.

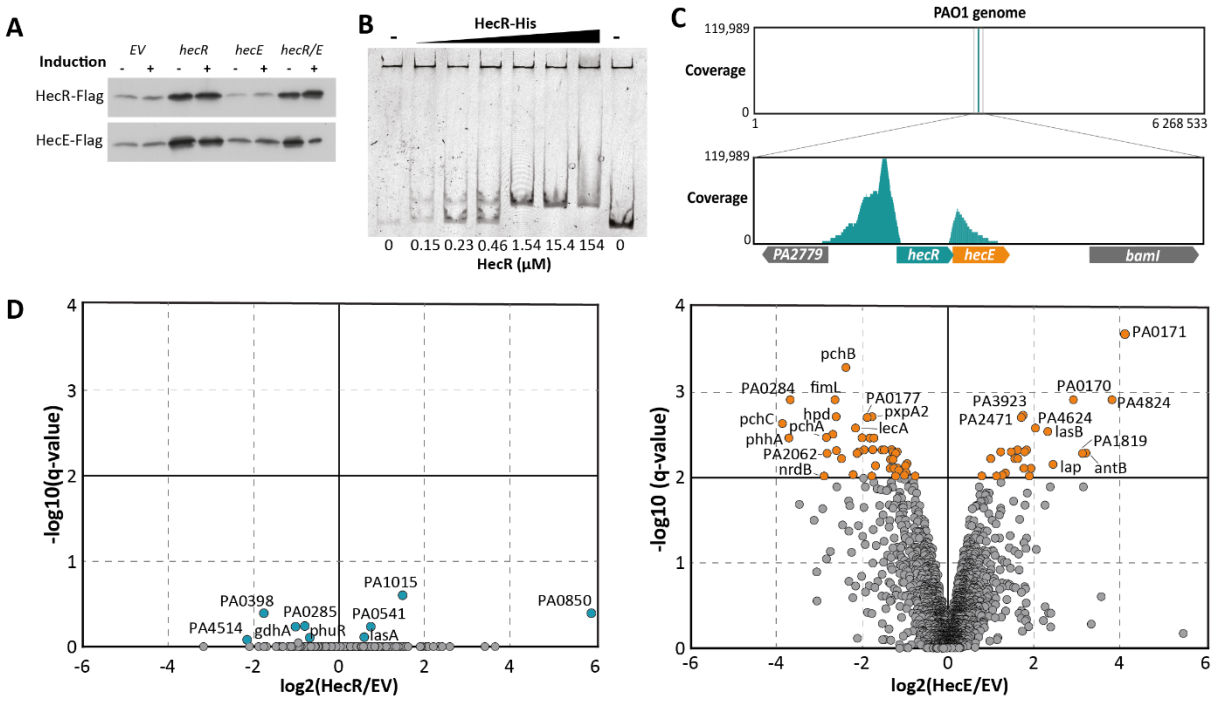

Figure 5: HecR binds to the *hecRE* promoter region and stimulates expression of *hecR* and *hecE*.
A: Expression of *hecR in trans* boosts cellular levels of HecR and HecE. Strains expressing Flag-tagged chromosomal copies of *hecR* or *hecE* under their natural promoters and containing either an empty control plasmid (EV) or a plasmid expressing *hecR*, *hecE* or both genes from an arabinose-inducible promoter were used. Cells were grown in the presence (+) or absence (-) of the inducer and extracts analyzed by immunoblots with an anti-Flag antibody. **B:** HecR binds to the *hecR* promoter region *in vitro*. EMSA assays were carried out with a Cy3-labelled DNA fragment containing the *hecRE* promoter region and with purified HecR-His. **C:** HecR binds to the chromosomal *hecR-hecE* locus *in vivo*. ChIP-seq experiments were performed with a strain expressing a HA-tagged copy of *hecR* from an IPTG-inducible promoter on a plasmid. Cells were grown in MOPS minimal medium containing 20 mM succinate to an optical density of 1.0 (exponential) or for 16 hours (stationary). Antibodies against the HA-tag were used for chromatin pull-down. Sequencing reads mapped to the *hec* locus are plotted on the y-axis. One representative example of a sample from exponential phase is shown. **D:** Volcano plots of *P. aeruginosa* proteins with altered abundance upon *hecR* or *hecE* expression. Log2-intensity ratios of detected peptides between Δ*hecRE* strain expressing *hecR* (left) or *hecE* (right) from an ITPG-inducible plasmid compared to the plasmid control (EV) were calculated and plotted versus values derived from significance analysis (modified t-statistic, empirical Bayes method, Smyth, 2004). Strains were grown in LB containing 100 µM IPTG for 20 hours.

This was confirmed when analyzing the proteome of a Δ*hecR* Δ*hecE* mutant expressing either *hecR* or *hecE* ectopically from a plasmid. While the overall proteome profile was virtually unchanged upon *hecR* expression, expression of *hecE* resulted in up- or downregulation of a considerable fraction of proteins **(Fig. 5D)**. Proteins experiencing strong HecE-mediated changes include PA0170, PA0171, and FimL, proteins involved in detergent-induced auto-aggregation (Klebensberger *et al*. 2009) and twitching motility (Inclan *et al*., 2011; Shan *et al*., 2004) or several virulence factors like the elastase LasB (Thayer *et al*., 1991),

the lectin LecA (Bajolet-Laudinat *et al*., 1994), Pch proteins involved in the biogenesis of the siderophore pyochelin (Serino *et al*. 1997), a novel surface receptor that binds to host laminin (PA3923) (Paulsson *et al*., 2019) or the anthranilate dioxygenase AntB, which is involved in the degradation of the *Pseudomonas* quinolone quorum signal (PQS) (Choi *et al*., 2011). We presume that these changes in protein expression result from the observed HecE-mediated increase in c-di-GMP.

Taken together, the transcription factor HecR exclusively regulates the *hec* genes establishing an autoregulatory feedback, which leads to HecE upregulation and an increase of c-di-GMP levels.

2.1.8 Expression of *hecE* is bimodal and growth phase dependent

Autoregulatory feedback loops can stabilize stochastic processes like transcription, thereby generating phenotypic heterogeneity in bacterial populations (Mcadams and Arkin, 1997). To test if HecR-mediated autoregulation causes cell-to-cell variations of *hecE* expression, we designed a transcriptional reporter suitable for single cell analysis. Two codon-optimized *mRuby2* reporter genes with synthetic ribosome binding sites were inserted between the stop codon of *hecE* and the transcriptional terminator of the module, therefore providing a readout for *hecE* expression (**Fig. 6A**) (in short: *hecRE-2mR*). In line with the observed increase of cellular HecR and HecE levels in stationary phase (**Fig. 6B**), *hecE* transcription was low during exponential phase but increased when cells entered stationary phase (**Fig. 6C, 4SA**). Ectopic expression of *hecR*, but not of *hecE*, from a plasmid increased transcription of the chromosomal *hecRE* reporter (**Fig. 6C, 4SA**). Of note, under these conditions, *hecRE* reporter expression set off at the same optical density where the aggregation-mediated nick was observed in the growth curves. Single cell analysis revealed that *hecE* is expressed only in a small subpopulation of cells in the stationary phase after growth in LB for 20 hours (**Fig. 6D**). This fraction of ON cells disappeared in a Δ*hecR* mutant, while a Δ*hecE* mutant retained heterogeneous reporter expression, although at a slightly lower level.

The above findings indicated that changes in *hecE* transcription and HecE protein concentration observed at the population level result from changing the fraction of ON cells as opposed to graded changes in *hec* promoter strength. In line with this, *hecRE-2mR* reporter

was uniformly expressed in all cells when *hecR* was ectopically expressed from an IPTG-inducible promoter.

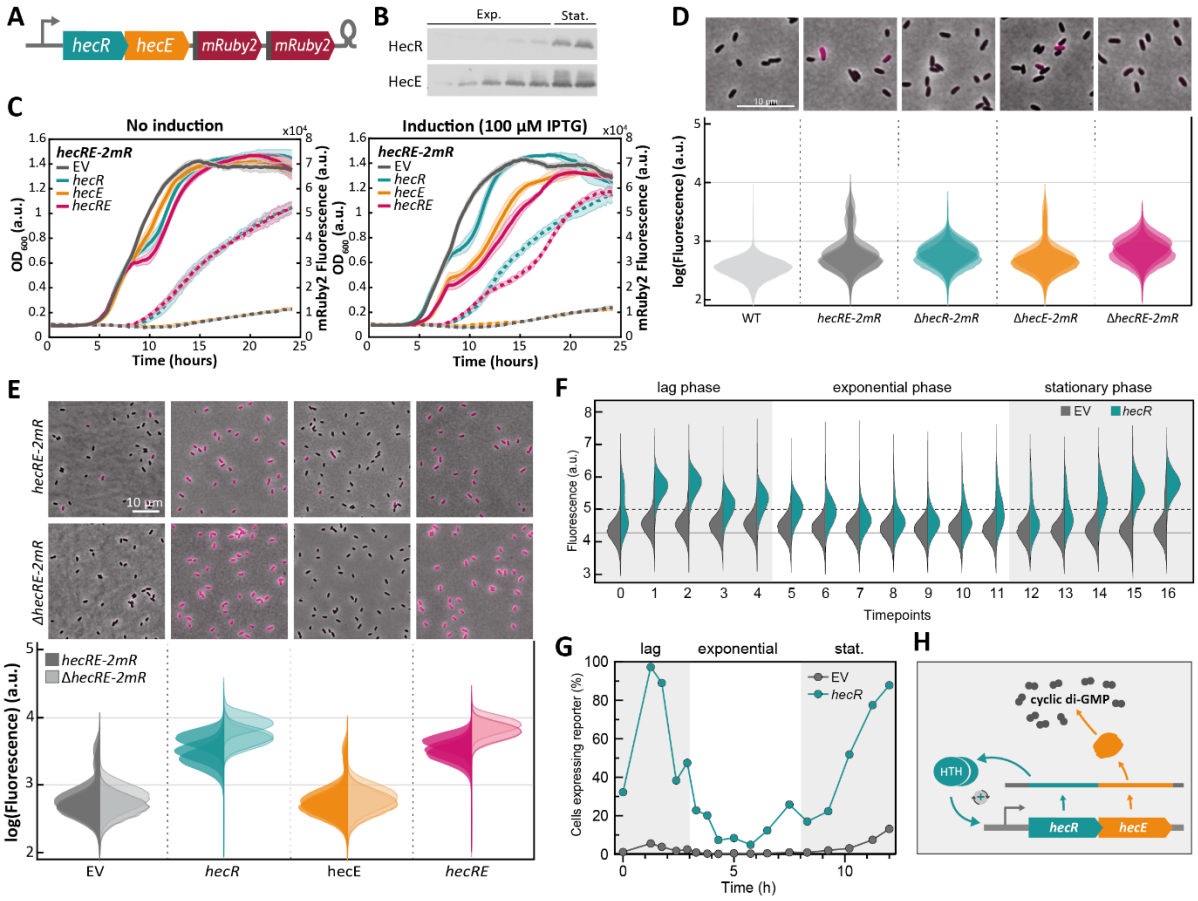

Figure 6: Expression of *hecE* is bimodal and changes during growth.
A: Schematic of the *hecRE-2mRuby2* transcriptional reporter used for these experiments. **B**: Protein levels of HecR and HecE are growth phase dependent. Strains expressing chromosomal Flag-tagged copies of *hecR* or *hecE* under their natural promoter were grown in LB. Extracts were analyzed by immunoblots with an anti-Flag antibody. **C:** Transcription of *hecE* increases in stationary phase. Growth (solid lines, left y-axis) and fluorescence (dashed line, right y-axis) of strains with an engineered fluorescent *mRuby2* reporter in the chromosomal *hec* locus (*hecRE-2mR*). Reporter strains contained an empty control plasmid (EV) or a plasmid carrying *hecR*, *hecE*, or both genes under the control of an IPTG-inducible promoter. LB media were supplemented with IPTG as indicated. Mean values and standard deviations of three biological replicates (with three technical replicates each) are shown. **D**: Transcription of *hecE* is bimodal. Microscopy and flow cytometry analysis of strains carrying the *hecRE-2mRuby2* reporter grown in LB supplemented with 100 µM IPTG for 20 hours. Microscopy experiments were done in triplicates; one representative image is shown. Flow cytometry experiments are shown for three biological replicates with the individual histograms stacked in the graph. For each sample, 100.000 events were recorded. **E:** Ectopic expression of *hecR* induces *hecE* transcription in a majority of cells. Microscopy and flow cytometry data of strains with an engineered fluorescent *mRuby2* reporter in the chromosomal *hec* locus (*hecRE-2mR*). Reporter strains contained an empty control plasmid (EV) or a plasmid carrying *hecR*, *hecE*, or both genes under the control of an IPTG-inducible promoter. Reporter strains were grown in LB supplemented with 100 µM IPTG for 20 hours. Microscopy experiments were done in triplicates; one representative image is shown. For flow cytometry, the histograms of the fluorescent intensities are overlaid for three biological replicates. For each sample, 100.000 events were recorded. **F, G:** The fraction of cells expressing *hecE* is strongly induced in stationary phase. The fractions of reporter ON cells of strains carrying an empty plasmid control (EV) or a plasmid expressing *hecR* from an IPTG-inducible promoter were determined by flow cytometry. The dotted line in (**F**) corresponds to the negative control strain without reporter and was used as threshold to distinguish between reporter ON and OFF cells. **H:** Autoregulation by HecR regulates *hecE* expression.

As expected, ectopic expression of *hecE* had no effect on the fraction of ON cells (**Fig. 6E**). Moreover, the gradual increase of *hec* gene expression observed during exponential growth

and upon entry into stationary phase (**Fig. 6A**) could be correlated to gradual changes of the fraction of ON in the population of *P. aeruginosa* cells (**Fig. 6F, G**). While *hecE* expression was OFF in growing *P. aeruginosa* wild type cells, up to 10% of the population showed *hecRE* reporter activity upon entry into stationary phase. Ectopic expression of *hecR* from a plasmid increased the fraction of ON cells in stationary phase to almost 100%. Surprisingly, the fraction of ON cells during the exponential growth phase remained low (**Fig. 6G**), indicating that additional factors control *hecE* expression and subsequently c-di-GMP levels (**Fig. 6H**) in growing cells, possibly at the post-transcriptional level.

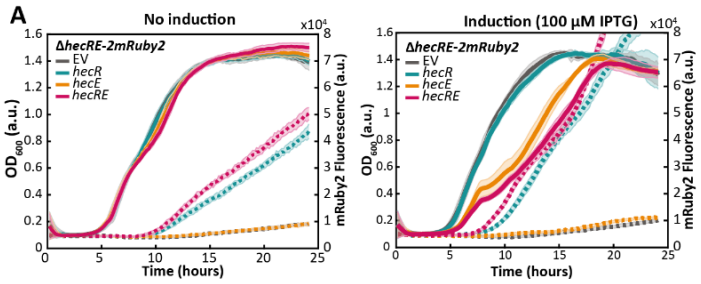

Supplementary Figure 4: Expression of *hecE* changes during growth.
A: Transcription of *hecE* increases in stationary phase. Growth (solid lines, left y-axis) and fluorescence (dashed line, right y-axis) of strains with an engineered fluorescent *mRuby2* reporter in the chromosomal *hec* locus of a Δ*hecR* Δ*hecE* mutant (Δ*hecRE-2mR*). Reporter strains contained an empty control plasmid (EV) or a plasmid carrying *hecR*, *hecE*, or both genes under the control of an IPTG-inducible promoter. LB media were supplemented with IPTG as indicated. Mean values and standard deviations of three biological replicates (with three technical replicates each) are shown.

2.1.9 Levels and frequency of *hecE* expression are regulated by the Gac/Rsm cascade

Previous reports had indicated that the *hec* module is regulated by the post-transcriptional regulator RsmA and its small RNA control units, RsmY and RsmZ (**Fig. 7A**) (Brencic and Lory, 2009). While RsmA binds to the untranslated 5' regions of specific mRNAs to block their access to the ribosome, RsmY and RsmZ compete for RsmA binding thereby sequestering RsmA away from mRNA (Francis *et al*., 2017). In addition, HecR was reported to engage in a feedback loop activating the transcription of *rsmZ* (Wang *et al*., 2014) **(Fig. 7A)**. To investigate the relevance of RsmA-mediated translation control of *hecE*, we first engineered transcriptional fusions of *mRuby2* to monitor *rsmY* and *rsmZ* expression. Both *rsmY* and *rsmZ* transcription increased in stationary phase, and their expression was reduced upon ectopic expression of *hecR* (**Fig. 7B**). Expressing *rsmY* or *rsmZ* from a plasmid stimulated the expression of the *hec* transcriptional reporter (**Fig. 7C**). Although the small RNAs control *hecRE* via RsmA on the post-transcriptional level, induction of the transcriptional *mRuby2* reporter likely results from elevated levels of the HecR transcription factor and its autoregulatory effect on *hecE* transcription (**Fig. 7A**). A strain with both *rsmY* and *rsmZ* deleted on the chromosome, but not single deletion strains, showed a slight reduction in *hecE* reporter activity in stationary phase **(Fig. S5A).**

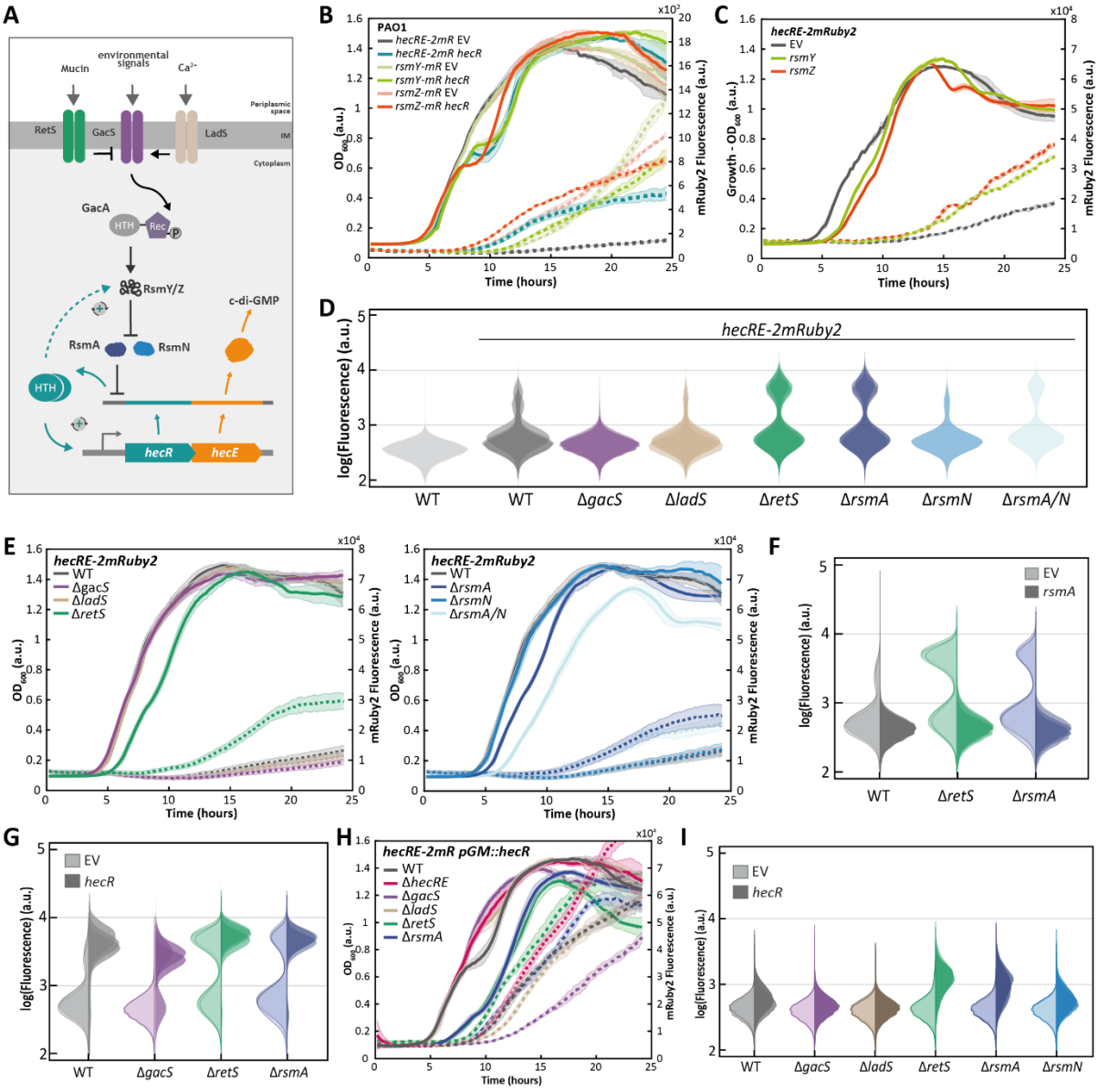

<u>Figure 7:</u> The global Gac/Rsm signaling cascade controls *hecE* expression.
A: Schematic of the Gac/Rsm cascade and its regulation of the *hecRE* module. **B**: Expression of *rsmY/Z* is repressed by HecR in stationary phase. Growth (solid lines, left y-axis) and fluorescence (dashed line, right y-axis) of *hecRE*, *rsmY* and *rsmZ* transcriptional promoter fusion strains. Reporter strains contained an empty control plasmid (EV) or a plasmid expressing *hecR* under the control of an IPTG-inducible promoter. LB media were supplemented with 100 µM IPTG. Mean values and standard deviations of one biological replicate (with three technical replicates) are shown. **C:** Expression of *hecE* is modulated by small RNAs. Growth (solid lines, left y-axis) and fluorescence (dashed line, right y-axis) of strains with an engineered fluorescent *mRuby2* reporter in the chromosomal *hec* locus (*hecRE-2mRuby2*) containing an empty control plasmid (EV) or plasmids expressing *rsmY* or *rsmZ* under the control of an IPTG-inducible promoter. LB media were supplemented with 100 µM IPTG. Mean values and standard deviations of three biological replicates (with three technical replicates each) are shown. **D:** The Gac/Rsm cascade controls frequency and intensity of *hecRE* expression. Flow cytometry analysis of strains with an engineered fluorescent *mRuby2* reporter in the chromosomal *hec* locus (*hecRE-2mRuby2*) in wild type (WT) and indicated mutants. Reporter strains were grown in LB for 20 hours. Flow cytometry experiments are shown for three biological replicates with the individual histograms stacked in the graph (for *rsmN* and *rsmA/N* mutants, one biological replicate is shown). For each sample, 100.000 events were recorded. **E:** The Gac/Rsm controls *hecRE* expression. Growth (solid lines, left y-axis) and fluorescence (dashed line, right y-axis) of strains with an engineered fluorescent *mRuby2* reporter in the chromosomal *hec* locus (*hecRE-2mRuby2*) in wild type (WT) and indicated mutants grown in LB. Mean values and standard deviations of three biological replicates (with six technical replicates each) are shown. **F:** *HecE* expression is repressed by RsmA. Flow cytometry analysis of strains with an engineered fluorescent *mRuby2* reporter in the chromosomal *hec* locus in wild type (WT) and indicated mutants. Reporter strains contained an empty control plasmid (EV) or a plasmid carrying *rsmA* under the control of an IPTG-inducible promoter and were grown in LB supplemented with 100 µM IPTG for 20 hours. Flow cytometry experiments are shown for three biological replicates with the individual histograms stacked in the graph. For each

sample, 100.000 events were recorded. **G:** Ectopic expression of *hecR* induces *hecE* transcription in Gac/Rsm mutants. Flow cytometry analysis of strains with an engineered fluorescent *mRuby2* reporter in the chromosomal *hec* locus in wild type (WT) and indicated mutants. Reporter strains contained an empty control plasmid (EV) or a plasmid expressing *hecR* under the control of an IPTG-inducible promoter and were grown in LB supplemented with 100 µM IPTG for 20 hours. Flow cytometry experiments are shown for three biological replicates with the individual histograms stacked in the graph. For each sample, 100.000 events were recorded. **H:** The Gac/Rsm cascade controls onset of *hecE* expression. Growth (solid lines, left y-axis) and fluorescence (dashed line, right y-axis) of strains with an engineered fluorescent *mRuby2* reporter in the chromosomal *hec* locus (*hecRE-2mR*) in wild type (WT) and indicated mutants. Reporter strains contained a plasmid carrying *hecR* under the control of an IPTG-inducible promoter and were grown in LB supplemented with 100 µM IPTG. Mean values and standard deviations of three biological replicates (with three technical replicates each) are shown. **I:** Control by the Gac/Rsm is not responsible for the repression in exponential phase. Flow cytometry analysis of strains with an engineered fluorescent *mRuby2* reporter in the chromosomal *hec* locus (*hecRE-2mR*) in wild type (WT) and indicated mutants. Reporter strains contained an empty control plasmid (EV) or a plasmid carrying *hecR* under the control of an IPTG-inducible promoter and were grown in LB supplemented with 100 µM IPTG to exponential phase. Flow cytometry experiments are shown for three biological replicates with the individual histograms stacked in the graph. For each sample, 100.000 events were recorded.

The findings above confirmed that the *hecRE* module is regulated by the Gac/Rsm cascade, but also indicated that this regulatory pathway is almost fully repressed under the conditions used for these experiments (20 hours in LB).

Expression of *rsmY* and *rsmZ* is ultimately controlled by three sensor histidine kinases, GacS, RetS, and LadS *(Francis et al*., 2017), through the activation of the response regulator and transcription factor GacA (**Fig. 7A**). While GacS and LadS stimulate GacA, RetS attenuates GacA activity (Ventre *et al*., 2006). In line with this, bimodality of *hecE* expression was strongly reduced in a Δ*gacS* and a Δ*ladS* mutant, while the fraction of cells expressing the *hecRE-mRuby2* reporter was strongly increased in a Δ*retS* mutant (**Fig. 7D,E**). Similarly, a strain lacking the translational repressor RsmA (Δ*rsmA*) also showed significantly more *hecE* ON cells than an isogenic wild-type strain (**Fig. 7D,E**). Deletion of the RsmA homolog, RsmN, showed no effect on the bimodal distribution of *hecE* expression (**Fig. 7D,E**). Of note, genetic derepression of the Gac/Rsm pathway not only increased the frequency of *hecE* ON cells, but also the fluorescence intensity in individual cells of the ON population (**Fig. 7D**). Importantly, *hecE* expression retained its bimodal nature in a ∆*rsmA* mutant, arguing that the Gac/Rsm cascade can tune *hecE* bimodality, but is not the cause of its heterogeneous expression **(Fig. 7D)**.

The above findings were further strengthened by *hecE* reporter analyses of strains in which individual components of the Gac/Rsm pathway were ectopically expressed (**Fig. 7F; S5C,D**). *E.g.*, ectopic expression of *rsmA* reduced the number of ON cells in wild type and in a Δ*retS* mutant, confirming its epistatic position in the Gac/Rsm pathway (**Fig. 7F**).

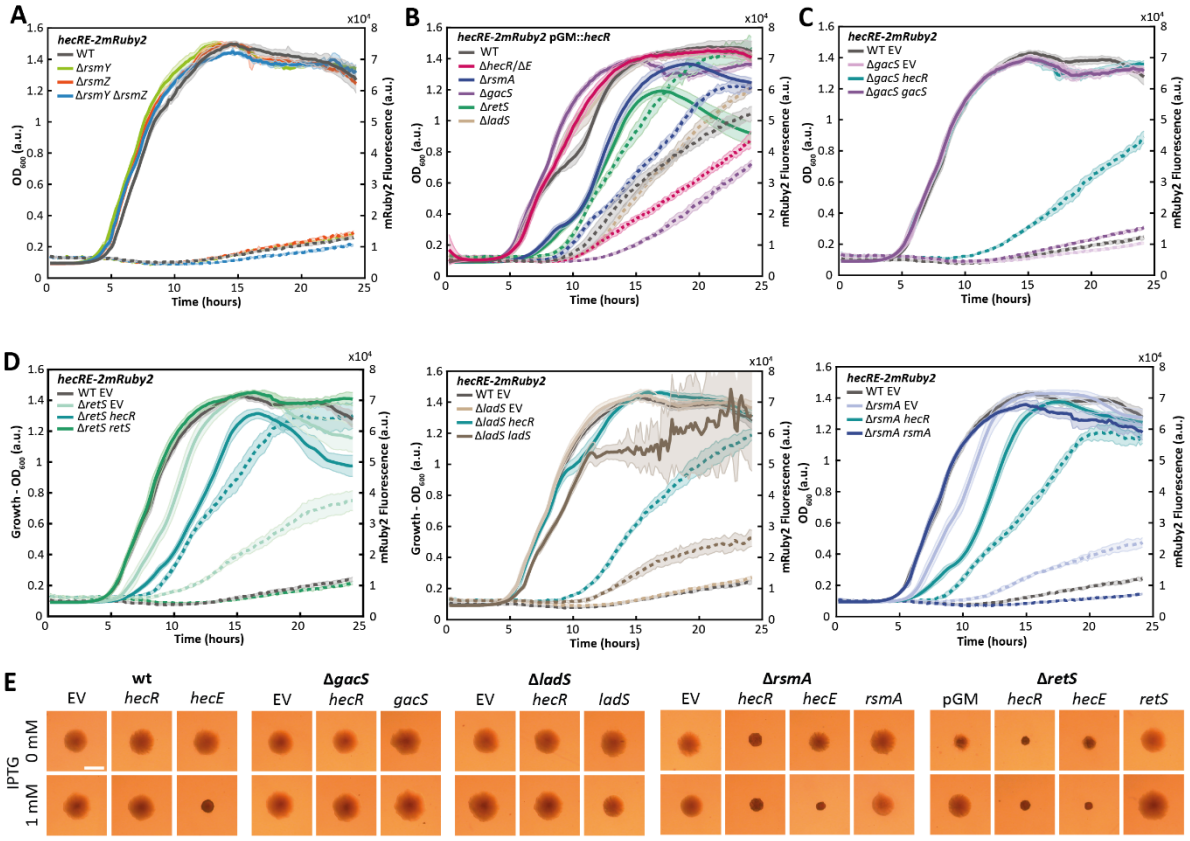

Supplementary Figure 5: The global Gac/Rsm signaling cascade controls *hecE* expression.
A: *HecRE* expression is reduced in *rsmY/Z* mutants in stationary phase. Growth (solid lines, left y-axis) and fluorescence (dashed line, right y-axis) of strains with an engineered fluorescent *mRuby2* reporter in the chromosomal *hec* locus (*hecRE-2mR*) in wild type (WT) and indicated mutants grown in LB. Mean values and standard deviations of one biological replicates (with six technical replicates) are shown. **B:** The Gac/Rsm cascade controls onset of *hecE* expression. Growth (solid lines, left y-axis) and fluorescence (dashed line, right y-axis) of strains with an engineered fluorescent *mRuby2* reporter in the chromosomal *hec* locus (*hecRE-2mRuby2*) in wild type (WT) and indicated mutants. Reporter strains a plasmid carrying *hecR* under the control of an IPTG-inducible promoter and were grown in LB. Mean values and standard deviations of three biological replicates (with three technical replicates each) are shown. **C,D:** The Gac/Rsm cascade controls *hecE* expression. Growth (solid lines, left y-axis) and fluorescence (dashed line, right y-axis) of strains with an engineered fluorescent *mRuby2* reporter in the chromosomal *hec* locus (*hecRE-2mR*) in wild type (WT) and indicated mutants. Reporter strains contained an empty control plasmid (EV) or plasmid carrying indicated genes under the control of an IPTG-inducible promoter and were grown in LB supplemented with 100 µM IPTG. Mean values and standard deviations of three biological replicates (with three technical replicates each) are shown. **E:** Colony morphology of *P. aeruginosa* with an engineered fluorescent *mRuby2* reporter in the chromosomal *hec* locus in wild type (WT) or indicated mutant strains expressing the indicated genes under control of an IPTG-inducible promoter. Strains were grown on LB plates containing Congo Red and Coomassie Brilliant Blue and the indicated amount of IPTG. Experiments were done in triplicates; one representative image is shown.

Also, the reporter signal in *hecE* ON fraction observed in cultures that ectopically express *hecR* from an IPTG-inducible promoter was partially dependent on GacS (**Fig. 7G**), arguing that translational control by the Gac/Rsm system contributes to expression of *hecE*, which is in line with HecRE-mediated SCV formation in mutants of the Gac/Rsm cascade (**Fig. S5E**).

Moreover, *hecE* expression increased prematurely when a Δ*rsmA* or a Δ*retS* mutant entered stationary phase, but was delayed in isogenic strains lacking GacS or LadS **(Fig. 7H; S5B,C,D)**. These data indicated that control by the Gac/Rsm cascade may contribute to the

observed strong repression of *hecE* in exponentially growing populations of *P. aeruginosa* **(Fig. 6F,G)**. To test this, we repeated the above experiments but instead of scoring *hecE* reporter activity in stationary phase (time point 20 hours) we analyzed populations in early log phase. The observation that even in the Δ*rsmA* and Δ*retS* mutants reporter intensity failed to reach the levels observed in stationary phase **(Fig. 7I)**, argues for additional factors contributing to *hec* expression control during the exponential growth phase.

2.1.10 Stochastic expression of *hecE* is induced by environmental stress

The observation that *hecE* bimodality is strongly tuned during different stages of growth, prompted us to investigate additional environmental factors that may regulate this system. The *hec* expression pattern was unchanged in MOPS minimal medium supplemented with either glycolytic or gluconeogenetic substrates (**Fig. 8A**), indicating that the central carbon metabolism does not impact *hecE* regulation. Cells grown in synthetic cystic fibrosis medium (SCFM) also showed bimodal *hecE* expression, arguing that this is an intrinsic property of the module. Interestingly, growth in artificial sputum medium (ASM) repressed the *hecE* ON fraction (**Fig. 8A**). In contrast to SCFM, ASM is supplemented with mucins, protein components of the human lung epithelial mucus layer (Ridley and Thornton, 2018), which were shown recently to be involved in RetS activation (Wang *et al*., 2021). Thus, although *hecE* expression appears independent of the primary carbon source, specific media supplements can influence its regulation via the Gac/Rsm cascade.

We next asked if the concentration of key nutrients in the medium affect *hecE* expression. Diluting succinate as the sole carbon source in MOPS minimal media resulted in increasingly premature *hecE* expression during growth, despite of largely unchanged growth kinetics (**Fig. 8B**). Intriguingly, the subpopulation of *hecE* ON cells emerged long before nutrient limitation caused a decline in growth rates. This, and the observation that the fraction of cells expressing *hecE* reached similar levels, argued that the stochastic expression of *hecE* is dictated by nutritional signals preceding growth limitation and entry into stationary phase. Similar nutrient-dependent shifts in *hecE* expression were observed in Δ*rsmA* and Δ*retS* mutants (**Fig. 8C, S6A**), arguing that this response is not mediated by the Gac/Rsm pathway. Likewise, *hecE* induction is not mediated by the stationary phase sigma factor RpoS, as a Δ*rpoS* mutant also maintained the *hecE* response at different succinate concentrations (**Fig. S8A**).

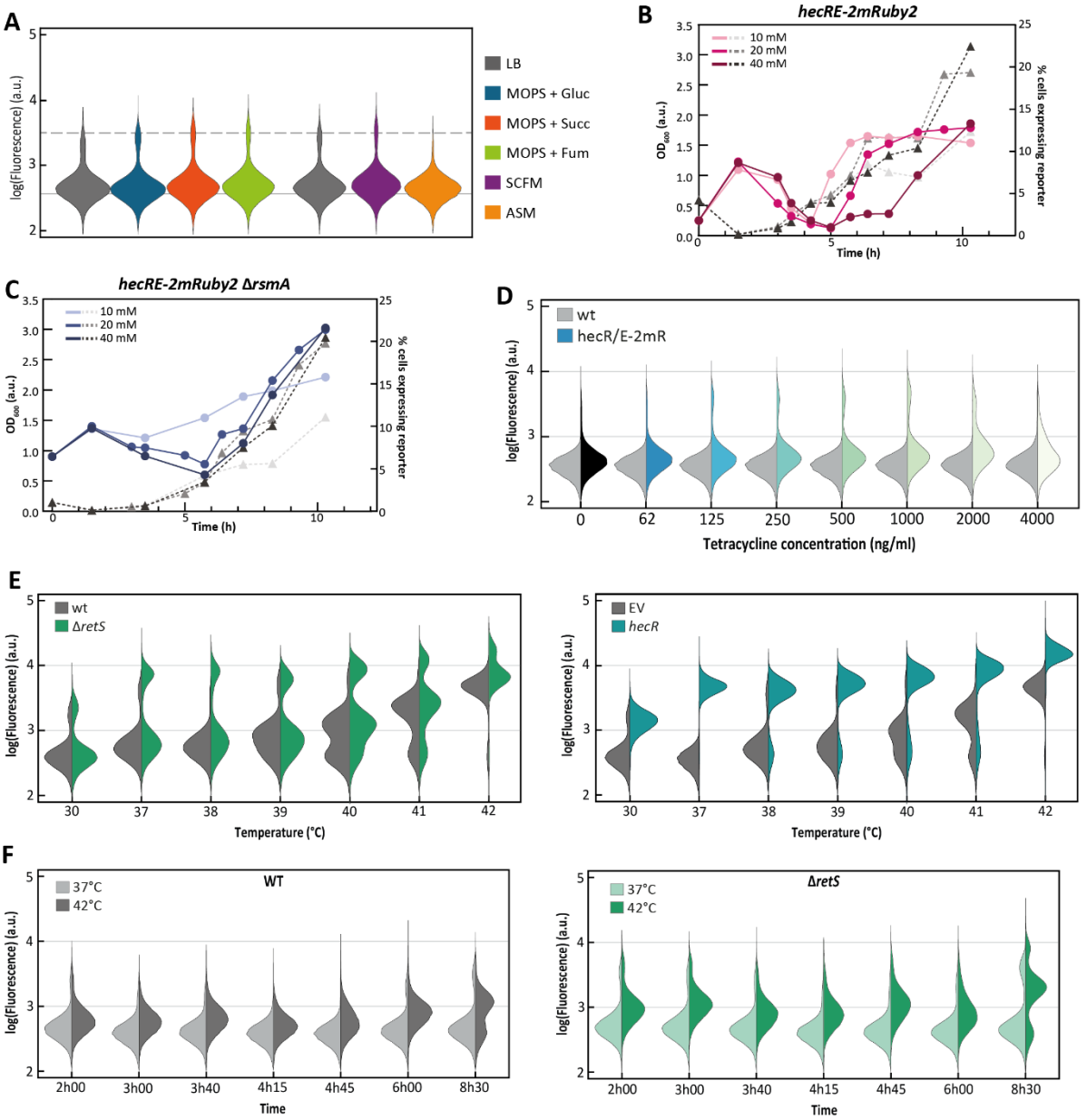

Figure 8: The expression of *hecE* responds to nutrients, subinhibitory antibiotic concentrations, and temperature.
A: Expression of *hecE* is independent of the primary carbon source. Flow cytometry analysis of strains with an engineered fluorescent *mRuby2* reporter in the chromosomal *hec* locus (*hecRE-2mR*). Reporter strains were grown in the indicated medium for 20 hours (left) or 24 hours (right). Flow cytometry experiments are shown for one biological replicate, with 100.000 events recorded. **B, C:** Nutrient availability controls *hecE* expression. Flow cytometry data of *hecRE*-reporter strains in wild type (WT) (**B**) and Δ*rsmA* (**C**) background, grown in MOPS with indicated amounts of succinate at 37°C. Cells with higher fluorescence intensity than the PAO1 wild type strain were quantified (right axis). The optical density of the culture before flow cytometry is indicated on the left axis. **D:** Subinhibitory concentrations of tetracycline induce *hecE* expression. Flow cytometry data of *hecRE*-reporter strains grown in MOPS + 20mM succinate and indicated amounts of tetracycline at 37°C overnight. Cells with higher fluorescence intensity than the PAO1 wild type strain were quantified (right axis). The optical density of the culture before flow cytometry is indicated on the left axis. **E:** Expression of *hecE* responds to temperature. Flow cytometry data of *hecRE*-reporter strains in wild type (WT) and Δ*retS* background (left figure) or expressing *hecR* from an IPTG-inducible promoter (right figure) were grown in MOPS with 20 mM succinate (supplemented with 100 µM IPTG where appropriate) at the indicated temperature for 16 hours. For each sample, one biological replicate with 100.000 events was recorded. **E:** HecE induction at 42°C is growth phase dependent. Flow cytometry data of *hecRE*-reporter strains in WT and Δ*retS* background were grown in MOPS + 20 mM succinate at 37 or 42 °C for indicated time. For each sample, one biological replicate with 100.000 events was recorded

Knowing that HecE controls c-di-GMP levels and biofilm formation and that subinhibitory concentrations of antibiotics stimulate biofilm formation in *P. aeruginosa* (Hoffman *et al*., 2005; Stoitsova *et al*., 2016), we also investigated *hecE* expression upon exposure of *P. aeruginosa* to antibiotics. Although we tested several antibiotics (carbenicillin, rifampicin, gentamycin, spectinomycin, tetracycline and tobramycin), only tetracycline showed a reproducible effect on the fraction of *hecE* ON cells at concentrations close to the MIC (**Fig. 8D, S6B**).

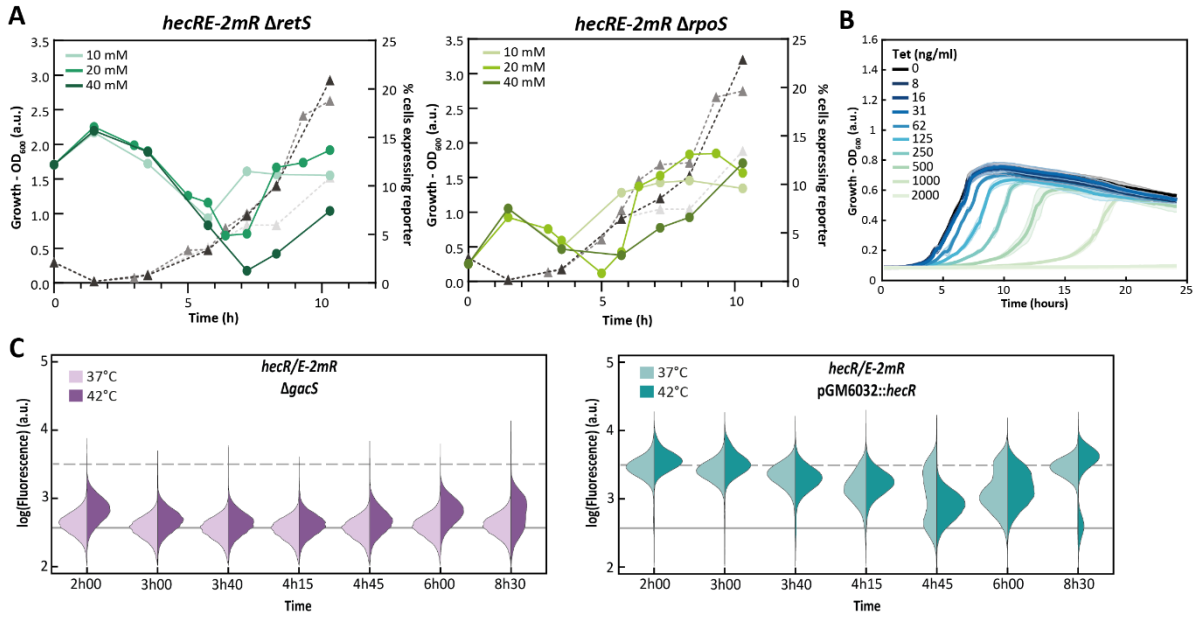

<u>Supplementary Figure 6:</u> *HecE* expression responds to nutrients, subinhibitory antibiotic concentrations, and temperature. **A:** Flow cytometry data of *hecRE*-reporter strains in Δ*retS* and Δ*rpoS* background, grown in MOPS with indicated amounts of succinate at 37°C. Cells with higher fluorescence intensity than the PAO1 wild type strain were counted as positive (right axis). The optical density of the culture before flow cytometry is indicated on the left axis. **B:** Growth curves of *hecRE-2mR* reporter strains in MOPS + 20mM succinate with indicated concentrations of Tetracycline at 37°C. The means and standard deviations of one biological replicate (with three technical replicates) are shown. **C:** Expression of *hecE* responds to temperature. Flow cytometry data of *hecRE*-reporter strains in wild type (WT) and Δ*gacS* background (left figure) or expressing *hecR* from an IPTG-inducible promoter were grown in MOPS + 20 mM succinate (supplemented with 100 µM IPTG where appropriate) at indicated temperature for 16 hours. For each sample, one biological replicate with 100.000 events was recorded.

Because *P. aeruginosa* is both an environmental organism and an opportunistic pathogen that successfully invades warm-blooded host environments, we also asked if temperature influenced *hec* expression. Surprisingly, fractions of *hecE* ON cells differed greatly at 30°C, 37°C or at 42°C. While both fluorescence intensity and frequency of ON cells was minimal at lower temperatures, *hecE* transcription gradually increased with increasing temperature and was strongly derepressed at 40°C and above with unimodal populations of ON cells at 42°C (**Fig. 8E**). This behavior was more pronounced in a Δ*retS* mutant, which generated even three distinct sub-populations of *hecE* expression strength as temperature was increased.

Intriguingly, *hecE* induction at elevated temperatures was limited to the late exponential and stationary growth phase and was fully suppressed during early exponential growth (**Fig. 8F**). This repression was not dependent on the Gac/Rsm cascade, as a similar hecE expression profile was observed during exponential growth of a Δ*gacS* mutant **(Fig. S6C)**.

Altogether, these experiments demonstrated that *hecE* expression is strongly stimulated by different environmental stressors like nutrient depletion, increased temperature or exposure to antibiotics. Expression of the module, especially expression of HecE increases c-di-GMP levels both by directly inactivating the phosphodiesterase BifA and activating the diguanylate cyclase WspR. The heterogeneous expression of the module likely creates a subpopulation of cells with higher c-di-GMP levels, thus splitting the population in phenotypically distinct subpopulations (**Fig. 9**).

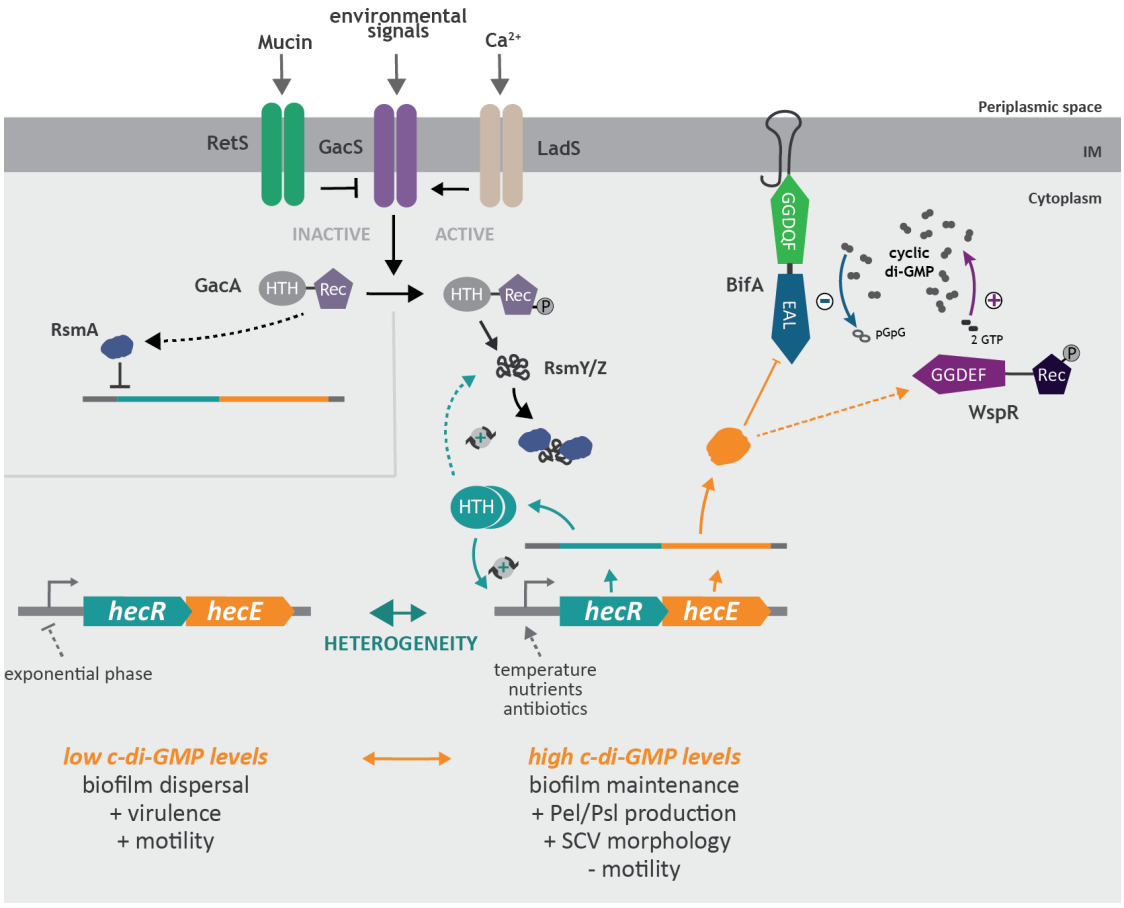

Figure 9: Current model of regulation and downstream effects of the *hecRE* module.
Expression of the *hecRE* module is dependent on HecR and is post-transcriptionally controlled by RsmA. When GacS is active, the transcription factor GacA is activated and upregulates expression of the sRNAs *rsmY* and *rsmZ*. RsmY/Z can sequester RsmA away from its mRNA targets, including the *hecRE* mRNA. HecRE expression is bimodal in stationary phase and repressed during exponential phase. Elevated temperature, reduced nutrient availability, and subinhibitory concentrations of tetracycline induce expression of *hecRE*. HecE specifically inhibits the phosphodiesterase BifA and increases activity of the diguanylate cyclase WspR, thereby increasing cyclic di-GMP levels. The *hecRE* module controls production of the Pel and Psl exopolysaccharides, biofilm formation, SCV morphology and motility in *P. aeruginosa*.

2.2 Supplementary Tables

HecR	
Considered sequences	**7580**
Wt	7518
A99V	18
H43R	5
E51D	4
A62V	4
E51Q|K77Q|S104G	3
S44P	3
F85L	3
G3V	2
R5W	2
S44F	2
V59I	2
V108A	2
T4I	1
Q19K	1
H43P	1
Q58L	1
M61V	1
A72T	1
L81P	1
A99T	1
R109H	1
H43D|Q58R	1
N46D|L81P	1
K7N|A8V|G14E|S50F|L57F	1

HecE	
Considered sequences	**7620**
Wt	7391
A55T	183
Q81P	16
A55T|Q81P	6
D48E	4
E85G	3
S47N	2
M1V	1
T11P	1
R19H	1
H24Q	1
E26Q	1
V44I	1
R53W	1
T57K	1
Q69H	1
N76S	1
E85K	1
R106H	1
T11P|T12P	1
Y28H|D48E	1
Q83I|I84E|E85S|S86L|L87Y|Y88S|S89I|I90V|V91E|E92G|G93I|I94R|R95S|S96C|C97R|R98P|P99L|L100M|M101Q|Q102E	1

Supplementary Table 1: Single Nucleotide Polymorphism (SNP) analysis of *hecR* (*PA2780*) and *hecE* (*PA2781*).
The nucleotide sequences of *PA2780* and *PA2781* of the Jenal Lab PAO1 strain were compared to 7580 and 7620 sequenced *P. aeruginosa* strains from NCBI.

Protein	Name	Global PBS score (confidence)	Protein Description	Selected Interaction Domain
PA1223		moderate	probable transcription regulator	HTH,LysR and LysR substrate-binding domains
PA1243		very high	probable sensor/response regulator hybrid, contains 2 PAS/PAC, a GAF, a histidine kinase, ATPase and signal transduction domain	signal transduction histidine kinase domain
PA1525	*alkB2*	very high	alkane-1-monooxygenase 2, contains multiple transmembrane domains and fatty acid desaturase type 1 domain	transmembrane domain
PA2366	*hsiC3*	moderate	uricase	DUF877
PA2707		moderate	AAA-type ATPase domain	AAA-type ATPase domain
PA3133	*sawR*	moderate	regulator, contains HTH-domain	unknown
PA3420		moderate	probable transcription regulator	LuxR, C-terminal domain
PA4024	*eutB*	moderate	ethanolamine-ammonia lyase, large subunit	N-terminal part of the protein
PA4367	*bifA*	very high	cyclic-Di-GMP phosphodiesterase, contains 2 transmembrane domains, GGDEF and EAL domains	EAL domain
PA4659		moderate	probable transcription regulator, contains MerR HTH family regulatory protein, cobalamin-binding module	HTH and cobalamine-binding domain
PA4726	*cbrB*	moderate	two-component response regulator, contains signal transduction response regulator and AAA+ ATPase domain	response regulator and ATPase domain
PA5246		very high	contains thioesterase superfamily domain	thioesterase superfamily domain
PA5269		moderate	hypothetical protein	unknown

Supplementary Table 2: Proteins interacting with HecE identified in a Yeast Two-Hybrid screen.
A yeast two-hybrid screen with HecE as bait against the PAO1 genome as prey was performed by Hybrigenics Services.

Gene(s)	Name(s)	# Hits	Description
PA0285		1	putative phosphodiesterase, containing a membrane domain, an EAL and a GGDEF domain
PA0286	*desA*	1	delta-9 fatty acid desaturase
PA0413	*chpA*	1	chemotaxis protein histidine kinase and related kinases, next to pilK, cell motility and secretion / Signal transduction mechanisms
PA0464	*creC*	1	two-component sensor CreC, Signal transduction histidine kinase
PA0820		4	hypothetical protein, unknown structure, predicted restriction endonuclease
PA0855		1	hypothetical protein, near bolA morphogene (involved in growth or morphogenesis)
PA1112-1113		1	intergenic region between PA1112-1113
PA1414		1	transcriptional regulator (1413)/unknown hypothetical pair
PA2060	*sppC*	1	ABC transporter permease

PA2130	*cupA3*	3	usher CupA3
PA2130 & PA2104/2105	*cupA3 & PA2104/PA2105*	2	usher CupA3; probable cysteine synthase; probable acetyltransferase
PA2130/PA2131	*cupA3/cupA4*	1	usher CupA3/A4
PA2131	*cupA4*	1	fimbrial subunit CupA4, putative fimbrial usher protein
PA2131 & PA3879 & PA5303	*cupA4 & narL & PA5303*	1	fimbrial subunit CupA4; two-component response regulator NarL; hypothetical protein
PA2373	*vgrG3*	1	type VI secretion system Vgr family protein
PA2788		1	probable chemotaxis transducer
PA2932	*morB*	1	morphinone reductase, could drive cifR
PA3048		1	hypothetical protein, could drive rmf - ribosome modulation factor
PA3331	cytochrome P450	1	cytochrome P450
PA3620	*mutS*	1	DNA mismatch repair
PA3702	*wspR*	2	response regulator with a GGDEF output domain
PA3702 & PA1191	*wspR & PA1191*	1	response regulator with a GGDEF output domain; hypothetical protein
PA3704	*wspE*	2	chemotaxis protein histidine kinase and related kinases
PA3705/3706	*wspC/wspD*	1	methylase of chemotaxis methyl-accepting proteins / chemotaxis signal transduction protein
PA3708	*wspA*	3	methyl-accepting chemotaxis protein
PA3708 & PA5242	*wspA & ppk*	5	methyl-accepting chemotaxis protein; polyphosphate kinase activity (nucleotide metabolic process)
PA3709		1	probable major facilitator superfamily (MFS) transporter, next to wspA
PA3766		1	probable aromatic amino acid transporter
PA3825		1	cyclic-guanylate-specific phosphodiesterase, contains EAL domain
PA4733	*acsB*	1	acetyl-coenzyme A synthetase
PA4981	*lysP*	1	lysine-specific permease
PA5042/PA5043	*pilO/pilN*	2	type 4 fimbrial biogenesis protein PilO & pilN
PA5059		1	probable transcriptional regulator
PA5252		1	probable ATP-binding component of ABC transporter
PA5443	*uvrD*	1	DNA helicase II, DNA repair
Transposase	Transposase	1	transposase, DNA replication, recombination, and repair

Supplementary Table 3: List of genes identified in a Mariner transposon suppressor screen resulting in the reversion of the HecE-mediated SCV morphotype.
Genes linked to the Wsp chemosensory system are highlighted in yellow, genes linked to cup fimbrae are highlighted in green and genes linked to T4P/Chp are highlighted in blue.

2.3 Additional Results

The following chapter comprises results, which are beyond the scope of the main results, but contribute to the overall understanding or might be influential for future experiments.

2.3.1 HecE induces SCV formation in multiple *P. aeruginosa* strains

Our results indicated that ectopic *hecE* expression induced SCV morphology in PAO1 by upregulating production of Pel and Psl (**Fig. 2F**). To test if this was a strain specific effect, *hecE* was expressed in *P. aeruginosa* strains PA14 and PAK, revealing that HecE-mediated SCV formation could be observed in the PAO1, PA14 and PAK strains (**Fig. 10**). While PAO1 and PAK produce both Psl and Pel exopolysaccharides, PA14 only produces Pel. A *pel* mutant in PAO1 shows HecE-mediated SCV formation, but this is lost in a PA14 *pel* mutant. These results confirm that HecE increases production of both Pel and Psl in different strains of *P. aeruginosa*.

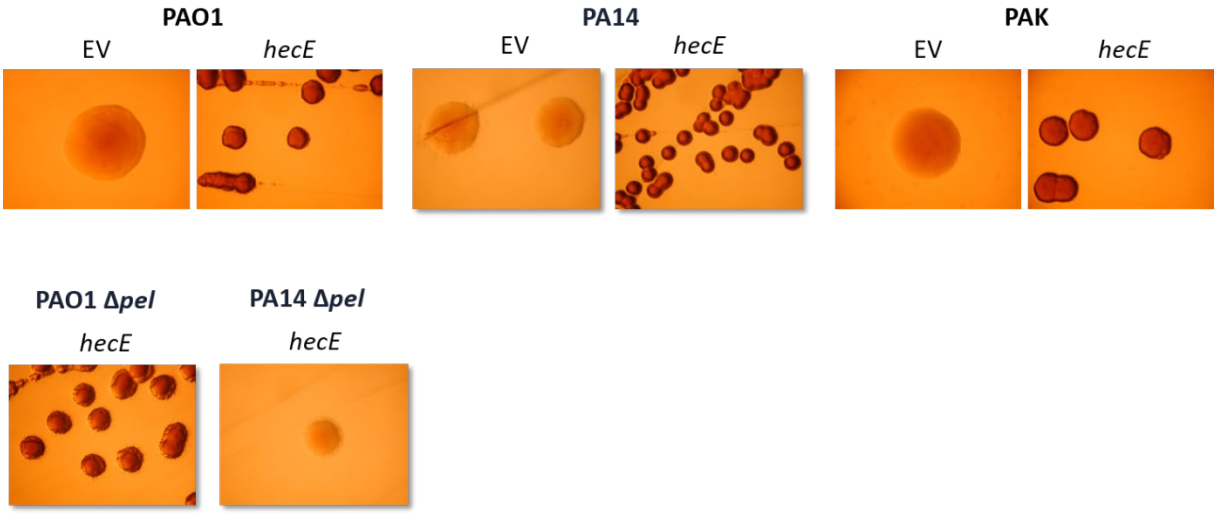

Figure 10: HecE induces SCV formation in PAO1, PA14 and PAK by increasing production of Pel and Psl.
Colony morphology of *P. aeruginosa* PAO1, PA14, and PAK wild type and mutant strains expressing *hecE* from an IPTG-inducible promoter. Strains were grown on LB plates containing Congo Red and 1 mM IPTG.

2.3.2 HecE-mediated aggregation is medium dependent

We had observed that ectopic expression of *hecE* leads to Psl-dependent aggregation in liquid cultures of LB. Intriguingly, ectopic expression of neither *hecR* nor *hecE* had an impact on growth in MOPS minimal medium supplemented with a glycolytic (glucose) or gluconeogenetic (succinate) carbon source or synthetic cystic fibrosis medium (**Fig. 11A, B**), while a change in growth similar to aggregation in LB could be observed in MOPS supplemented with both succinate and glucose (**Fig. 11 A**). This suggests that the HecE-mediated effects in liquid culture depend on the medium, probably due altered presence/activity of downstream factors. In contrast, inactivation of the phosphodiesterases BifA, Pch, and RbdA led to strong aggregation in MOPS supplemented with glucose and succinate, corroborating our findings that HecE-mediated aggregation is caused by WspR activity and not by inactivation of the phosphodiesterases.

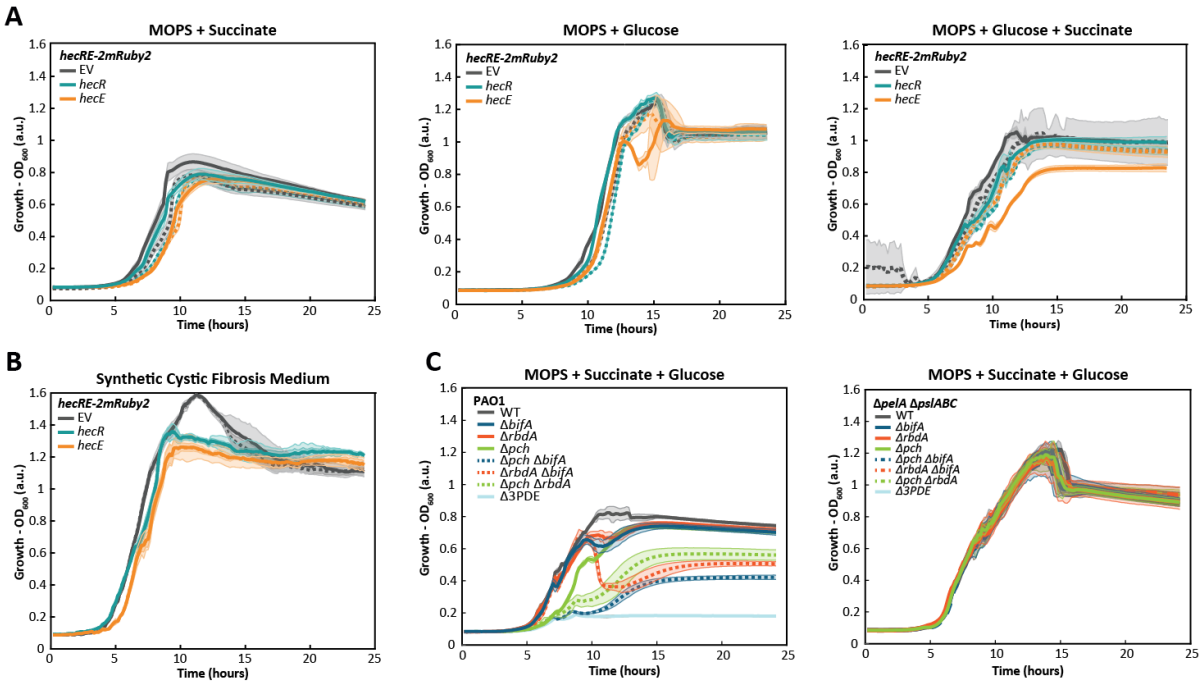

Figure 11: Cellular aggregation is medium dependent.
A,B: HecE-mediated aggregation is medium dependent. Growth of *P. aeruginosa hecRE* reporter strains (*hecRE*-2mRuby2) expressing *hecR* or *hecE* from an IPTG-inducible promoter in MOPS supplemented with 20 mM glucose, 20 mM succinate or 10 mM glucose and 10 mM succinate (**A**) or synthetic cystic fibrosis medium (**B**). Growth in indicated media (dashed lines) or in media supplemented with 100 µM IPTG (solid lines) was recorded and mean values and standard deviations of one biological replicate (with three technical replicates) are shown. **C:** Growth effects in the phosphodiesterase mutants are Pel and Psl dependent. Growth of *P. aeruginosa* PDE mutant strains in wild type (PAO1) and Δ*pelA* Δ*pslABC* background in MOPS supplemented with 10 mM glucose and 10 mM succinate. Mean values and standard deviations of one biological replicate (with three technical replicates) are shown.

2.3.3 Growth and twitching phenotypes of the *bifA* mutant are independent of *hecRE* and *wspR*

We had observed that a Δ*bifA* mutant exhibits a nick in growth curves, similar to ectopic expression of the *hec* genes and that this HecRE-mediated nick was dependent on WspR activity. Interestingly, the growth phenotype observed in the Δ*bifA* mutant is unaltered in isogenic strains harboring a deletion in *wspR* or *hecRE*. Similarly, twitching motility of the Δ*bifA* mutant was unaltered in isogenic strains harboring a deletion in *wspR* or *hecRE*. Together, these data support a model in which BifA acts downstream of HecE and independent of WspR.

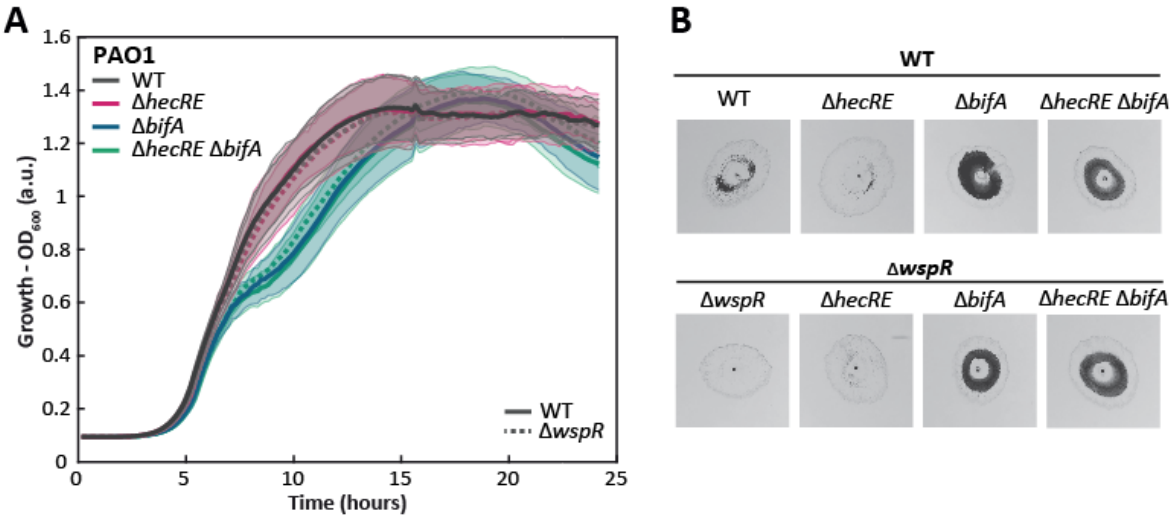

Figure 12: Growth and twitching phenotypes of the *bifA* mutant are independent of *hecRE* and *wspR*.
A: Deletion of *wspR* or *hecRE* does not restore normal growth of *bifA* deletion mutants. Growth of *P. aeruginosa* wild type and indicated deletion strains was scored in LB (solid lines) and compared to isogenic strains harboring a deletion in *wspR* (Δ*wspR,* dashed lines). Mean values and standard deviations of three biological replicates (with three technical replicates) are shown. **B:** Deletion of *wspR* or *hecRE* does not restore normal twitching phenotype of *bifA* deletion mutants. Twitching motility of *P. aeruginosa* wild type and indicated deletion strains was scored on LB 1.5% agar plates and compared to isogenic strains harboring a deletion in *wspR* (Δ*wspR*). Mean values and standard deviations of three biological replicates (with three technical replicates) are shown. Experiments were done in triplicates; one representative image is shown.

2.3.4 Phage Knedl is related to two unclassified Siphoviridae of *P. aeruginosa*

Our findings that HecE upregulates production of the Pel and Psl exopolysaccharides (**Fig. 2E,F**), together with the fact that surface glycans are frequent phage receptors (Bertozzi Silva *et al*., 2016; Sellner *et al*., 2021) prompted us to test whether the *hec* module would sensitize *P. aeruginosa* for phage infection. This lead to the identification of a novel phage called Knedl that infects *P. aeruginosa* in a Psl-dependent manner (**Fig. 2H**). To characterize phage Knedl in more detail, we sequenced its genome. The genome of Knedl has 59205 bp with a GC content

of 56.4%. A BLAST search (https://blast.ncbi.nlm.nih.gov/Blast.cgi) revealed that Knedl is closely related to the unclassified Siphoviridae Iggy and PBPA162, sharing a sequence identity of 92.45 % and 95.51 %, respectively. The novelty of Knedl and its related phages could be an opportunity to discover new phage-host interactions and underlying mechanisms.

Scientific Name	Max Score	Total Score	Query Cover	E value	Per. Ident	Acc. Len	Accession
Pseudomonas phage Iggy	39776	85906	95%	0.0	92.45%	60628	MN029011.1
Pseudomonas virus PBPA162	19054	82315	93%	0.0	95.51%	60626	MK816297.1

Figure 13: Knedl is related to phages Iggy and PBPA162.
A BLAST using the genomic sequence of Knedl revealed sequence identities with two other unclassified *P. aeruginosa* Siphoviridae.

2.3.5 Infection by phage Knedl relies on high c-di-GMP levels and is T4P independent

Since phage Knedl was isolated on a strain ectopically expressing *hecR*, thereby inducing expression of *hecE* and subsequently increasing c-di-GMP levels, we wanted to test whether phage sensitivity was mediated by c-di-GMP or HecE-specific effects (**Fig. 2G**). Sensitivity for infection by Knedl was increased in strains expressing either the diguanylate cyclase *dgcZ* from *E. coli* or *wspR* from *P. aeruginosa* (**Fig. 13A**), indicating that sensitivity is due to high c-di-GMP levels. Additionally, we found that type IV pili (T4P), a common entry point for phages in *P. aeruginosa* (Bertozzi Silva *et al*., 2016), were not required for Knedl infection (**Fig. 13B**), in line with our findings that Psl is the primary receptor for Knedl (**Fig. 2H**).

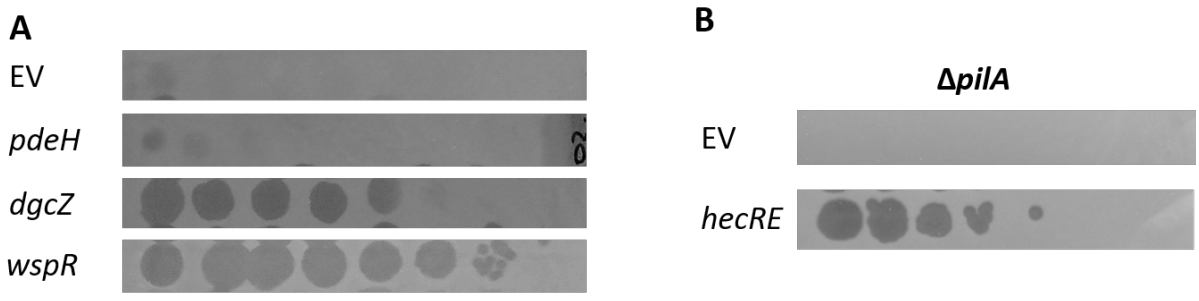

Figure 14: Knedl infection relies on high c-di-GMP levels but not type IV pili.
A: Phage sensitivity depends on c-di-GMP levels. Ten-fold dilutions of phages Knedl were applied in LB top agar containing 100 µM IPTG and the *P. aeruginosa* strains indicated. Strains contained either an empty control plasmid (EV) or a plasmid expressing *pdeH, dgcZ* or *wspR* from an IPTG-inducible promoter. **B:** Knedl infection is independent of type IV pili. Ten-fold dilutions of phages Knedl were applied in LB top agar containing 100 µM IPTG and the *P. aeruginosa* strains indicated. Strains contained either an empty control plasmid (EV) or a plasmid expressing *hecRE* from an IPTG-inducible promoter.

2.3.6 Sensitivity to KnedI is changed between liquid culture and top agar assays

We had observed that KnedI can infect PAO1 strains ectopically expressing *hecR* or *hecE* in top agar assays in a Psl-dependent manner (**Fig. 2H**). Furthermore, expression of *hecE* is heterogeneous in liquid cultures, thus we expected that the subpopulation expressing *hecE* would be sensitive to KnedI infection in liquid cultures. Surprisingly, PAO1 wild type was also sensitive to KnedI infection in liquid culture (**Fig. 15A**), which stands in clear contrast to top agar assays where PAO1 wild type was not infected (**Fig. S2C**). Sensitivity to KnedI infection in liquid culture was abolished in strains lacking the exopolysaccharide Psl, which is the receptor of KnedI.

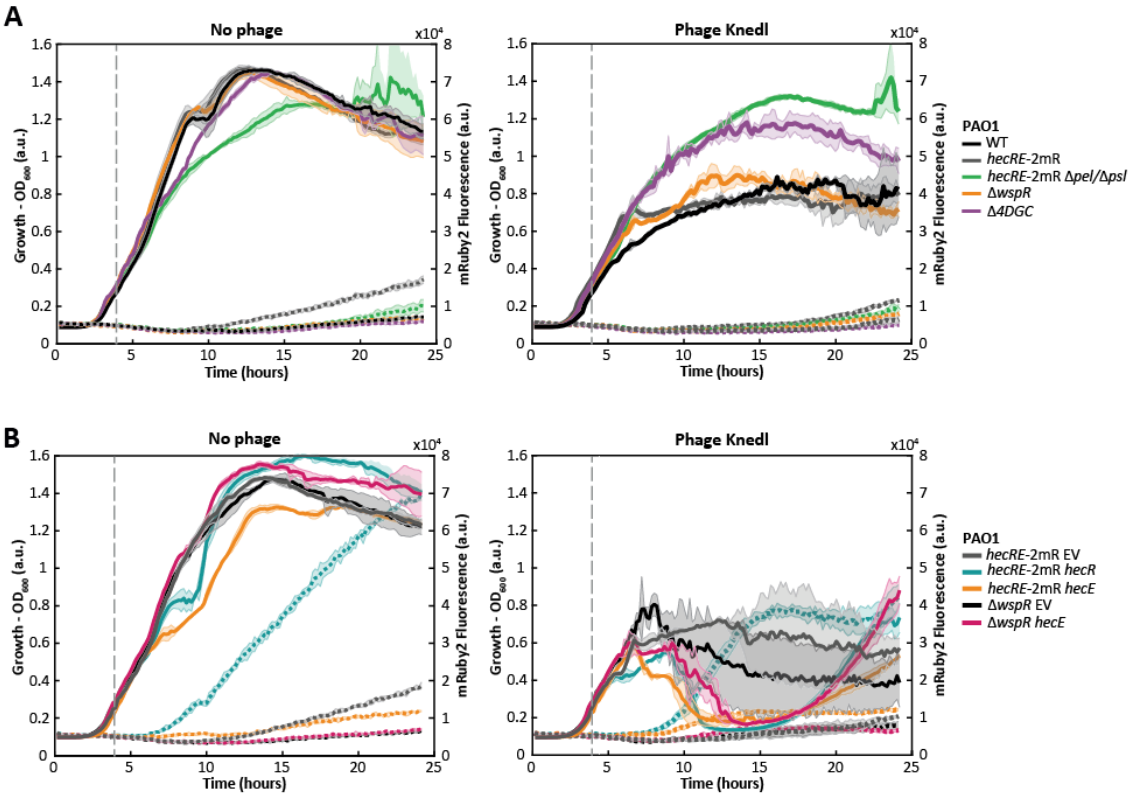

Figure 15: Liquid cultures are more sensitive to KnedI infection.
A: Sensitivity to KnedI in liquid cultures is c-di-GMP dependent**.** Growth (solid lines, left y-axis) and fluorescence (dashed line, right y-axis) of strains with an engineered fluorescent *mRuby2* reporter in the chromosomal *hec* locus (*hecRE-2mR*) or of indicated deletion strains. Strains were grown in LB and KnedI was added at the indicated time (vertical dashed line) at a multiplicity of infection (MOI) of 1. Mean values and standard deviations of one biological replicate (with three technical replicates) are shown. **B:** HecR and HecE increase sensitivity to KnedI infection in liquid cultures. Growth (solid lines, left y-axis) and fluorescence (dashed line, right y-axis) of strains with an engineered fluorescent *mRuby2* reporter in the chromosomal *hec* locus (*hecRE-2mR*) or *wspR* deletion strains (Δ*wspR*). Strains contained an empty control plasmid (EV) or a plasmid carrying *hecR* or *hecE* under the control of an IPTG-inducible promoter. Strains were grown in LB supplemented with 100 µM IPTG and KnedI was added at the indicated time (vertical dashed line) at a multiplicity of infection (MOI) of 1. LB media were Mean values and standard deviations of one biological replicate (with three technical replicates) are shown.

In line with previous findings (Irie *et al*., 2012; Kragh *et al*., 2018; Overhage *et al*., 2005), this suggested that *P. aeruginosa* cells produce Psl in liquid cultures, allowing for Knedl infection. A strain lacking the four diguanylate cyclases s*adC, dgcH, PA0338* and *PA0847* (Δ*4DGC*), exhibited similar immunity to Knedl as the *pel*/*psl* mutant (**Fig. 15A**), suggesting that basal levels of c-di-GMP are needed for Psl production in this condition. Interestingly, a Δ*wspR* mutant showed only slightly reduced Knedl sensitivity, supporting the notion that WspR is not active in this condition. Ectopic expression of *hecE* increased sensitivity to Knedl infection in both wild type (*hecRE-2mR*) and a *wspR* deletion strain (Δ*wspR*), indicating that an additional boost in c-di-GMP levels and Psl production promotes sensitivity to Knedl (**Fig. 15B**).

Taken together, these results show that the production of Psl differs between liquid cultures and top agar assays. The sensitivity to Knedl in liquid culture without ectopic expression of *hecE* impedes measurement of single cell phage sensitivity, but the Δ4DGC strain could provide a good background for such experiments.

2.3.7 Expression of *hecRE* is strongly increased in biofilms

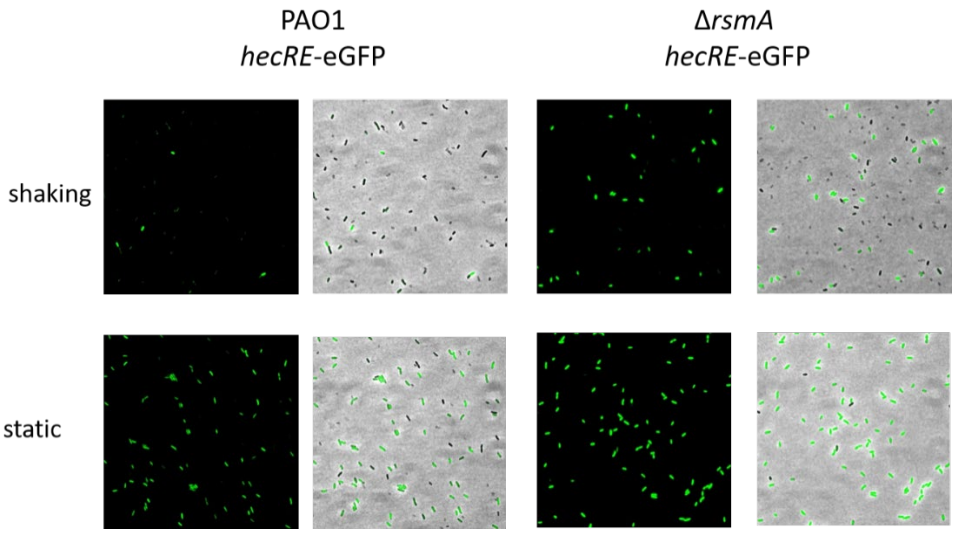

Figure 16: ***HecRE*** **expression is increased in static cultures.**
Microscopy data of strains with an engineered fluorescent *eGFP* reporter in the chromosomal *hec* locus (*hecRE-eGFP*) in wild type (PAO1) or *rsmA* deletion background (Δ*rsmA*). Reporter strains were grown in LB shaking or static cultures for 48 hours. For static cultures the cells from the air-liquid interface were taken and resuspended in LB.

Knowing that a *hec* mutants exhibited decreased biofilm formation at time points after 15 hours (**Fig. 1D; S1B**), we expected that the *hec* module was more frequently expressed in biofilms than in liquid cultures. Indeed, most cells taken from the pellicle formed on the air-liquid interface after 48 hours of static culture expressed the *hecRE* reporter, compared to the small subpopulation expressing it in shaking cultures (**Fig. 16**). Similarly to shaking cultures, expression of the *hecRE* reporter was increased in both frequency and intensity in a Δ*rsmA* strain. This confirmed that the *hecRE* module is upregulated in biofilms, mediating biofilm maintenance and that this upregulation is only partially controlled by the Gac/Rsm cascade.

2.3.8 Expression of *hecRE* is reduced in the periphery of the swarming zone

Swarming experiments revealed that *hec* mutants showed a hyperswarming phenotype (**Fig. 2A**), indicating that in this condition the *hec* module is usually expressed. Since we had observed heterogeneous expression of the *hecRE* genes in liquid cultures, we wanted to know the expression pattern during swarming motility.

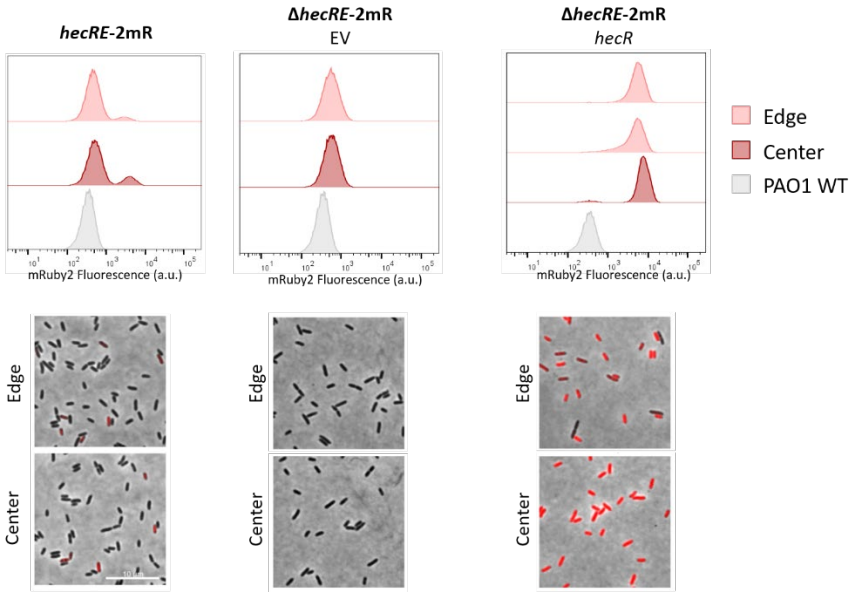

Figure 17: *HecRE* expression varies between edge and center of the swarm zone.
Microscopy and flow cytometry data of strains with an engineered fluorescent *mRuby2* reporter in the chromosomal *hec* locus in wild type (*hecRE-2mR*) or *hecRE* deletion background (Δ*hecRE-2mR*). Reporter strains contained an empty control plasmid (EV) or a plasmid carrying *hecR* under the control of an IPTG-inducible promoter. Swarming assays of reporter strains were performed on M8 agar plates (0.5% agar) supplemented with 0.4% glucose and 0.05% casamino acids for 24 hours. Cells from the edge and center of the swarm zones were taken for microscopy and flow cytometry.

Surprisingly, *hecRE* expression was also heterogeneous during swarming, although the subpopulation of cells expressing *hecRE* was reduced in the edge of the swarm compared to

the center. In line with this, reporter expression levels upon ectopic *hecR* expression were also reduced in the edge of the swarm. These findings suggest that *hecRE* expression is tightly regulated during swarming and that the number of cells expressing the module differs within the swarm. Recent findings showed that a small proportion of non-motile cells (5%) is sufficient to inhibit swarming of the entire population in a exopolysaccharide dependent manner (Lewis *et al*., 2021). In line with this, small changes in the frequency of cells expressing *hecRE* thereby exhibiting increased c-di-GMP levels and exopolysaccharide production, would be sufficient to control swarming motility.

2.3.9 *P. aeruginosa* exhibits heterogeneous c-di-GMP levels in stationary phase

The heterogeneous expression of *hecE* in stationary phase (**Fig. 7E**) together with the fact that HecE controls activity of the phosphodiesterase BifA (**Fig. 3**) and the diguanylate cyclase WspR (**Fig. 4**), thereby increasing c-di-GMP levels (**Fig. 1B**), suggest that the *hec* module creates subpopulations with different c-di-GMP levels. Heterogeneity in cellular c-di-GMP levels of *P. aeruginosa* had been previously observed after cell division and during surface colonization (Armbruster *et al*., 2020; Christen *et al*., 2010; Kulasekara *et al*., 2013; Laventie *et al*., 2019). Using our novel c-di-GMP sensor, we could show that c-di-GMP levels are also heterogeneous in planktonic cultures, in line with findings that c-di-GMP controlled production of Psl is heterogeneous in this condition (Yang *et al*., 2018). Surprisingly, we observed many cells that have high c-di-GMP levels and low *hec* expression and *vice versa*, suggesting that the conditions used are unsuitable for studying HecRE-mediated c-di-GMP increase in single cells.

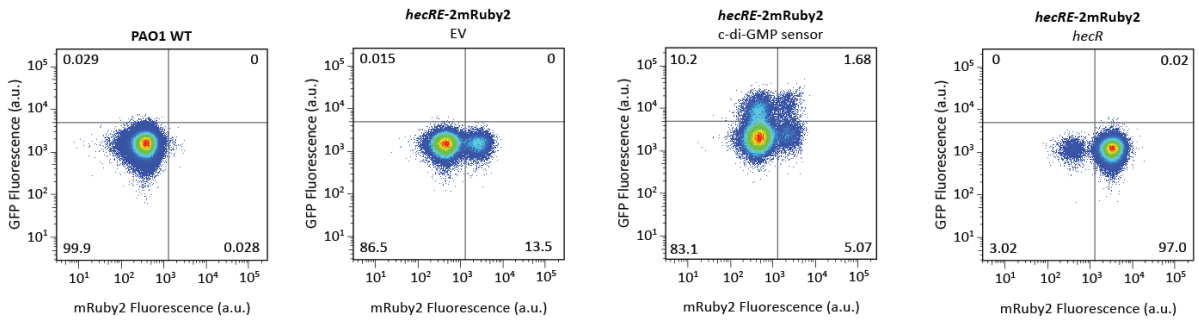

Figure 18: ***HecRE*** **expression and c-di-GMP levels are heterogeneous in** ***P. aeruginosa*** **stationary phase.**
Flow cytometry data of PAO1 wild type (WT) and strains with an engineered fluorescent *mRuby2* reporter in the chromosomal *hec* locus (*hecRE-2mR*). Reporter strains contained an empty control plasmid (EV) or a plasmid carrying *hec* under the control of an IPTG-inducible promoter or the BldD2-eGFP based c-di-GMP sensor under the control of the constitutive Bba_J23115 promoter. Strains were grown in LB for 20 hours at 37°C. *HecRE* reporter signal (mRuby2 fluorescence, x-axis) and c-di-GMP levels (GFP fluorescence, y-axis) of each cell are shown.

2.3.10 Expression levels of *hecRE* at 42°C are independent of the reporter system

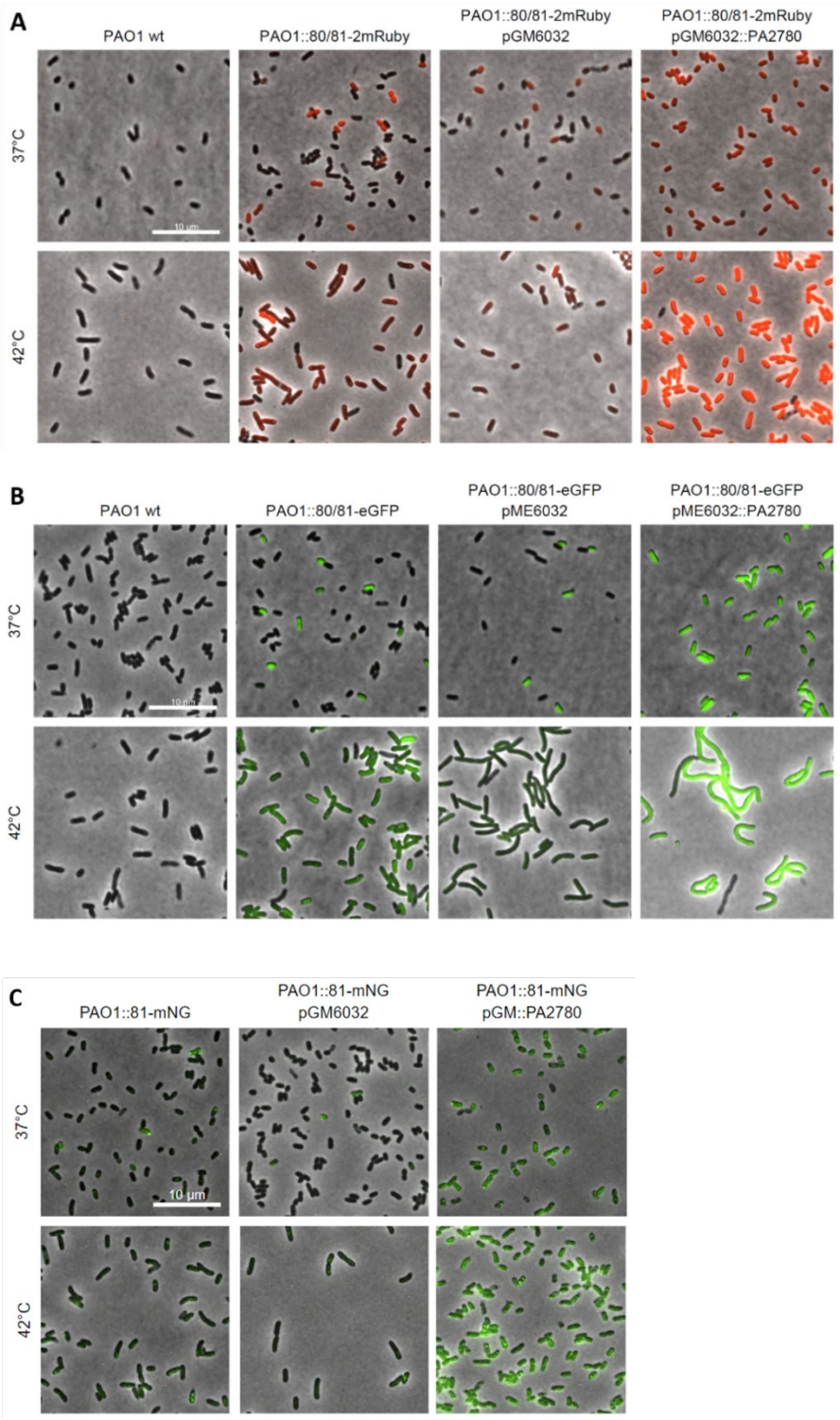

Figure 19: Induction of *hecRE* expression at 42°C is independent of the reporter system.
Microscopy data of strains with different fluorescent *hecRE* reporters: transcriptional *mRuby2* reporter (PAO1::*80/81-2mRuby*) (**A**), transcriptional *eGFP* reporter (PAO1::*80/81-eGFP*) (**B**) or a translational fusion of HecE with *mNeonGreen* (PAO1::*81-mNG*) in the chromosomal *hec* locus. Reporter strains contained an empty control plasmid (pGM6032 or pME6032) or a plasmid carrying *hecR* under the control of an IPTG-inducible (pGM::PA2780) or arabinose inducible (pME6032::PA2780) promoter. Strains were grown in MOPS supplemented with 20 mM succinate for 16 hours at the indicated temperature.

Cells grown at 42°C exhibited increased *hecRE* expression compared to cells grown at 37°C when the *mRuby2* based *hecRE* reporter intensity was scored (**Fig. 8E**). To verify that this temperature mediated effect was independent of the mRuby2 based reporter, we repeated the experiments at 42°C using a GFP based *hecRE* transcriptional reporter (PAO1::*80/81-eGFP*, **Fig. 19B**) and a HecE-mNeonGreen fusion reporter (PAO1::*81-mNG*, **Fig. 19C**). All reporters showed increased intensity at 42°C compared to 37°C (**Fig. 19**). Additionally, ectopic *hecR* expression boosted reporter intensity at 37°C and 42°C. These results confirmed that the observed temperature dependent effects were reporter independent.

2.4 Materials and Methods

Preparation of culture media

For Lysogeny broth (LB) 10 g/l tryptone, 5 g/l yeast extract and 10 g/l NaCl were dissolved in MilliQ water and sterilized by autoclaving. LB agar was prepared by adding 15 g/l bacteriology grade agar before autoclaving. Liquid cultures of *Escherichia coli* and *Pseudomonas aeruginosa* strains were grown in LB at 37°C, shaking in glass tubes at 170 rpm unless stated otherwise. LB agar plates (1.5% agar) were used as solid medium for routine lab work. The following antibiotic concentrations were used for selection for plasmid maintenance: for *E. coli* Gentamicin at 20 µg/ml, Tetracycline at 12.5 µg/ml, for *P. aeruginosa* Gentamicin at 30 µg/ml, Tetracycline at 100 µg/ml.

Bacteriophage handling and culturing

Bacteriophage handling protocols are based on Maffei *et al*., 2021. High-titer stocks of bacteriophages were generated using the plate overlay method. Top agar plates (see qualitative top agar assays) were set up to grow almost confluent plaques of a given phage and then covered with 12 ml of SM buffer (0.1 M NaCl, 10 mM MgSO4, and 0.05 M Tris (pH 7.5)). The suspension was removed after agitation for 24 hours at 4°C, and centrifuged at 8000 g for 10 minutes. Supernatants were sterilized with chloroform (10% final concentration) and stored in the dark at 4°C.

Molecular Biology Procedures

Cloning was carried out using standard molecular biology techniques. DNA fragments were PCR amplified using Phusion polymerase. Vectors were cut by restriction and dephosphorylated using Calf Intestinal alkaline phosphatase. Vectors and inserts were gel or column purified then ligated at 16°C overnight or room temperature for 10 minutes using T4 DNA Ligase. After ligase deactivation at 65°C for 10 min, chemically competent *E*. *coli* DH5α were transformed by heat shock at 42°C for 45 seconds, followed by phenotypic expression and plating on LB agar containing the appropriate antibiotic. Constructs were validated by sequencing.

Deletion of genes by homologous recombination

Gene deletions in *P*. *aeruginosa* strain PAO1 were generated by two-step allelic exchange. The integrative plasmid pEX18 (Gm^R) in which we cloned the regions flanking the target gene to delete (ca. 700bp) was used. The two flanking regions were amplified individually by PCR then fused in a second step by overlap extension PCR (SOE-PCR). *P. aeruginosa* was transformed by electroporation or di-parental conjugation using *E. coli* ST-18 as donor strain. Mutants were selected by sucrose counter selection using LB (no salt) plates supplemented with 8% sucrose. Positives clones were selected by pick and patching clones on LB and LB supplemented with 30 µg/mL Gentamicin agar plates. Mutants were validated by colony PCR and sequencing.

Qualitative top agar assays

The assay was adapted from Maffei *et al*., 2021. Top agars were prepared for each bacterial strain on LB agar plates. LB plates were prepared using square Petri dishes (ca. 12 cm x 12 cm, REF Z617679 Greiner Bio-One), filled with 50ml LB agar (stored at 60°C), left to cool down and dry for 48 hours at room temperature. *P. aeruginosa* strains were cultured in LB (supplemented with appropriate antibiotic, no induction) at 37 °C, 170 RPM for approx. 24 h. The plates were overlaid with 10 ml of top agar (LB with 0.5% agar, 20 mM $MgSO_4$ and 5 mM $CaCl_2$; stored at 60°C) supplemented with 300 µl of the bacterial culture, appropriate antibiotics and inducers where indicated. High-titer stocks of all tested bacteriophages were diluted in a 10-fold dilution series in 1X PBS at room temperature. 2.5 µl of each dilution were spotted onto the top agar plates and air-dried before the plates were incubated upside-down for 20 hours at 37°C. Due to low stability of Phage Knedl in high-titer stocks, phage infectivity was only qualitatively analysed, by interpreting the lysis zones.

Transposon mutagenesis

Screening for SCV morphology

The transposon mutagenesis was performed in Malone *et al*., 2010. In short, the pALMAR3 plasmid was introduced into PAO1 via biparental mating with *E. coli* S17-1. Transposon insertion was selected on LB agar containing tetracycline, chloramphenicol and Congo Red. Insertions leading to small colony morphology were restreaked on fresh plates and the location of the transposon was determined by semi-random PCR.

Screening for SCV morphology

The pALMAR3 plasmid was introduced into PAO1 via biparental mating with *E. coli* S17-1. Transposon insertion was selected on LB agar containing tetracycline, chloramphenicol and Congo Red. Pooled cells were transformed with the pGM6032::HecE plasmid and selected on LB agar containing gentamicin, chloramphenicol and Congo Red. Insertions leading to smooth colony morphology were restreaked on fresh plates and the location of the transposon was determined by semi-random PCR.

Colony morphology

P. aeruginosa strains were cultured in LB (supplemented with appropriate antibiotics but no inducers) at 37 °C, 170 RPM for approx. 24 h. Strains were then diluted back 10^{-6}-fold in fresh LB and 20 µl plated on LB agar plates supplemented with Congo Red (40 µg/ml) and Coomassie Brilliant Blue (20 µg/ml). Antibiotics and inducers were added to the indicated amounts. Plates were incubated statically at 37°C for 24 hours. Pictures were taken using a Coolpix 995 camera (Nikon) with a MDC Coolpix Camera Adapter Lens (Nikon) at an M3Z stereomicroscope (Wild Heerbrugg).

Growth assays

Liquid cultures of *P. aeruginosa* strains were grown in the indicated medium at 37 °C, 170 RPM for approx. 24 h. The OD_{600} was measured and adjusted to a final OD_{600} of 0.01 in the indicated medium. Supplements such as antibiotics and inducers were added to the indicated final concentrations. 200 µl were distributed to each well of the 96-well plate [REF353072, Falcon or REF83.3924, Sarstedt]. Wells on the edge were filled with the respective uninoculated medium. Cultures were grown at the indicated temperature under shaking in Microplate readers (Synergy H1 or Epoch 2: Double Orbital: Continuous, Frequency 425 cpm (3mm)). Cell density was measured by absorption at OD_{600} (Read Speed: Normal, Delay 100 msec, Measurements/Data Point: 8). Fluorescence was measured using Synergy H1 machines with the following settings (Light source: Xenon Flash, Lamp Energy: High, Read Speed: Normal, Delay 100 msec, Measurements/Data Point: 10, Read Height: 7mm, Optics: Bottom). Fluorescence signals were measured for mRuby2 using Ex: 558 nm, Em: 600 nm, Gain: 150 for GFP using Ex: 482 nm, Em: 520 nm, Gain: 60. The analysis was done with Matlab [Version 9.5 (R2018b)].

Attachment assay / biofilm assay

The assay was adapted from Malone *et al*. 2010. Cultures of *P. aeruginosa* strains were grown in LB (supplemented with appropriate antibiotics, no induction) at 37 °C, 170 RPM for approx. 24 h. The OD_{600} was measured and adjusted to a final OD_{600} of 0.01 in the indicated medium. Supplements such as antibiotics and inducers were added to the indicated final concentrations. 200 µl were distributed to each well of the 96-well plate [REF353072, Falcon or REF83.3924, Sarstedt]. Wells on the edge were not inoculated, but filled with the respective medium. Cultures were grown statically for indicated time at 37°C. Afterwards, the cell density was measured at OD_{600} with a plate reader [Epoch 2, BioTek or Synergy H1, BioTek], the supernatant was discarded and wells were washed three times with tap water. The 96-well plate was put to air-dry, up-side-down on a paper-towel. 210 µL of crystal violetCV Staining solution (0.1 % crystal violet, 1 % methanol, 1 % isopropanol in ddH_2O) were added to the wells and incubated statically for 30 min at room temperature. The staining solution was discarded and the wells were rinsed three times with tap water. 215 µL of destaining solution (20 % acetic acid, 80% ddH_2O) were added to re-dissolve the crystal violet stain and incubated 30-60 min at room temperature. The OD_{600} was measured with a plate reader.

Motility

Twitching motility

LB agar (1.5%) plates supplemented with antibiotics and inducers where indicated, were stab-inoculated with *P. aeruginosa* strains and incubated for 24 hours at 37°C. The agar was removed and twitching zones were stained with CV Staining solution (0.1 % crystal violet, 1 % methanol, 1 % isopropanol in ddH_2O) for 5 minutes at room temperature. Plates were carefully rinsed with tap water to remove residual staining and put to air-dry.

Swimming and swarming motility

Swimming and swarming motility were carried out as previously described (Malone *et al*., 2010). In short, swarm agar was based on TB and solidified with 0.5% agar. Plates were dried overnight and then inoculated on the surface with colonies re-suspended in LB. Plates were incubated at 37°C for 19h. Swimming motility was assayed using TB plates containing 0.3% agar. Colonies were stabbed into the agar using toothpicks and plates incubated at 37°C for 8 hours.

Co-immunoprecipitation (co-IP)

Strains were grown in LB supplemented with 100 µg/ml tetracycline overnight and diluted back in fresh medium 1:100 and grown until an OD_{600} between 1.5 and 2 was reached. Cells were pelleted and resuspended in PBS at 37°C, then crosslinked with Formaldehyde (250 mM) and incubated for 12 minutes at 37°C. The crosslinking reaction was quenched by addition of Glycine (375 mM). Cells were washed in ice-cold 1x PBS and stored at -20°C. Pellets were resuspended in lysis buffer (20 mM HEPES pH 7.4, 150 mM NaCl, 5% v/v glycerol, 1mM EDTA, 0.2 mg/ml DNAse1, 0.2 mg/ml RNAse, 0.4 mg/ml lysozyme and cOmplete mini antiprotease and PhosSTOP antiphosphatase tabs), lysed by two runs on the French press at 130 PSI and split into soluble and membrane fraction by ultracentrifugation (100 000 g for 30 minutes). The membrane fraction was resuspended in resuspension buffer (20 mM HEPES pH 7.4, 150 mM NaCl, 5% v/v glycerol, 1 mM EDTA, 1% w/v DMM and cOmplete mini antiprotease and PhosSTOP antiphosphatase tabs), incubated for 1 hour at 4°C and the supernatant after ultracentrifugation (100 000 g for 30 minutes) was collected. Samples were mixed with anti-Flag-magnetic beads, incubated 1 hour at 4°C and washed three times with 100 mM ammonium bicarbonate. Elution is performed by on-bead digest with 1.6 M urea, 100 mM ammonium bicarbonate and 5 µg/ml trypsin for 30 minutes at 27°C.

The resulting peptides were prepared for MS (reduction of cysteines, acidification, C18 column purification) and loaded on a PicoFrit fused silica LC column. Mass spectra of ionized peptides were acquired on an Orbitrap Elite. The experiment was replicated 3 times.

Yeast two-hybrid screen for identification of binding partners of PA2781

A yeast two-hybrid screen was performed (Hybrigenics Services) using the full-length *P. aeruginosa* protein PA2781 (amino acids 1-113, vector: pB29 (N-PA2781-LexA-C fusion)) as bait. The prey library was based on the *P. aeruginos*a PAO1 genome, 262 clones were processed. A total of 18.7 million interactions were screened.

Protein expression and purification

BifA histag-GGDEF-EAL (250-678) and histag-EAL (413-678) constructs were expressed in BL21 (DE3) at 18˚C for 16 hours by adding 400 µM IPTG at an O.D600 of 0.6. Cells were lysed by sonication in 20 mM Tris pH 8.0, 200 mM NaCl, 5 mM B-mercaptoethanol, 0.5 mg/ml lysozyme, and protease inhibitor. The proteins were submitted to affinity purification in a HisTrap column (Cytiva) using 20 mM Tris pH 8.0, 200 mM NaCl, 5 mM MgCl2, 5 mM β-mercaptoethanol with a gradient of 10–500 mM imidazole. The fractions containing the target

protein were pooled, concentrated and loaded onto a S200 26/600 gel filtration column (Cytiva) in 20 mM Tris pH 8.0, 5 mM MgCl2, 200 mM NaCl and 2 mM DTT. The peak corresponding to BifA was analyzed by SDS-PAGE to check the purity and the protein was immediately frozen in liquid nitrogen and stored at -80˚C.

PA2781-GB1-histag construct was expressed in BL21 (DE3) under the same conditions as described above for BifA constructs. Cells were lysed by sonication in 20 mM Tris pH 8.0; 200 mM NaCl; 5mM β-mercaptoethanol, 0.5 mg/ml lysozyme, and protease inhibitor. The lysate was loaded onto a HisTrap column (Cytiva) equilibrated with the same buffer and eluted with a gradient of 10–500 mM imidazole. Fractions containing PA2781-GB1-histag were pooled and loaded onto a S200 26/600 gel filtration column in 20 mM Tris pH 8.0, 200 mM NaCl, 5 mM β-mercaptoethanol and 50 mM Arginine/Glutamate. Purified PA2781-GB1-histag was submitted to treatment with TEV protease to cleave the phusion protein GB1. The sample was again loaded onto a HisTrap (Cytiva) column and the flow through containing PA2781 alone was collected and stored at -80˚ C. As for BifA, SDS-PAGE was performed to check the quality of protein purification.

Phosphodiesterase activity

Phosphodiesterase activity of BifA_GGDEF-EAL-histag (250-678) in absence and in presence of various concentrations of PA2781 was measured by online ion exchange chromatography (oIEC) (manuscript under preparation). A reaction mix containing 200 mM Tris pH 8.0, 200 mM NaCl, 5 mM MgCl2, 2 mM DTT, 5 µM BifA_GGDEF-EAL and the appropriate amount of HecE (PA2781) was prepared and left at room temperature for 15 minutes for equilibration. After the pre-incubation time, the reaction was started by the addition of c-di-GMP. Peaks corresponding to c-di-GMP and pGpG were integrated and the amount of nucleotide calculated accordingly to known nucleotide standards.

Microscale thermophoresis (MST)

BifA_GGDEF-EAL-histag (250-678) and HecE were both dialyzed against PBS 1X supplemented with 50 mM Arginine/Glutamate and 5 mM MgCl2. BifA at 200 nM was incubated for 30 min with RED-tris-NTA 2nd Generation Dye for his-tag labelling accordingly to manufacturer's instructions. After centrifugation for 10 min at 4˚ C and 15000 rcf the protein was ready to use. PA2781 was titrated by the employment of serial dilutions (2:1) using 152.5 µM as initial concentration in 16 different capillary tubes. The assay was measured in a Nanotemper Monolith NT.115 MST machine. Settings used were 50 % for LED/excitation power and MST power low. Temperature used was 25 ˚C at excitation type Nano-RED.

Phostag Gels

Samples were grown overnight on LB agar plates supplemented with 100 µg/mL tetracycline at 37°C, cells were scraped from the plates and diluted in LB to an OD_{600} of 0.5. 100 µl were spotted on prewarmed LB plates supplemented with 100 µg/mL tetracycline and 0.5% arabinose where indicated. Plates were incubated at 37°C for 6 hours. Cells were scraped from plates, pelleted, frozen in liquid nitrogen and stored at -80°C. Boiled samples were heated to

95°C for 10 minutes before freezing. Samples were thawn on ice, resuspended in 60 µl lysis buffer and incubated at room temperature for 5 minutes. Samples were then centrifuged at max. speed for 5 minutes at room temperature and 80 µl of the supernatant were mixed with 2X loading buffer. Phostag gels (Separation buffer, 50 µM Phos-Tag Acrylamide, 100 µM MnCl2, 0.1% APS, 0.025% TEMED, 12% Acrylamide) were polymerized three hours at room temperature and stored overnight at 4°C. Samples were run at 100V for 225 minutes at 4°C, then transferred on a membrane by 'wet' transfer. Membranes were blocked overnight in milk. Proteins were detected using specific primary antibodies (anti-Flag 1:7000) and anti-mouse secondary antibodies (1:10000).

Immunoblots

Fig. 5A – Cells were grown overnight in LB supplemented with 100 µg/ml tetracycline, then diluted back 1:100 into fresh LB supplemented with 100 µg/ml tetracycline and 0.05% Triton and grown for 3 hours. Cells were diluted back in fresh LB supplemented with 100 µg/ml tetracycline and 0.05% Triton to a start OD_{600} of 0.05, grown for 1.5 hours then split to cultures with and without induction (0.2% arabinose). Cells were harvested 1.5 hours later.

Fig. *6B* - Cells were grown overnight in LB, then diluted back 1:100 into fresh LB and grown for 4 hours. Cells were diluted back in fresh LB to a start OD_{600} of 0.005 and samples were taken at the following optical densities: ~0.15 (t1, 1h30), ~0.29 (t2, 2h00), ~0.64 (t3, 2h30), ~1.0 (t4, 2h50), ~1.8 (t5, 3h25), ~1.95 (t6, 4h), ~2.5 (t7, 5h).

Harvested cells were normalized in loading buffer, boiled for 10 minutes at 95°C and separated on 15% SDS-acrylamide gel electrophoreses (PAGE). Proteins were detected using specific primary antibodies (anti-Flag 1:7000) and anti-mouse secondary antibodies (1:10000).

Electromobility Shift Assay

5' Cy3-labelled input DNA was generated by PCR (0.5 µM primers 5947 and 5948, PAO1 gDNA, 200 µM dNTPS, 1X GC buffer, 0.6 µl Fusion Polymerase; 98°C 2', 30x – 98°C 15'', 72°C 20'', 72°C 15'' – 72C 7'). 1nM of input DNA and the purified protein were incubated for 10 minutes at room temperature in binding buffer (50 mM Tris pH 8.0, 39 mM NaCl, 10 mM MgCl2, 1 mM DTT, 0.01% Triton, 0.1 mg/ml BSA, 10% Glycerol, 25 µg/ml λ-DNA). Samples were mixed 1:1 with loading buffer (binding buffer + 40% Glycerol and run on 4% native PAA gels (1x TBE, 4% Acrylamid, 0.0875% APS, 0.1% TEMED), BioRad 0.75mm gels) at 100V for 50 minutes.

Chromatin Immunoprecipitation Sequencing

Pre-cultures were grown for 16-24 h in MOPS minimal medium supplemented with 20 mM succinate and appropriate antibiotics and 10 µM IPTG. Cultures were diluted back into fresh medium to a start OD_{600} of 0.01 and grown until an OD_{600} of 1.0 (exponential phase) or for 16 hours (stationary). Cells were harvested and resuspended 10 mM sodium phosphate buffer. Formaldehyde was added to a final concentration of 1.25 % and samples were incubated at 37 °C for 7-10 min. Crosslinking was quenched by addition of 3 M Tris-HCl (pH 7.6) on ice for 30 min. Samples were pelleted, the supernatant discarded and the pellet was washed twice in 1x PBS and stored frozen at -80 °C. Samples were resuspended in ChIP-buffer (16.7 mM Tris-HCl, 167 mM NaCl, 1.2 mM EDTA, 1% Triton X-100, with cOmplete EDTA free protease inhibitor

and incubated on ice for 30 min. Cells were lysed by two passages through the French press at 1 bar. The lysate was sonicated (40 % duty cycle; Total time: 7.5 min; Time ON: 30 sec; Time OFF: 30 sec; 15 cycles) on ice. Samples were cleared by centrifugation and supernatants were transferred frozen at - 80 °C. Immunoprecipitation was performed with anti-HA agarose beads overnight at 4°C. Elution was performed with 1% SDS and 100 mM $NaHCO_3$ for 15 minutes at room temperature, 0.25 M NaCl was added before incubation at 75 °C for 12.5 h. Protein digestion was performed by addition of EDTA (3 mM), Tris-HCl (30 mM, pH 6.5) and Proteinase-K (33 µg/ml), incubated at 45 °C for 2 h. RNase was added and incubated at 37 °C for 1-2 h. DNA extraction was performed using Phenol:Chloroform:Isoamyl Alcohol. DNA was precipitated with 100% EtOH at -80°C for 1 hour and samples were dried at roomtemperature. Size of DNA fragments was confirmed by agarose gel electrophoresis (120 V, 30 min). Sequencing was done by the Quantitative Genomics Facility of Dr. Christian Beissel at the DBSSE. Reads were aligned to the reference genome using Geneious.

Mass spectrometry based proteome analysis

Sample Preparation

Cells were grown in LB supplemented with 30 µg/ml gentamicin and grown for approx. 24h, then diluted back to an OD_{600} of 0.01 in fresh LB supplemented with 30 µg/ml gentamicin and 100 µM IPTG and grown for 20h at 37°C. Cells were harvested and washed three times in ice-cold 1X PBS. After the third wash, the OD_{600} of the samples was measured and 2.5 10^8 bacteria/sample were harvested and stored at -80°C. Samples were lysed in 50 µL of lysis buffer (1% Sodium deoxycholate (SDC), 10 mM TCEP, 100 mM Tris, pH=8.5) using twenty cycles of sonication (30 s on, 30 s off per cycle) on a Bioruptor (Dianode). Following sonication, proteins in the bacterial lysate were reduced by TCEP at 95° C for 10 min. Proteins were alkylated using 15 mM chloroacetamide at 37° C for 30 min and further digested using sequencing-grade modified trypsin (1/50 w/w, ratio trypsin/protein; Promega, USA) at 37° C for 12 hours. After digestion, the samples were acidified using TFA (final 1%). Peptide desalting was performed using iST cartridges (PreOmics, Germany) following the manufactures instructions. After drying the samples under vacuum, peptides were stored at -20° C and dissolved in 0.1% aqueous formic acid solution at a concentration of 0.5 mg/ml upon use.

Mass spectrometry based analysis

Whole proteome analysis: For each sample, 0.5 µg total peptides including 5 fmol/µg were subjected to LC-MS analysis using Sample Block Randomization on a Q-Exactive HF mass spectrometer equipped with a nanoelectrospray ion source (both Thermo Fisher Scientific). Peptide separation was carried out using an EASY nLC-1000 system (Thermo Fisher Scientific) equipped with a RP-HPLC column (75µm × 30cm) packed in-house with C18 resin (ReproSil-Pur C18-AQ, 1.9 µm resin; Dr. Maisch GmbH, Germany) and a custom-made column heater (60° C). Peptides were separated using a linear gradient from 95% solvent A (0.1% formic acid, 99.9% water) and 5% solvent B (80% acetonitrile, 0.1% formic acid, 19.9% water) to 45% solvent B over 60 min, further to 95% solvent B over 2 min and 95% solvent B over 18 min at a flow rate of 0.2 µl/min.

For data dependent acquisition (DDA) analysis each MS1 scan was followed by high-collision-dissociation (HCD) of the 20 most abundant precursor ions with dynamic exclusion for 45 seconds. For MS1, $3x10^6$ ions were accumulated in the Orbitrap cell over a maximum time of 110 ms and scanned at a resolution of 60,000 FWHM (at 200 m/z). MS2 scans were acquired at a target setting of $1x10^5$ ions, accumulation time of 50 ms and a resolution of 15,000 FWHM (at 200 m/z). Singly charged ions and ions with unassigned charge state were excluded from triggering MS2 events. The normalized collision energy was set to 28%, the mass isolation window was set to 1.4 m/z and one microscan was acquired for each spectrum.

Microscopy

Images were acquired using softWoRx 6.0 (GE Healthcare) on a DeltaVision system (GE Healthcare), equipped with a pco.edge sCMOS camera, and an UPlan FL N 100X/1.30 oil objective (Olympus). Cells were grown for approx. 24h in LB (supplemented with appropriate antibiotics) and then diluted back in fresh medium (supplemented with appropriate antibiotics and inducers) to a start OD_{600} of 0.01 and grown for 20 hours. Bacteria were then spotted on 1 % agarose pads prepared with 1X PBS. Images were analyzed using OMERO.web 5.9.1 (University of Dundee & Open Microscopy Environment).

Flow cytometry

Flow cytometry was performed on a BD LSR Fortessa Analyzer. The filter sets were adjusted to the fluorophore mRuby2 which employed the dsRed-H filter. During the measurement, the flow rate was kept around 2-10 000 event/s and 100 000 events were recorded for each sample. Cells were grown in the indicated medium for approx. 24 hours, then diluted back into fresh medium with a starting OD_{600} 0.01 and grown at the indicated temperature and time. Cells were harvested and resuspended in fresh medium supplemented with 30 µg/ml chloramphenicol and incubated for 2 hours at the corresponding temperature. Samples were diluted in 1X filtered PBS for flow cytometry. Flow cytometry data were analysed using the software FlowJo 10.6.1 version. The samples were gated for FSC-H and SSC-H (intact/live bacteria) and the SSC-H and SSC-W (single cell). DsRed-H values for gated populations were exported and analysed using Python.

2.4.1 Culture media used in this study

Artificial Sputum Medium (based on Sriramulu *et al*. 2005)

5 g/l mucin from pig stomach mucosa
4 g/l DNA (low molecular-weight salmon sperm DNA)
5.9 mg/l DTPA (diethylene triamine pentaacetic acid)
5 g/l NaCl
2.2 g/l KCl
1.81 mg/l Tris base
5 g/l casamino acids

Synthetic Cystic Fibrosis Medium (based on Palmer *et al*., 2007)

1.3 mM NaH_2PO_4
1.25 mM Na_2HPO_4
0.348 mM KNO_3
0.271 mM K_2SO_4
0.122 g/l NH_4Cl
1.114 g/l KCl
3.03 g/l NaCl
10 mM MOPS
3.2 mM Glucose
9 mM Lactate
3.6 µM $FeSO_4$
0.2 mM Cysteine
0.6 mM Methionine
0.7 mM Ornithine
0.3 mM Arginine
1.4 mM Serine
1 mM Threonine
1.8 mM Alanine
1.2 mM Glycine
1.7 mM Proline
1.1 mM Isoleucine
1.1 mM Valine
0.8 mM Aspartate
1.5 mM Glutamate
0.5 mM Phenylalanine
0.8 mM Tyrosine
0.01 mM Tryptophan
2.1 mM Lysine
0.5 mM Histidine

MOPS Minimal medium (based on Neidhardt *et al*., 1974)

40 mM MOPS
4 mM Tricine
0.01 mM $FeSO_4$
9.52 mM NH_4Cl
0.5 µM $CaCl_2$
0.52 mM $MgCl_2$
50 mM NaCl
1 X Micronutrients

Micronutrients
3 µM ammonium molybdate tetrahydrate
400 µM boric acid
30 µM cobalt chloride
10 µM cupric sulfate
80 µM manganese chloride
10 µM zinc sulfate

2.4.2 Bacterial strains used in this study

Strains	Description	Reference	Identifier
PAO1	wild type *P. aeruginosa*	Malone *et al* ., 2010	505
PAO1 *hecR* ::Tn	PAO1 with Mariner transposon insertion in *hecR* (*PA2780*)	this study	CM531
Δ*hecR* (*PA2780*)	Unmarked deletion of *hecR* in PAO1	this study	314
Δ*hecRE* (*PA2780 /81*)	Unmarked deletion of *hecE* in PAO1	this study	315
Δ*hecE (PA2781)*	Unmarked deletion of *hecRE* in PAO1	this study	427
Δ*pelA*	Unmarked deletion of *pelA* in PAO1	Broder *et al* ., 2016	1820
Δ*pslABC*	Unmarked deletion of *pslABC* in PAO1	Broder *et al* ., 2016	2028
Δ*pelA* Δ*pslABC*	Unmarked deletion of *pslABC* in Δ*pelA*	Broder *et al* ., 2016	2029
Δ*bifA*	Unmarked deletion of *bifA* in PAO1	this study	3431
Δ*pch*	Unmarked deletion of *pch* in PAO1	Laventie *et al* ., 2019	3428
Δ*rbdA*	Unmarked deletion of *rbdA* in PAO1	this study	3429
Δ*pch* Δ*bifA*	Unmarked deletion of *bifA* in Δ*pch*	this study	3774
Δ*rbdA* Δ*bifA*	Unmarked deletion of *bifA* in Δ*rbdA*	this study	3775
Δ*pch* Δ*rbdA*	Unmarked deletion of *rbdA* in Δ*pch*	this study	3860
Δ3PDE	Unmarked deletion of *bifA* in Δ*pch* Δ*rbdA*	this study	3861
Δ*pelA* Δ*pslABC* Δ*3PDE*	Unmarked deletion of *bifA* in Δ*pelA* Δ*pslABC* Δ*pch* Δ*rbdA*	this study	3925
Δ4DGC	Unmarked deletions of *sadC PA0847 PA5487 PA0338*	this study	1303
Δ*wspR*	Unmarked deletion of *wspR* in PAO1	this study	1464
Δ*sadC*	Unmarked deletion of *sadC* in PAO1	this study	3528
Δ*yfiBNR*	Unmarked deletion of *yfiBNR* in PAO1	Malone *et al* ., 2010	517
PAO1::*wspR* -Flag	PAO1 with *wspR* -Flag, with the Flag tag fused on the 3' end at the original *wspR* locus	this study	2499
Δ*hecRE* ::*wspR* -Flag	PAO1 with *wspR* -Flag in Δ*hecRE*	this study	2500
Δ*wspF* ::*wspR* -Flag	PAO1 with *wspR* -Flag in Δ*wspF*	this study	2555
Δ*wspR* Δ*rbdA*	Unmarked deletion of *rbdA* in Δ*wspR*	this study	3879
Δ*wspR* Δ*bifA*	Unmarked deletion of *bifA* in Δ*wspR*	this study	CM512
Δ*wspR* Δ*rbdA* Δ*bifA*	Unmarked deletion of *bifA* in Δ*wspR* Δ*rbdA*	this study	3928
Δ*hecRE* Δ*bifA*	Unmarked deletion of *bifA* in Δ*hecRE*	this study	CM516
Δ*hecRE* Δ*wspR*	Unmarked deletion of *wspR* in ΔhecRE	this study	2383
Δ*hecRE* Δ*wspR* Δ*bifA*	Unmarked deletion of *bifA* in Δ*wspR* Δ*hecRE*	this study	CM529
Δ*hecR* attTn7::*hecR* -Flag	Δ*hecR* with *hecR* -Flag (C-terminal Flag tag) under the control of the native promoter, inserted at the att::Tn7 locus.	this study	636
Δ*hecRE* attTn7::*hecE* -Flag	Δ*hecRE* with *hecE* -Flag (C-terminal Flag tag) in the native operon organization, inserted at the att::Tn7 locus.	this study	637
hecRE -2mRuby2	*hecRE* -2x(RBSSYN-mRuby2)	this study	4179
Δ*hecR -2mRuby2*	Unmarked integration of *hecRE -2mRuby2* reporter with deletion of *hecR* in PAO1	this study	4965
Δ*hecRE -2mRuby2*	Unmarked integration of *hecRE -2mRuby2* reporter with deletion of *hecE* in PAO1	this study	4966
Δ*hecE -2mRuby2*	Unmarked integration of *hecRE -2mRuby2* reporter with deletion of *hecRE* in PAO1	this study	4967
Δ*rsmA hecRE -2mRuby2*	Unmarked integration of *hecRE -2mRuby2*	this study	4402

	reporter in Δ*rsmA*		
Δ*retS hecRE -2mRuby2*	Unmarked integration of *hecRE -2mRuby2* reporter in Δ*retS*	this study	4403
Δ*gacS hecRE -2mRuby2*	Unmarked integration of *hecRE -2mRuby2* reporter in Δ*gacS*	this study	5095
Δ*rsmN hecRE -2mRuby2*	Unmarked integration of *hecRE -2mRuby2* reporter in Δ*rsmN*	this study	4758
Δ*rsmA/ hecRE -2mRuby2*	Unmarked integration of *hecRE -2mRuby2* reporter in Δ*rsmA* Δ*rsmN*	this study	4929
Δ*ladS hecRE -2mRuby2*	Unmarked integration of hecRE-*2mRuby2* reporter in Δ*ladS*	this study	4961

2.4.3 Plasmids used in this study

Name	Description	Reference	Identifier
Episomal constructs			
pME6032	pVS1 derived shuttle vector, for gene expression under the control of the IPTG inducible Ptac promoter (Tet^R)	Heeb *et al* ., 2000	3897
pGM6032	pME6032 based vector, Tet cassette replaced with *aacCI* gentamycin resistance cassette (Gm^R)	Malone *et al* ., 2012	1142
pME-*araC*	pME6032 with the lac-promoter and *lacI* replaced with the *araC* pBAD promoter fragment from pBAD18s (Tet^R)	Malone *et al* ., 2010	3512
pMEaraC::*hecR*	pMEaraC carrying *hec* (*PA2780*) of *P. aeruginosa* PAO1 (Tet^R)	this study	1187
pMEaraC::*hecE*	pMEaraC carrying *hecE* (*PA2781*) of *P. aeruginosa* PAO1 (Tet^R)	this study	1188
pMEaraC::*hecRE*	pMEaraC carrying *hecRE* (*PA2780 /81*) of *P. aeruginosa* PAO1 (Tet^R)	this study	1189
pMEtac::*rsmZ*	pME6359 (ptac-rsmZ) (Tet^R)	Heeb *et al* ., 2002	566
pMEtac::*rsmY*	pME6918 (ptac-rsmY) (Tet^R)	Valverde *et al* ., 2003	567
pGM::*hecR*	pGM6032 carrying *hecR* of *P. aeruginosa* PAO1 (Gm^R)	this study	3588
pGM::*hecE*	pGM6032 carrying *hecE* of *P. aeruginosa* PAO1 (Gm^R)	this study	1209
pGM::*hecRE*	pGM6032 carrying *hecRE* of *P. aeruginosa* PAO1 (Gm^R)	this study	4954
pGM::*hecR*-HA	pGM6032 carrying *hecR*-HA of *P. aeruginosa* PAO1 (Gm^R)	this study	3511
pGM::*pdeH*	pGM6032 carrying *pdeH* of *E.coli* MG1655 (Gm^R)	this study	4260
pGM::*dgcZ*	pGM6032 carrying *dgcZ* of *E.coli* MG1655 (Gm^R)	this study	4261
pGM::*rsmA*	pGM6032 carrying *rsmA* of *P. aeruginosa* PAO1 (Gm^R)	this study	5092
pGM::*retS*	pGM6032 carrying *retS* of *P. aeruginosa* PAO1 (Gm^R)	this study	5093
pGM::*ladS*	pGM6032 carrying *ladS* of *P. aeruginosa* PAO1 (Gm^R)	this study	5303
pGM::*gacS*	pGM6032 carrying *gacS* of *P. aeruginosa* PAO1 (Gm^R)	this study	4937
pGM::BldD2-eGFP	pGM6032 carrying BldD2-eGFP with BBa_J23115 promoter (Gm^R)	Kazmierczak, unpubl.	6177

Name	Description	Reference	Identifier
Integrative constructs			
pEX18Gm::*wspR* -Flag	pEX18Gm carrying *wspR*-Flag as EcoRI-HindIII fragment	this study	2428
pME3087::Δ*hecR*	pME3087 carrying *hecR* deletion cassette as EcoRI-BamHI fragment	this study	1192
pME3087::Δ*hecE*	pME3087 carrying *hecE* deletion cassette as EcoRI-BamHI fragment	this study	1193
pME3087::Δ*hecRE*	pME3087 carrying *hecRE* deletion cassette as EcoRI-bamHI fragment	this study	1194
pEX18Gm::Δ*gacS*	pEX18Gm carrying *gacS* deletion cassette as HindIII-BamHI fragment	this study	4938
pEX18Gm::*hecRE -2mRuby2*	pEX18Gm carrying *hecRE -2mRuby2* reporter as EcoRI-bamHI fragment	this study	4118
pEX18Gm::Δ*hecR -2mRuby2*	pEX18Gm carrying Δ*hecR -2mRuby2* reporter as EcoRI-BamHI fragment	this study	4336
pEX18Gm::Δ*hecE -2mRuby2*	pEX18Gm carrying Δ*hecE -2mRuby2* reporter as EcoRI-BamHI fragment	this study	4120
pEX18Gm::Δ*hecRE -2mRuby2*	pEX18Gm carrying Δ*hecRE -2mRuby2* reporter as EcoRI-BamHI fragment	this study	4337
pEX18Gm::Δ*bifA*	pEX18Gm carrying *bifA* deletion cassette as XbaI-XmaI fragment	this study	3421
pEX18Gm::Δ*rbdA*	pEX18Gm carrying *rbdA* deletion cassette as BamHI-EcoRI fragment	this study	3776
pEX19::Δ*wspR*	pEX19 carrying WspR deletion cassette, GmR	Hickman *et al* ., 2005	677
pEX18Gm::Δ*rsmN*	pEX18Gm carrying *rsmN* deletion cassette as SacI-HindIII fragment	this study	4686
mCTX1::P*rsmY -mRuby2*	mCTX1-Ruby2 carrying rsmY-mRuby2 reporter as SacI-BamHI fragment	this study	4458
mCTX1::P*rsmZ -mRuby2*	mCTX1-Ruby2 carrying rsmZ-mRuby2 reporter as SacI-BamHI fragment	this study	4459
pUC18-Tn7Gm::*hecR*-Flag	pUC18-Tn7Gm carrying *hecR*-Flag under the control of its natural promoter as BamHI-SpeI fragment	this study	584
pUC18-Tn7Gm::*hecR*/*hecE*-Flag	pUC18-Tn7Gm carrying *hecE*-Flag in the native operon organization as BamHI-SpeI fragment	this study	585

2.4.4 Primers used in this study

Name	Sequence	Description
A	ccgaattcatgctaggtaccc	*hecR* F (pMEaraC)
B	cactcgagcctcacagttcactcc	*hecR* R (pMEaraC)
C	gcggataacaatttcacacaggaaacagaattcgagctcccatgctaggtacccggctaaaagc	*hecR* F (pGM)
D	gatcctcgagtcacagttcactccttgtgcgtac	*hecR* R (pGM)
E	ccgaattcgtgaacaaaagcttg	*hecE* F
F	cactcgagcctcagcctcgcgccag	*hecE* R
G	gatcctcgagtcagcctcgcgccagttgc	*hecRE* R (pGM)
H	tgcagaattcttcagtcgaggaagtagtaataaggagagtagtatgataaggcaggttatccagc	*pdeH* F
I	gtcaccatggttatagcgccagaaccgcc	*pdeH* R
J	tgcagaattccaccactgacctacaaaagtaaggaggaagactaatgatcaagaagacaacgg	*dgcZ* F
K	gtcaccatggttaaactcggttaatcacattttg	*dgcZ* R
L	gatccccggggtgttcaaggatctcggc	*gacS* F
M	gatcggtacctcagagttcgctggagtc	*gacS* R
N	gatcgaattcatgctgattctgactcgtcg	*rsmA* F
O	gatcctcgagttaatggtttggctcttgatctttc	*rsmA* R
P	gatcgaattcgtggtacggcttcggatc	*retS* F
Q	gatcctcgagtcaggagggcagggcg	*retS* R
R	gatcgaattcatgcggcactggctgattc	*ladS* F
S	gatcggtacctcaggcggacttggtgacg	*ladS* R
T	gatcggatcccaggagtgatattagcgattc	*rsmZ*p F
U	gatcaagcttgggaatgacctctgcgtg	*rsmZ*p R
V	gatcgagctcgctgggaaggctcgcg	*rsmY*p F
W	gatcggatccggtttgaagattacgcatctctg	*rsmY*p R
X	ccgaattcctgttgatgcgactc	*hecR* up F
Y	ttcactcctccgggtacctagcatc	*hecR* up R
Z	ggtacccggaggagtgaactgtgaac	*hecR* dn F
AA	ccggatccgcaaggctggcgttc	*hecR* dn R
AB	ccgaattcagtatcgtcccgatc	*hecE* up F
AC	tcgcgccagcaagcttttgttcac	*hecE* up R
AD	aaaagcttgctggcgcgaggctgag	hecE dn F
AE	ccggatcccgagcatgcgggtag	*hecE* dn R
AF	tcgcgccagccgggtacctagcatc	*hecRE* up R
AG	ggtacccggctggcgcgaggctgag	*hecRE* dn F
AH	gccaagcttgcatgcctgcaggtcgactctagaggatcccatggcctccagcttcttctgg	*hecRE*-2mR up F
AI	cctccttatcctcaaatctagcgtatgcgctctcagcctcgcgccagttg	*hecRE*-2mR up R
AJ	gctagatttgaggataaggaggccgttttatggttagcaaaggtgaagaac	*hecRE*-2mR mid F
AK	ctagccgcgccggggccttacttgtacagctcgtccatg	*hecRE*-2mR mid R
AL	catggacgagctgtacaagtaaggccccggcgcggctag	*hecRE*-2mR down F
AM	gcggataacaatttcacacaggaaacagctatgaccatgattacgaattccgccttcgcggctgcgc	*hecRE*-2mR dn R
AN	gctaggtacccggctaaaagccgagctgacgcgtttcatcgaacag	Δ*hecR*-2mR mid F
AO	ctgttcgatgaaacgcgtcagctcggcttttagccgggtacctagc	Δ*hecR*-2mR mid R
AP	caaaagcttggattcagactcgatactgcaactggcgcgag	Δ*hecE*-2mR mid F

AQ	ctcgcgccagttgcagtatcgagtctgaatccaagcttttg	Δ*hecE*-2mR mid R
AR	gatcgaattcctaccactcgcgttcgtacatcg	*wspR*-Flag up F
AS	catggtctttgtagtcgaagcccgccggggccggcggcaccggctgttcc	*wspR*-Flag up R
AT	gatgacgacgataaatagtaagcggcgcgcggcggccatgcgtcg	*wspR*-Flag dn F
AU	gatcaagcttctcggacagctcgatgatagtgg	*wspR*-Flag dn R
AV	gatctctagagatcgtcaagagctcctccg	Δ*bifA* up F
AW	gcctgttctgatcagggccgcagtttcaaggggccttccttg	Δ*bifA* up R
AX	gatccccgggcaccgatgcctgcctggtc	Δ*bifA* dn R
AY	caaggaaggccccttgaaactgcggccctgatcagaacaggc	Δ*bifA* dn F
AZ	atgcggatcctgtcgggcggtcagcggcag	Δ*rbdA* up F
BA	cttcgccccgcggtcacctacattccatctaccattcaaactggcgc	Δ*rbdA* up R
BB	gcgccagtttgaatggtagatggaatgtaggtgaccgcggggcgaag	Δ*rbdA* dn F
BC	gcatgaattccttggggaaggcgttttcgtagacg	Δ*rbdA* dn R
BD	gatcaagcttaggctgacatcgcagacatc	Δ*gacS* up F
BE	ctggtggaggacaggtgcagtacgcgcccttg	Δ*gacS* up R
BF	caaggggcgcgtactgcacctgtcctccaccag	Δ*gacS* dn F
BG	gatcggatccgtattgatcagcatcgcgcc	Δ*gacS* dn R
BH	gatcgagctcgaagcgccacaagcatcatc	Δ*rsmN* up F
BI	gcaaggacgcggaacatgtgacgaacggtagaaagtaaaagc	Δ*rsmN* up R
BJ	gcttttactttctaccgttcgtcacatgttccgcgtccttgc	Δ*rsmN* dn F
BK	ctcaagcttctgaatggcgggagtatgaaaagtctcgagaggttgagctgattgaggcg	Δ*rsmN* dn R
BL	gcggataacaatttcacacaggaaacag	pEX18 R
BM	gaaggtgagcaggtgcagcgctgc	*hec* promoter F
BN	gcttttagccgggtacctagcatcc	*hec* promoter R

3 DISCUSSION AND PERSPECTIVES

Pseudomonas aeruginosa is a ubiquitous opportunistic human pathogen that can cause both acute and chronic infections. In patients with cystic fibrosis (CF) *P. aeruginosa* infections are the leading cause of morbidity and mortality due to the establishment of persistent lung infections (Malhotra *et al*., 2019). Adaptation during lung infection in CF patients leads to the formation of distinct phenotypes, such as small colony variants (SCV), that have been linked to increased antibiotic resistance and poor clinical outcomes (Malone, 2015).

Due to the implication of SCVs in persistent lung infections, we decided to study the formation of SCVs in *P. aeruginosa* in more detail. We used a transposon screen to identify new regulators of SCV formation and found many transposon insertions mapped to the *PA2780* gene, besides insertions in genes of the Yfi and Wsp systems that have been previously linked to the SCV morphotype (D'Argenio *et al*., 2002; Malone *et al*., 2010). Surprisingly, the frequency of transposon insertions in *PA2780* (*hecR*) was higher than in the regulators of the Yfi and Wsp systems (*yfiR* and *wspF),* even though these genes are larger, indicating that the *hec* module is a potent regulator of SCV formation.

In detail study of the *hec* module revealed that the SCV morphology in the *hecR* transposon mutant was due to increased expression of *hecE* and not *hecR* disruption. Ectopic expression of *hecE* augmented c-di-GMP levels and affected biofilm formation, cellular aggregation, and swimming, swarming, and twitching motility. Our findings indicated that the regulation of c-di-GMP dependent phenotypes was mediated by HecE independently of HecR. This stands in contrast to previously published results (Wang *et al*., 2014), although the absence of certain data together with vague descriptions of methods and conditions, make it difficult to compare the datasets in detail. We found that HecR had no impact on c-di-GMP dependent phenotypes in the absence of HecE and that the observed phenotypes of the Δ*hecR* mutant could be explained via autoregulation of the module by HecR.

While our findings indicated that HecE boosts c-di-GMP levels, the mechanism behind remained unclear. The absence of known c-di-GMP regulating domains in HecE prompted us to explore possible interaction partners and led to identification of the phosphodiesterase BifA in both the Y2H and the Co-IP assay. The interaction of HecE with BifA was confirmed *in vitro* revealing that HecE inhibited the phosphodiesterase activity of BifA. Intriguingly, BifA inactivation alone was not sufficient to reproduce HecE-mediated phenotypes, a notion that

was supported by the absence of SCVs formed upon transposon insertions in *bifA*. In line with this, no other phosphodiesterase was identified in the transposon screen, indicating that inactivation of a single phosphodiesterase was not sufficient to induce SCV formation in our conditions. This notion, together with the observation that even a mutant lacking the three potent phosphodiesterases BifA, Pch, and RbdA did not induce the strong SCV phenotype observed by ectopic expression of *hecE* led us to the conclusion that HecE must affect diguanylate cyclases in addition.

A subsequent SCV-suppressor transposon screen revealed the Wsp chemosensory system as downstream target of HecE, in line with findings that the Wsp cascade is a frequent target for mutations leading to SCVs in CF lung infections (Smith *et al*., 2008). Indeed, most of the HecE-mediated phenotypes were lost in a *wspR* deletion strain, arguing that WspR activity was the main cause of the observed phenotypes. The diguanylate cyclase activity of WspR depends on its phosphorylation status (Hickman *et al*., 2005), and our results confirmed that WspR phosphorylation was increased upon *hecE* expression, thereby upregulating WspR activity and increasing c-di-GMP levels. Since neither WspR nor other components of the Wsp system had been identified in the Y2H or Co-IP assays, this suggested that the effects of HecE on WspR activity are mediated by additional factors. PA1243, an orphan histidine kinase response regulator hybrid (Hsu *et al*., 2008), was identified as probable interaction partner of HecE in the Y2H screen and could be the link between HecE and WspR activity. A mutant in *PA1243* showed reduced biofilm formation (Müsken *et al*. 2010) and one could speculate that PA1243 controls WspR phosphorylation and thereby c-di-GMP synthesis and biofilm formation in a HecE-mediated manner.

Even though the exact mechanism of WspR activation by HecE remains unclear, our observations imply that regulation of BifA and WspR activity is enough to explain HecE-mediated phenotypes, since ectopic *hecE* expression in a *wspR bifA* double mutant had no additional impact on biofilm formation. Intriguingly, some phenotypes like biofilm formation were more dependent on BifA activity, while SCV formation relied on WspR activity, arguing that it is the dual activity of HecE that confers such wide ranged effects.

One of the effects we observed were HecE-mediated nicks in the growth curves, likely caused by c-di-GMP mediated cell aggregation (Borlee *et al*., 2010; Hickman *et al*., 2005; Irie *et al*., 2012). In line with previous findings, the HecE-mediated effects on growth were abolished in mutants lacking the Psl exopolysaccharide. Together with the observation that

HecE induced the SCV morphotype in mutants lacking either the Pel or Psl exopolysaccharides, this indicated that the *hec* module upregulates production of both Pel and Psl. Since surface glycans are exploited by bacteriophages as primary receptors (Bertozzi Silva *et al*., 2016) the finding that HecE upregulates their production encouraged us to investigate if the *hec* module would sensitize *P. aeruginosa* for phage infection. The screening of sewage water samples resulted in the discovery of a new phage named Knedl that infects *P. aeruginosa* upon high c-di-GMP levels in a Psl-dependent manner. Besides the role as primary (or secondary) receptor, surface glycans might act as support for directional movement of the phage towards the cell surface by employing enzymes like polysaccharide depolymerases (Broeker and Barbirz, 2017; Latka *et al*. 2017). If Knedl also encodes for such an enzyme, this would open up an opportunity for controlling *P. aeruginosa* infections, as a loss of Psl would reduce biofilm formation and pathogenicity. To our knowledge this is the first time that *P. aeruginosa* exopolysaccharides were described as phage receptors. Also, our data present one of the few direct links between c-di-GMP and phage infection (Junkermeier and Hengge 2021; Sellner *et al*., 2021; De Smet *et al*., 2021), despite the significance of the c-di-GMP signaling network.

Intrigued by the findings that HecE upregulates exopolysaccharide production and thereby increases phage sensitivity and biofilm formation, we next focused on determining under which conditions *hecE* is expressed. The initial characterization of the *hec* module suggested autoregulation by the transcription factor HecR. In line with these observations, we found that HecR binds specifically to the *hec* promoter region and increases expression and cellular levels of HecR and HecE. In contrast to our results showing that HecR did not bind to regions beyond the *hecRE* locus, Wang *et al*. had demonstrated that HecR binds to the *rsmZ* promoter region *in vitro* suggesting that our ChIP-seq conditions favored binding of HecR to the *hecRE* locus instead of the *rsmZ* promoter region. In agreement with previous findings that HecR increases *rsmZ* expression (Wang *et al*., 2014), we observed that HecR increased *rsmZ* expression between 10 and 15 hours, even though it repressed expression at later times. A similar repression effect was found for *rsmY*.

Expression of the small regulatory RNAs *rsmY*/*Z* is under control of GacS/A two-component system a network controlling the acute to chronic infection switch. When expressed, *RsmY* and *RsmZ* control activity of the RNA binding protein RsmA, by sequestering it away from its mRNA targets (Francis, *et al*., 2017). Therefore the control of *rsmY*/*Z* expression by *HecR* together with the post-transcriptional control of RsmA on *hec* expression

(Brencic and Lory, 2009) provide a second feedback loop on top of HecR autoregulation. These feedback loops are likely the cause for the heterogeneous expression of the *hec* module, as they stabilize stochastic fluctuations in gene expression (Mcadams and Arkin, 1997).

Heterogeneous expression in stationary phase was dependent on HecR since the subpopulation expressing the *hec* reporter disappeared in a Δ*hecR* mutant, while leaky expression of *hecR* under control of an IPTG-inducible promoter stimulated expression in all cells. Therefore, autoregulation by HecR is the key factor for the heterogeneous expression. Surprisingly, heterogeneity was still observed in the Δ*rsmA* mutant where the post-transcriptional control of RsmA on *hec* expression was relieved. This strengthened the notion, that heterogeneity is a characteristic of the *hec* module, while the Gac/Rsm cascade acts as "gatekeeper", controlling both frequency and intensity of *hec* expression.

Furthermore, we observed that *hec* expression was repressed during exponential phase and that even ectopic expression of *hecR* could not boost expression levels to those observed in stationary phase. Intriguingly, the effects during exponential phase are not mediated by the Gac/Rsm cascade. Consequently, there must be additional factors controlling *hec* expression during exponential phase. It is possible that additional growth dependent transcription factors interfere with *hec* expression (Babin *et al*., 2016) or that HecR protein stability is controlled by growth phase dependent proteases (Kamal *et al.*, 2019).

In addition to growth phase dependent effects on *hec* expression, we observed that subinhibitory concentrations of tetracycline and changes in temperature also impact expression. Since temperature plays an important role during infection of warm-blooded hosts, this cue could be used to increase c-di-GMP levels in a HecE dependent manner, thereby promoting chronic infections.

Taken together, we identified a new c-di-GMP controlling effector, HecE that interacts with two key players of c-di-GMP turnover. Due to the control of both the phosphodiesterase BifA and the diguanylate cyclase WspR activity, the HecE-mediated downstream affects are wide ranged, including induction of SCV formation, biofilm formation, as well as modulation of swimming, swarming, and twitching motility. Furthermore, we observed that *hecE* expression is stochastic in stationary phase and that this heterogeneity is relying on HecR and can be overwritten by the control of the global Gac/Rsm cascade. The Gac/Rsm cascade inversely regulates factors involved in acute infection (type III secretion system, motility) and chronic

infection (type VI secretion system, biofilm formation, pyocyanin). Since the *hec* module also controls exopolysaccharide production and c-di-GMP levels, certain outputs of the Gac/Rsm cascade could therefore be assigned to HecE-mediated effects.

The Gac/Rsm cascade had been previously linked to the c-di-GMP network via translational inhibition of the diguanylate cyclase SadC by RsmA (Moscoso *et al*., 2014) and activation of the diguanylate cyclase HsbD via the HptB branch of the cascade (Valentini *et al*., 2016). Our findings provide therefore an additional link to c-di-GMP by connecting the Gac/Rsm cascade with the phosphodiesterase BifA and the diguanylate cyclase WspR. BifA seems to counterbalance c-di-GMP levels produced by SadC and at least one additional diguanylate cyclase, thereby controlling swarming motility and exopolysaccharide production (Kuchma *et al*., 2007; Merritt *et al*., 2007). Thus, the Gac/Rsm controlled HecE-BifA interaction would affect SadC downstream signals beyond the translational regulation by RsmA. Not only do our findings strengthen the link between the Gac/Rsm cascade and regulation of motility via the HecE/BifA/SadC axis but they also add a link to WspR-mediated changes in c-di-GMP levels and SCV formation. This is in line with the RsmA-controlled production of the exopolysaccharides Pel and Psl. RsmA has an overall negative effect on Pel and Psl production by direct repression of *psl* translation (Irie *et al*., 2010) and indirectly via repressing translation of the transcription factor *vfr* (Irie *et al*. 2020). Vfr inhibits *fleQ* expression (Dasgupta *et al*., 2002) and thereby FleQ-related *pel* and *psl* expression (Hickman and Harwood, 2009). As FleQ repression of *pel* and *psl* expression is relieved by c-di-GMP (Hickman and Harwood, 2009), the before mentioned connections between the Gac/Rsm cascade and c-di-GMP reinforce the effects of RsmA on exopolysaccharide production. HecE-mediated upregulation of Pel and Psl production of Pel and Psl strengthens thereby control imposed by the Gac/Rsm cascade.

One of the questions needed to be answered next is the implication of heterogeneous *hecE* expression on phenotypes such as swarming, biofilm formation, and phage sensitivity. We had observed that swarming motility was suppressed in wild type PAO1 compared to the hyperswarming phenotype of *hecRE* deletion strains. Recent findings indicated that a small subpopulation of non-motile cells could suppress swarming of the wild type majority in a T4P and exopolysaccharide dependent manner (Lewis *et al*., 2021). This strengthens the idea that stochastic expression of *hecRE* impairs swarming motility and that small changes in the frequency of *hec*-expressing cells would be sufficient to switch between a motile and a non-motile population. Additionally the heterogeneous expression of *hec* and subsequent Psl

exopolysaccharide production could act as nucleation centers for biofilm formation (Kragh *et al*., 2018), while the boost in *hecE* expression during biofilm formation would serve as aid to maintain high c-di-GMP levels and exopolysaccharide production.

Considering these interconnections, the *hecRE* module plays a key role in mediating the switch from acute to chronic infection governed by the Gac/Rsm cascade and the heterogeneous expression of *hecRE* could serve as additional bet-hedging strategy to provide fitness advantages during infection.

4 LIST OF FIGURES AND TABLES

4.1 List of Figures

4.2 List of Supplementary Figures

4.3 List of Tables

4.4 List of Supplementary Tables

5 BIBLIOGRAPHY

An, Shuwen, Ji Wu, and Lian-hui Zhang. 2010. "Modulation of Pseudomonas Aeruginosa Biofilm Dispersal by a Cyclic-Di-GMP Phosphodiesterase with a Putative Hypoxia-Sensing Domain □ †." 76(24): 8160–73.

Andersen, Jens Bo et al. 2021. "Induction of Native C-Di-GMP Phosphodiesterases Leads to Dispersal of Pseudomonas Aeruginosa Biofilms." *Antimicrobial Agents and Chemotherapy* 65(4).

Armbruster, Catherine R. et al. 2020. "Erratum: Correction: Heterogeneity in Surface Sensing Suggests a Division of Labor in Pseudomonas Aeruginosa Populations (ELife (2019) 8 PII: E59154)." *eLife* 9: 1–29.

Arora, Naveen Kumar. 2015. *Plant Microbes Symbiosis: Applied Facets*. ed. Naveen Kumar Arora. Springer India.

Aspedon, Arden, Kelli Palmer, and Marvin Whiteley. 2006. "Microarray Analysis of the Osmotic Stress Response in Pseudomonas Aeruginosa." 188(7): 2721–25.

Babin, Brett M. et al. 2016. "SutA Is a Bacterial Transcription Factor Expressed during Slow Growth in Pseudomonas Aeruginosa." *Proceedings of the National Academy of Sciences of the United States of America* 113(5): E597–605.

Bajolet-Laudinat, O. et al. 1994. "Cytotoxicity of Pseudomonas Aeruginosa Internal Lectin PA-I to Respiratory Epithelial Cells in Primary Culture." *Infection and Immunity* 62(10): 4481–87.

Balasubramanian, Deepak, Hansi Kumari, and Kalai Mathee. 2014. "Pseudomonas Aeruginosa AmpR: An Acute-Chronic Switch Regulator." *Pathogens and Disease* 73(2): 1–14.

Bantinaki, Eleni et al. 2007. "Adaptive Divergence in Experimental Populations of Pseudomonas Fluorescens. III. Mutational Origins of Wrinkly Spreader Diversity." *Genetics* 176(1): 441–53.

Bar-On, Yinon M., Rob Phillips, and Ron Milo. 2018. "The Biomass Distribution on Earth." *Proceedings of the National Academy of Sciences of the United States of America* 115(25): 6506–11.

Baraquet, Claudine, and Caroline S. Harwood. 2013. "Cyclic Diguanosine Monophosphate Represses Bacterial Flagella Synthesis by Interacting with the Walker a Motif of the Enhancer-Binding Protein FleQ." *Proceedings of the National Academy of Sciences of the United States of America* 110(46): 18478–83.

Barbier, Mariette et al. 2014. "From the Environment to the Host: Re-Wiring of the Transcriptome of Pseudomonas Aeruginosa from 22°C to 37°C." *PLoS ONE* 9(2).

Bellini, Dom et al. 2014. "Crystal Structure of an HD-GYP Domain Cyclic-Di-GMP Phosphodiesterase Reveals an Enzyme with a Novel Trinuclear Catalytic Iron Centre." *Molecular Microbiology* 91(1): 26–38.

Bertozzi Silva, Juliano, Zachary Storms, and Dominic Sauvageau. 2016. "Host Receptors for Bacteriophage Adsorption." *FEMS Microbiology Letters* 363(4): 1–11.

Bhagirath, Anjali Y. et al. 2017. "Characterization of the Direct Interaction between Hybrid Sensor Kinases PA1611 and RetS That Controls Biofilm Formation and the Type III Secretion System in Pseudomonas Aeruginosa." *ACS Infectious Diseases* 3(2): 162–75.

Boedicker, James Q., Meghan E. Vincent, and Rustem F. Ismagilov. 2009. "Microfluidic Confinement of Single Cells of Bacteria in Small Volumes Initiates High-Density Behavior of Quorum Sensing and Growth and Reveals Its Variability." *Angewandte Chemie - International Edition* 48(32):

5908–11.

Booth, Ian R. 2002. “Stress and the Single Cell: Intrapopulation Diversity Is a Mechanism to Ensure Survival upon Exposure to Stress.” *International Journal of Food Microbiology* 78(1–2): 19–30.

Borlee, Bradley R. et al. 2010. “Pseudomonas Aeruginosa Uses a Cyclic-Di-GMP-Regulated Adhesin to Reinforce the Biofilm Extracellular Matrix.” *Molecular Microbiology* 75(4): 827–42.

Brencic, Anja et al. 2009. “The GacS/GacA Signal Transduction System of Pseudomonas Aeruginosa Acts Exclusively through Its Control over the Transcription of the RsmY and RsmZ Regulatory Small RNAs.” *Molecular Microbiology* 73(3): 434–45.

Brencic, Anja, and Stephen Lory. 2009a. “Determination of the Regulon and Identification of Novel MRNA Targets of Pseudomonas Aeruginosa RsmA.” *Molecular microbiology* 72(3): 612–32. http://www.ncbi.nlm.nih.gov/pubmed/19426209.

———. 2009b. “Determination of the Regulon and Identification of Novel MRNA Targets of Pseudomonas Aeruginosa RsmA.” *Molecular Microbiology* 72(3): 612–32.

Broder, Ursula N., Tina Jaeger, and Urs Jenal. 2016. “LadS Is a Calcium-Responsive Kinase That Induces Acute-to-Chronic Virulence Switch in Pseudomonas Aeruginosa.” *Nature Microbiology* 2(1): 1–11. http://dx.doi.org/10.1038/nmicrobiol.2016.184.

Broeker, Nina K., and Stefanie Barbirz. 2017. “Not a Barrier but a Key: How Bacteriophages Exploit Host’s O-Antigen as an Essential Receptor to Initiate Infection.” *Molecular Microbiology* 105(3): 353–57.

Camilli, Andrew, and Bonnie L Bassler. 2006. “Bacterial Small-Molecule Signaling Pathways.” *Science* 311(5764): 1113–16. http://www.ncbi.nlm.nih.gov/pubmed/16497924%0Ahttp://www.ncbi.nlm.nih.gov/pubmed/16497924.

Chambonnier, Gaël et al. 2016. “The Hybrid Histidine Kinase LadS Forms a Multicomponent Signal Transduction System with the GacS/GacA Two-Component System in Pseudomonas Aeruginosa.” *PLoS Genetics* 12(5): 1–30.

Chan, Benjamin K. et al. 2016. “Phage Selection Restores Antibiotic Sensitivity in MDR Pseudomonas Aeruginosa.” *Scientific Reports* 6(March): 1–8. http://dx.doi.org/10.1038/srep26717.

Chihara, Kotaro et al. 2021. “Global Identification of RsmA/N Binding Sites in Pseudomonas Aeruginosa by in Vivo UV CLIP-Seq.” *RNA Biology* 00(00): 1–16. https://doi.org/10.1080/15476286.2021.1917184.

Choi, Yusang et al. 2011. “Growth Phase-Differential Quorum Sensing Regulation of Anthranilate Metabolism in Pseudomonas Aeruginosa.” *Molecules and Cells* 32(1): 57–65.

Choy, Weng-keong et al. 2004. “MorA Defines a New Class of Regulators Affecting Flagellar Development and Biofilm Formation in Diverse Pseudomonas Species.” 186(21): 7221–28.

Christen, Matthias et al. 2010. “Asymmetrical Distribution of the Second Messenger C-Di-GMP upon Bacterial Cell Division.” *Science* 328(5983): 1295–97.

Cobián Güemes, Ana Georgina et al. 2016. “Viruses as Winners in the Game of Life.” *Annual Review of Virology* 3: 197–214.

D’Argenio, David A., M. Worth Calfee, Paul B. Rainey, and Everett C. Pesci. 2002. “Autolysis and Autoaggregation in Pseudomonas Aeruginosa Colony Morphology Mutants.” *Journal of Bacteriology* 184(23): 6481–89.

Dasgupta, Nandini et al. 2002. “FleQ, the Gene Encoding the Major Flagellar Regulator of Pseudomonas Aeruginosa, Is Σ70 Dependent and Is Downregulated by Vfr, a Homolog of Escherichia Coli Cyclic AMP Receptor Protein.” *Journal of Bacteriology* 184(19): 5240–50.

———. 2003. “A Four-Tiered Transcriptional Regulatory Circuit Controls Flagellar Biogenesis in Pseudomonas Aeruginosa.” *Molecular Microbiology* 50(3): 809–24.

Déziel, Eric, Yves Comeau, and Richard Villemur. 2001. “Initiation of Biofilm Formation by Pseudomonas Aeruginosa 57RP Correlates with Emergence of Hyperpiliated and Highly Adherent Phenotypic Variants Deficient in Swimming , Swarming , and Twitching Motilities.” *Journal of Bacteriology* 183(4): 1195–1204.

Dion, Moïra B., Frank Oechslin, and Sylvain Moineau. 2020. “Phage Diversity, Genomics and Phylogeny.” *Nature Reviews Microbiology* 18(3): 125–38. http://dx.doi.org/10.1038/s41579-019-0311-5.

Dötsch, Andreas et al. 2009. “Genomewide Identification of Genetic Determinants of Antimicrobial Drug Resistance in Pseudomonas Aeruginosa □.” 53(6): 2522–31.

Driscoll, James A., Steven L. Brody, and Marin H. Kollef. 2007. “The Epidemiology, Pathogenesis and Treatment of Pseudomonas Aeruginosa Infections.” *Drugs* 67(3): 351–68.

Dubey, Ashok K. et al. 2003. “CsrA Regulates Translation of the Escherichia Coli Carbon Starvation Gene, CstA, by Blocking Ribosome Access to the CstA Transcript.” *Journal of Bacteriology* 185(15): 4450–60.

Duerig, Anna et al. 2009. “Second Messenger-Mediated Spatiotemporal Control of Protein Degradation Regulates Bacterial Cell Cycle Progression.” *Genes and Development* 23(1): 93–104.

Fang, Ferric C., Elaine R. Frawley, Timothy Tapscott, and Andrés Vázquez-Torres. 2016. “Bacterial Stress Responses during Host Infection.” *Cell Host and Microbe* 20(2): 133–43.

Fazli, Mustafa et al. 2014. “Regulation of Biofilm Formation in Pseudomonas and Burkholderia Species.” *Environmental Microbiology* 16(7): 1961–81. http://doi.wiley.com/10.1111/1462-2920.12448.

Francis, Vanessa I. et al. 2018. “Multiple Communication Mechanisms between Sensor Kinases Are Crucial for Virulence in Pseudomonas Aeruginosa.” *Nature Communications* 9(1). http://dx.doi.org/10.1038/s41467-018-04640-8.

Francis, Vanessa I., Emma C. Stevenson, and Steven L. Porter. 2017. “Two-Component Systems Required for Virulence in Pseudomonas Aeruginosa.” *FEMS Microbiology Letters* 364(11): 1–22.

Goodman, Andrew L. et al. 2004. “A Signaling Network Reciprocally Regulates Genes Associated with Acute Infection and Chronic Persistence in Pseudomonas Aeruginosa.” *Developmental Cell* 7(5): 745–54.

———. 2009. “Direct Interaction between Sensor Kinase Proteins Mediates Acute and Chronic Disease Phenotypes in a Bacterial Pathogen.” *Genes and Development* 23(2): 249–59.

Goymer, Patrick et al. 2006. “Adaptive Divergence in Experimental Populations of Pseudomonas Fluorescens. II. Role of the GGDEF Regulator WspR in Evolution and Development of the Wrinkly Spreader Phenotype.” *Genetics* 173(2): 515–26.

Granato, Elisa T., Thomas A. Meiller-Legrand, and Kevin R. Foster. 2019. “The Evolution and Ecology of Bacterial Warfare.” *Current Biology* 29(11): R521–37. https://doi.org/10.1016/j.cub.2019.04.024.

Güvener, Zehra Tüzün, and Caroline S. Harwood. 2007. “Subcellular Location Characteristics of the

Pseudomonas Aeruginosa GGDEF Protein, WspR, Indicate That It Produces Cyclic-Di-GMP in Response to Growth on Surfaces." *Molecular Microbiology* 66(6): 1459–73.

Haiko, Johanna, and Benita Westerlund-Wikström. 2013. "The Role of the Bacterial Flagellum in Adhesion and Virulence." *Biology* 2(4): 1242–67.

Hampton, Hannah G., Bridget N.J. Watson, and Peter C. Fineran. 2020. "The Arms Race between Bacteria and Their Phage Foes." *Nature* 577(7790): 327–36. http://dx.doi.org/10.1038/s41586-019-1894-8.

Hancock, Robert E.W., and David P. Speert. 2000. "Antibiotic Resistance in Pseudomonas Aeruginosa: Mechanisms and Impact on Treatment." *Drug Resistance Updates* 3(4): 247–55.

Harshey, Rasika M. 2003. "Bacterial Motility on a Surface: Many Ways to a Common Goal." *Annual Review of Microbiology* 57: 249–73.

Harvey, Hanjeong et al. 2018. "Pseudomonas Aeruginosa Defends against Phages through Type IV Pilus Glycosylation." *Nature Microbiology* 3: 47–52. http://dx.doi.org/10.1038/s41564-017-0061-y.

Hecht, G. B., and A. Newton. 1995. "Identification of a Novel Response Regulator Required for the Swarmer-to- Stalked-Cell Transition in Caulobacter Crescentus." *Journal of Bacteriology* 177(21): 6223–29.

Heeb, Stephan, Caroline Blumer, and Dieter Haas. 2002. "Regulatory RNA as Mediator in GacA / RsmA-Dependent Global Control of Exoproduct Formation in Pseudomonas Fluorescens CHA0." 184(4): 1046–56.

Heeb, Stephan, and Dieter Haas. 2001. "Regulatory Roles of the GacS / GacA Two-Component System in Plant-Associated and Other Gram-Negative Bacteria." *The American Phytopathological Society* 14(12): 1351–63.

Hendrix, Roger W. et al. 1999. "Evolutionary Relationships among Diverse Bacteriophages and Prophages: All the World's a Phage." *Proceedings of the National Academy of Sciences of the United States of America* 96(5): 2192–97.

Heurlier, Karin et al. 2004. "Positive Control of Swarming, Rhamnolipid Synthesis, and Lipase Production by the Posttranscriptional RsmA / RsmZ System in Pseudomonas Aeruginosa PAO1." *Journal of bacteriology* 186(10): 2936–45.

Hickman, Jason W, and Caroline S. Harwood. 2009. "Identification of FleQ from Pseudomonas Aeruginosa as a C-Di- GMP-Responsive Transcription Factor." *Molecular Microbiology* 69(2): 376–89.

Hickman, Jason W, Delia F Tifrea, and Caroline S Harwood. 2005. "A Chemosensory System That Regulates Biofilm Formation through Modulation of Cyclic Diguanylate Levels." *Proceedings of the National Academy of Sciences* 102(40): 14422–27.

Hoffman, Lucas R. et al. 2005. "Aminoglycoside Antibiotics Induce Bacterial Biofilm Formation." *Nature* 436(7054): 1171–75.

Hsu, Jye L., Hsuan Cheng Chen, Hwei Ling Peng, and Hwan Y. Chang. 2008. "Characterization of the Histidine-Containing Phosphotransfer Protein B-Mediated Multistep Phosphorelay System in Pseudomonas Aeruginosa PAO1." *Journal of Biological Chemistry* 283(15): 9933–44.

Huangyutitham, Varisa, Zehra Tüzün Güvener, and Caroline S. Harwood. 2013. "Subcellular Clustering of the Phosphorylated WspR Response Regulator Protein Stimulates Its Diguanylate Cyclase Activity." *mBio* 4(3): 1–8.

Inclan, Yuki F., Medora J. Huseby, and Joanne N. Engel. 2011. “FimL Regulates CAMP Synthesis in Pseudomonas Aeruginosa.” *PLoS ONE* 6(1).

Irie, Yasuhiko et al. 2010. “Pseudomonas Aeruginosa Biofilm Matrix Polysaccharide Psl Is Regulated Transcriptionally by RpoS and Post-Transcriptionally by RsmA.” *Molecular Microbiology* 78(1): 158–72.

———. 2012. “Self-Produced Exopolysaccharide Is a Signal That Stimulates Biofilm Formation in Pseudomonas Aeruginosa.” *Proceedings of the National Academy of Sciences of the United States of America* 109(50): 20632–36.

———. 2020. “Hfq-Assisted RsmA Regulation Is Central to Pseudomonas Aeruginosa Biofilm Polysaccharide PEL Expression.” *Frontiers in Microbiology* 11(November): 1–15.

Irving, Sophie E., Naznin R. Choudhury, and Rebecca M. Corrigan. 2021. “The Stringent Response and Physiological Roles of (Pp)PGpp in Bacteria.” *Nature Reviews Microbiology* 19(4): 256–71. http://dx.doi.org/10.1038/s41579-020-00470-y.

Janssen, Kayley H. et al. 2018. “RsmV , a Small Noncoding Regulatory RNA in Pseudomonas MRNAs.” *Journal of Bacteriology* 200(16): 1–13.

Jenal, Urs, Alberto Reinders, and Christian Lori. 2017. “Cyclic Di - GMP : Second Messenger Extraordinaire.” *Nature Reviews Microbiology* 15: 271–84.

Johnke, Julia, Jens Boenigk, Hauke Harms, and Antonis Chatzinotas. 2017. “Killing the Killer: Predation between Protists and Predatory Bacteria.” *FEMS Microbiology Letters* 364(9): 1–8.

Junkermeier, Eike H, and Regine Hengge. 2021. “A Novel Locally C-Di-GMP-Controlled Exopolysaccharide Synthase Required for N4 Phage Infection of E . Coli.” *bioRxiv*.

Kalelkar, Pranav P., Milan Riddick, and Andrés J. García. 2021. “Biomaterial-Based Antimicrobial Therapies for the Treatment of Bacterial Infections.” *Nature Reviews Materials* 0123456789.

Kamal, Shady Mansour et al. 2019. “Two FtsH Proteases Contribute to Fitness and Adaptation of Pseudomonas Aeruginosa Clone C Strains.” *Frontiers in Microbiology* 10(JULY): 1–18.

Katharios-Lanwermeyer, Stefan, Gregory B. Whitfield, P Lynne Howell, and George A. O’Toole. 2021. “Pseudomonas Aeruginosa Uses C-Di-GMP Phosphodiesterases RmcA and MorA To Regulate Biofilm Maintenance.” *mBio* 12(1).

Kazmierczak, Barbara I., Maren Schniederberend, and Ruchi Jain. 2015. “Cross-Regulation of Pseudomonas Motility Systems: The Intimate Relationship between Flagella, Pili and Virulence.” *Current Opinion in Microbiology* 28: 78–82. http://dx.doi.org/10.1016/j.mib.2015.07.017.

Kearns, Daniel B. 2010. “A Field Guide to Bacterial Swarming Motility.” *Nature Reviews Microbiology* 8(9): 634–44.

Keto-Timonen, Riikka et al. 2016. “Cold Shock Proteins: A Minireview with Special Emphasis on Csp-Family of Enteropathogenic Yersinia.” *Frontiers in Microbiology* 7(July): 1–7.

Kim, Suran, Xi-hui Li, Hyeon-ji Hwang, and Joon-hee Lee. 2020. “Thermoregulation of Pseudomonas Aeruginosa Biofilm Formation.” *Applied and Environmental Microbiology* 86(22): 1–11.

Klebensberger, Janosch et al. 2009. “SiaA and SiaD Are Essential for Inducing Autoaggregation as a Specific Response to Detergent Stress in Pseudomonas Aeruginosa.” *Environmental Microbiology* 11(12): 3073–86.

Köhler, Thilo et al. 2000. “Swarming of Pseudomonas Aeruginosa Is Dependent on Cell-to-Cell Signaling and Requires Flagella and Pili.” *Journal of Bacteriology* 182(21): 5990–96.

Kong, Weina et al. 2013. “Hybrid Sensor Kinase PA1611 in Pseudomonas Aeruginosa Regulates Transitions between Acute and Chronic Infection through Direct Interaction with RetS.” *Molecular Microbiology* 88(4): 784–97.

Kragh, Kasper Nørskov et al. 2018. “The Inoculation Method Could Impact the Outcome of Microbiological Experiments Kasper.” *Applied and Environmental Microbiology* 84(5): 1–14.

Krylov, Victor N. 2014. 88 Advances in Virus Research *Bacteriophages of Pseudomonas Aeruginosa: Long-Term Prospects for Use in Phage Therapy*. 1st ed. Elsevier Inc. http://dx.doi.org/10.1016/B978-0-12-800098-4.00005-2.

Kuchma, Sherry L. et al. 2007. “BifA, a Cyclic-Di-GMP Phosphodiesterase, Inversely Regulates Biofilm Formation and Swarming Motility by Pseudomonas Aeruginosa PA14.” *Journal of Bacteriology* 189(22): 8165–78.

Kulasakara, Hemantha et al. 2006. “Analysis of Pseudomonas Aeruginosa Diguanylate Cyclases and Phosphodiesterases Reveals a Role for Bis-(3’-5’)-Cyclic-GMP in Virulence.” *Proceedings of the National Academy of Sciences of the United States of America* 103(8): 2839–44. http://www.ncbi.nlm.nih.gov/pubmed/16477007.

Kulasekara, Bridget R et al. 2013. “C-Di-GMP Heterogeneity Is Generated by the Chemotaxis Machinery to Regulate Flagellar Motility.” : 1–19.

Kumari, Hansi et al. 2014. “LTQ-XL Mass Spectrometry Proteome Analysis Expands the Pseudomonas Aeruginosa AmpR Regulon to Include Cyclic Di- GMP Phosphodiesterases and Phosphoproteins, and Identifies Novel Open Reading Frames.” *Journal of Proteomics* 96: 328–42.

Laskowski, Michelle A., and Barbara I. Kazmierczak. 2006. “Mutational Analysis of RetS, an Unusual Sensor Kinase-Response Regulator Hybrid Required for Pseudomonas Aeruginosa Virulence.” *Infection and Immunity* 74(8): 4462–73.

Laskowski, Michelle A., Ellice Osborn, and Barbara I. Kazmierczak. 2004. “A Novel Sensor Kinase-Response Regulator Hybrid Regulates Type III Secretion and Is Required for Virulence in Pseudomonas Aeruginosa.” *Molecular Microbiology* 54(4): 1090–1103.

Latka, Agnieszka et al. 2017. “Bacteriophage-Encoded Virion-Associated Enzymes to Overcome the Carbohydrate Barriers during the Infection Process.” *Applied Microbiology and Biotechnology* 101(8): 3103–19.

Laventie, Benoît Joseph et al. 2019. “A Surface-Induced Asymmetric Program Promotes Tissue Colonization by Pseudomonas Aeruginosa.” *Cell Host and Microbe* 25(1): 140-152.e6.

Lee, Keehoon, and Sang Sun Yoon. 2017. “Pseudomonas Aeruginosa Biofilm, a Programmed Bacterial Life for Fitness.” *Journal of Microbiology and Biotechnology* 27(6): 1053–64.

Leighton, Tiffany L., Ryan N.C. Buensuceso, P. Lynne Howell, and Lori L. Burrows. 2015. “Biogenesis of Pseudomonas Aeruginosa Type IV Pili and Regulation of Their Function.” *Environmental Microbiology* 17(11): 4148–63.

Lennon, Jay T., and Stuart E. Jones. 2011. “Microbial Seed Banks: The Ecological and Evolutionary Implications of Dormancy.” *Nature Reviews Microbiology* 9(2): 119–30.

Lewis, Kimberley A. et al. 2021. “Non-Motile Subpopulations of Pseudomonas Aeruginosa Repress Flagellar Motility 2 in Motile Cells through a Type IV Pili- and Pel-Dependent Mechanism.” *bioRxiv*.

Li, Kewei et al. 2013. “SuhB Is a Regulator of Multiple Virulence Genes and Essential for Pathogenesis of Pseudomonas Aeruginosa.” *mBio* 4(6).

———. 2017. “SuhB Regulates the Motile-Sessile Switch in Pseudomonas Aeruginosa through the Gac/Rsm Pathway and c-Di-GMP Signaling.” *Frontiers in Microbiology* 8(JUN): 1–11.

Liu, Chong et al. 2018. “Insights into Biofilm Dispersal Regulation from the Crystal Structure of the PAS-GGDEF-EAL Region of RbdA from Pseudomonas Aeruginosa.” *Journal of bacteriology* 200(3): 1–19.

Liu, Cong, Di Sun, Jingrong Zhu, and Weijie Liu. 2019. “Two-Component Signal Transduction Systems: A Major Strategy for Connecting Input Stimuli to Biofilm Formation.” *Frontiers in Microbiology* 9.

Lo, Yi Ling et al. 2016. “Regulation of Motility and Phenazine Pigment Production by FliA Is Cyclic-Di-Gmp Dependent in Pseudomonas Aeruginosa PAO1.” *PLoS ONE* 11(5): 1–16. http://dx.doi.org/10.1371/journal.pone.0155397.

Locey, Kenneth J., and Jay T. Lennon. 2016. “Scaling Laws Predict Global Microbial Diversity.” *Proceedings of the National Academy of Sciences of the United States of America* 113(21): 5970–75.

Maffei, Enea et al. 2021. “Systematic Exploration of Escherichia Coli Phage-Host Interactions with the BASEL Phage Collection.” *bioRxiv*: 2021.03.08.434280. https://www.biorxiv.org/content/10.1101/2021.03.08.434280v1%0Ahttps://www.biorxiv.org/content/10.1101/2021.03.08.434280v1.abstract.

Malhotra, Sankalp, Don Jr. Hayes, and Daniel J. Wozniak. 2019. “Cystic Fibrosis and Pseudomonas Aeruginosa: The Host-Microbe Interface.” *Clinical Microbiology Reviews* 32(3).

Malone, Jacob G. et al. 2010. “YfiBNR Mediates Cyclic Di-GMP Dependent Small Colony Variant Formation and Persistence in Pseudomonas Aeruginosa.” *PLoS Pathogens* 6(3).

———. 2015. “Role of Small Colony Variants in Persistence of Pseudomonas Aeruginosa Infections in Cystic Fibrosis Lungs.” *Infection and Drug Resistance* 8: 237–47.

Malone, Jacob G et al. 2012. “The YfiBNR Signal Transduction Mechanism Reveals Novel Targets for the Evolution of Persistent Pseudomonas Aeruginosa in Cystic Fibrosis Airways.” 8(6).

Marden, J. N. et al. 2013. “An Unusual CsrA Family Member Operates in Series with RsmA to Amplify Posttranscriptional Responses in Pseudomonas Aeruginosa.” *Proceedings of the National Academy of Sciences* 110(37): 15055–60.

Marín, Mercedes M, Luis Yuste, and Fernando Rojo. 2003. “Differential Expression of the Components of the Two Alkane Hydroxylases from Pseudomonas Aeruginosa.” 185(10): 3232–37.

Marles-Wright, Jon, and Richard J. Lewis. 2007. “Stress Responses of Bacteria.” *Current Opinion in Structural Biology* 17(6): 755–60.

Matilla, Miguel A., David Martín-Mora, Jose A. Gavira, and Tino Krell. 2021. “ Pseudomonas Aeruginosa as a Model To Study Chemosensory Pathway Signaling .” *Microbiology and Molecular Biology Reviews* 85(1): 1–32.

Mcadams, Harley H., and Adam Arkin. 1997. “Stochastic Mechanisms in Gene Expression.” *Proceedings of the National Academy of Sciences of the United States of America* 94(3): 814–19.

Merighi, Massimo et al. 2007. “The Second Messenger Bis-(3′-5′)-Cyclic-GMP and Its PilZ Domain-Containing Receptor Alg44 Are Required for Alginate Biosynthesis in Pseudomonas Aeruginosa.” *Molecular Microbiology* 65(4): 876–95.

Merino, Nancy et al. 2019. “Living at the Extremes: Extremophiles and the Limits of Life in a Planetary

Context." *Frontiers in Microbiology* 10(MAR).

Merritt, Judith H. et al. 2010. "Specific Control of Pseudomonas Aeruginosa Surface-Associated Behaviors by Two c-Di-GMP Diguanylate Cyclases." *mBio* 1(4).

Merritt, Judith H, Kimberly M Brothers, Sherry L Kuchma, and George A O Toole. 2007. "SadC Reciprocally Influences Biofilm Formation and Swarming Motility via Modulation of Exopolysaccharide Production and Flagellar Function □." 189(22): 8154–64.

Miller, Christine L et al. 2016. "RsmW , Pseudomonas Aeruginosa Small Non- Coding RsmA-Binding RNA Upregulated in Biofilm versus Planktonic Growth Conditions." *BMC Microbiology*: 1–16. http://dx.doi.org/10.1186/s12866-016-0771-y.

Monard, C. et al. 2016. "Habitat Generalists and Specialists in Microbial Communities across a Terrestrial-Freshwater Gradient." *Scientific Reports* 6: 1–10.

Morris, Elizabeth R et al. 2013. "Structural Rearrangement in an RsmA / CsrA Ortholog of Pseudomonas Aeruginosa Creates." *Structure* 21(9): 1659–71.

Moscoso, Joana A. et al. 2014. "The Diguanylate Cyclase SadC Is a Central Player in Gac/Rsm-Mediated Biofilm Formation in Pseudomonas Aeruginosa." *Journal of Bacteriology* 196(23): 4081–88.

Murphy, Timothy F. 2008. "The Many Faces of Pseudomonas Aeruginosa in Chronic Obstructive Pulmonary Disease." *Clinical Infectious Diseases* 47(12): 1534–36.

Murray, Thomas S., and Barbara I. Kazmierczak. 2008. "Pseudomonas Aeruginosa Exhibits Sliding Motility in the Absence of Type IV Pili and Flagella." *Journal of Bacteriology* 190(8): 2700–2708.

Müsken, Mathias et al. 2010. "Genetic Determinants of Pseudomonas Aeruginosa Biofilm Establishment." *Microbiology* 156(2): 431–41.

Nadal Jimenez, P. et al. 2012. "The Multiple Signaling Systems Regulating Virulence in Pseudomonas Aeruginosa." *Microbiology and Molecular Biology Reviews* 76(1): 46–65. http://mmbr.asm.org/cgi/doi/10.1128/MMBR.05007-11.

Neidhardt, F. C., P. L. Bloch, and D. F. Smith. 1974. "Culture Medium for Enterobacteria." *Journal of Bacteriology* 119(3): 736–47.

Neves, P. R., J. A. McCulloch, E. M. Mamizuka, and N. Lincopan. 2014. 3 Encyclopedia of Food Microbiology: Second Edition *Pseudomonas: Pseudomonas Aeruginosa*. Second Edi. Elsevier. http://dx.doi.org/10.1016/B978-0-12-384730-0.00283-4.

Niepa, Tagbo H R et al. 2017. "Films of Bacteria at Interfaces (FBI): Remodeling of Fluid Interfaces by Pseudomonas Aeruginosa." *Scientific Reports*: 1–11. http://dx.doi.org/10.1038/s41598-017-17721-3.

Nobrega, Franklin L, Marnix Vlot, Patrick A De Jonge, and Lisa L Dreesens. 2018. "Targeting Mechanisms of Tailed Bacteriophages." *Nature Reviews Microbiology* 16(December): 760–73. http://dx.doi.org/10.1038/s41579-018-0070-8.

Norman, Thomas M., Nathan D. Lord, Johan Paulsson, and Richard Losick. 2015. "Stochastic Switching of Cell Fate in Microbes." *Annual Review of Microbiology* 69(1): 381–403.

O'Toole, George, Heidi B Kaplan, and Roberto Kolter. 2000. "Biofilm Formation As Mirobial Development." *Annual Review of Microbiology* 54: 49–79.

Overhage, Jörg, Mirle Schemionek, Jeremy S. Webb, and Bernd H.A. Rehm. 2005. "Expression of the Psl Operon in Pseudomonas Aeruginosa PAO1 Biofilms: PslA Performs an Essential Function in

Biofilm Formation." *Applied and Environmental Microbiology* 71(8): 4407–13.

Palmer, Kelli L., Lindsay M. Aye, and Marvin Whiteley. 2007. "Nutritional Cues Control Pseudomonas Aeruginosa Multicellular Behavior in Cystic Fibrosis Sputum." *Journal of Bacteriology* 189(22): 8079–87.

Pang, Zheng et al. 2019. "Antibiotic Resistance in Pseudomonas Aeruginosa: Mechanisms and Alternative Therapeutic Strategies." *Biotechnology Advances* 37(1): 177–92. https://doi.org/10.1016/j.biotechadv.2018.11.013.

Paulsson, Magnus et al. 2019. "Pseudomonas Aeruginosa Uses Multiple Receptors for Adherence to Laminin during Infection of the Respiratory Tract and Skin Wounds." *Scientific Reports* 9(1): 1–10.

Pessi, Gabriella et al. 2001. "The Global Posttranscriptional Regulator RsmA Modulates Production of Virulence Determinants and N-Acylhomoserine Lactones in Pseudomonas Aeruginosa." *Journal of bacteriology* 183(22): 6676–83.

Pierson, Leland S., and Elizabeth A. Pierson. 2010. "Metabolism and Function of Phenazines in Bacteria: Impacts on the Behavior of Bacteria in the Environment and Biotechnological Processes." *Applied Microbiology and Biotechnology* 86(6): 1659–70.

Pourciau, Christine et al. 2020. "Diverse Mechanisms and Circuitry for Global Regulation by the RNA-Binding Protein CsrA." *Frontiers in Microbiology* 11(October).

Rainey, Paul B, and Michael Travisano. 1998. "Adaptive Radiation in a Heterogeneous Environment." *Nature* 394: 69–72.

Rashid, M. Harunur, and Arthur Kornberg. 2000. "Inorganic Polyphosphate Is Needed for Swimming, Swarming, and Twitching Motilities of Pseudomonas Aeruginosa." *Proceedings of the National Academy of Sciences of the United States of America* 97(9): 4885–90.

Ridley, Caroline, and David J. Thornton. 2018. "Mucins: The Frontline Defence of the Lung." *Biochemical Society Transactions* 46(5): 1099–1106.

Rife, Chris et al. 2005. "Crystal Structure of the Global Regulatory Protein CsrA from Pseudomonas Putida at 2.05 Å Resolution Reveals a New Fold." *Proteins: Structure, Function and Genetics* 61(2): 449–53.

Romero, Manuel et al. 2018. "Genome-Wide Mapping of the RNA Targets of the Pseudomonas Aeruginosa Riboregulatory Protein RsmN." *Nucleic Acids Research* 46(13): 6823–40.

Römling, U., and C. Balsalobre. 2012. "Biofilm Infections, Their Resilience to Therapy and Innovative Treatment Strategies." *Journal of Internal Medicine* 272(6): 541–61.

Roncarati, Davide, and Vincenzo Scarlato. 2017. "Regulation of Heat-Shock Genes in Bacteria: From Signal Sensing to Gene Expression Output." *FEMS microbiology reviews* 41(4): 549–74.

Ross, P et al. 1986. "Regulation of Cellulose Synthesis in Acetobacter Xylinum by Cyclic Diguanylic Acid." *Nature* 325(15): 279–81.

Le Roux, Michele et al. 2015. "Kin Cell Lysis Is a Danger Signal That Activates Antibacterial Pathways of Pseudomonas Aeruginosa." *eLife* 2015(4): 1–65.

Roy, Ankita Basu, Olga E Petrova, and Karin Sauer. 2012. "The Phosphodiesterase DipA (PA5017) Is Essential for Pseudomonas Aeruginosa Biofilm Dispersion." *Journal of Bacteriology* 194(11): 2904–15.

Rumbaugh, Kendra P., and Karin Sauer. 2020. "Biofilm Dispersion." *Nature Reviews Microbiology*

18(10): 571–86. http://dx.doi.org/10.1038/s41579-020-0385-0.

Ryan Kaler, Kylie M., Jay C. Nix, and Florian D. Schubot. 2021. “RetS Inhibits Pseudomonas Aeruginosa Biofilm Formation by Disrupting the Canonical Histidine Kinase Dimerization Interface of GacS.” *Journal of Biological Chemistry* 297(4): 101193. https://doi.org/10.1016/j.jbc.2021.101193.

Ryjenkov, Dmitri A, Marina Tarutina, Oleg V Moskvin, and Mark Gomelsky. 2005. “Cyclic Diguanylate Is a Ubiquitous Signaling Molecule in Bacteria : Insights into Biochemistry of the GGDEF Protein Domain †.” 187(5): 1792–98.

Schmidt, Andrew J, Dmitri A Ryjenkov, and Mark Gomelsky. 2005. “The Ubiquitous Protein Domain EAL Is a Cyclic Diguanylate-Specific Phosphodiesterase : Enzymatically Active and Inactive EAL Domains †.” 187(14): 4774–81.

Schulmeyer, Kayley H. et al. 2016. “Primary and Secondary Sequence Structure Requirements for Recognition and Discrimination of Target RNAs by Pseudomonas Aeruginosa RsmA and RsmF.” *Journal of Bacteriology* 198(18): 2458–69.

Sellner, Benjamin et al. 2021. “A New Sugar for an Old Phage: A c-Di-GMP Dependent Polysaccharide Pathway Sensitizes E. Coli for Bacteriophage Infection.” *bioRxiv*: 2021.09.27.461960. https://www.biorxiv.org/content/10.1101/2021.09.27.461960v1%0Ahttps://www.biorxiv.org/content/10.1101/2021.09.27.461960v1.abstract.

Senior, Andrew W et al. 2020. “Improved Protein Structure Prediction Using Potentials from Deep Learning.” *Nature* 577(January). http://dx.doi.org/10.1038/s41586-019-1923-7.

Serino, Laura et al. 1997. “Biosynthesis of Pyochelin and Dihydroaeruginoic Acid Requires the Iron-Regulated PchDCBA Operon in Pseudomonas Aeruginosa.” *Journal of Bacteriology* 179(1): 248–57.

Sevin, Emeric W., and Frédérique Barloy-Hubler. 2007. “RASTA-Bacteria: A Web-Based Tool for Identifying Toxin-Antitoxin Loci in Prokaryotes.” *Genome Biology* 8(8).

Shan, Zhiying et al. 2004. “Identification of Two New Genes Involved in Twitching Motility in Pseudomonas Aeruginosa.” *Microbiology* 150(8): 2653–61.

De Smet, Jeroen et al. 2021. “Bacteriophage-Mediated Interference of the c-Di-GMP Signalling Pathway in Pseudomonas Aeruginosa.” *Microbial Biotechnology* 14(3): 967–78.

Smith, Daniel J., Iain L. Lamont, Greg J. Anderson, and David W. Reid. 2013. “Targeting Iron Uptake to Control Pseudomonas Aeruginosa Infections in Cystic Fibrosis.” *European Respiratory Journal* 42(6): 1723–36.

Smith, Eric E. et al. 2008. “Genetic Adaptation of Pseudomonas Aeruginosa to the Airways of Cystic Fibrosis Patients Is Catalyzed by Hypermutation.” *Journal of Bacteriology* 190(24): 7910–17.

Smyth, Gordon K. 2004. “Linear Models and Empirical Bayes Methods for Assessing Differential Expression in Microarray Experiments.” *Statistical Applications in Genetics and Molecular Biology* 3(1).

Soares, Anaïs, Kévin Alexandre, and Manuel Etienne. 2020. “Tolerance and Persistence of Pseudomonas Aeruginosa in Biofilms Exposed to Antibiotics: Molecular Mechanisms, Antibiotic Strategies and Therapeutic Perspectives.” *Frontiers in Microbiology* 11(August): 1–11.

Sousa, Ana Margarida, and Maria Olívia Pereira. 2014. “Pseudomonas Aeruginosa Diversification during Infection Development in Cystic Fibrosis Lungs-A Review.” *Pathogens* 3(3): 680–703.

Spiers, Andrew J. et al. 2002. “Adaptive Divergence in Experimental Populations of Pseudomonas Fluorescens. I. Genetic and Phenotypic Bases of Wrinkly Spreader Fitness.” *Genetics* 161(1): 33–

46.

Sriramulu, Dinesh D., Heinrich Lünsdorf, Joseph S. Lam, and Ute Römling. 2005. “Microcolony Formation: A Novel Biofilm Model of Pseudomonas Aeruginosa for the Cystic Fibrosis Lung.” *Journal of Medical Microbiology* 54(7): 667–76.

Starnbach, M. N., and S. Lory. 1992. “The FilA (RpoF) Gene of Pseudomonas Aeruginosa Encodes an Alternative Sigma Factor Required for Flagellin Synthesis.” *Molecular Microbiology* 6(4): 459–69.

Stoitsova, Stoyanka R., Tsvetelina S. Paunova-Krasteva, and Dayana B. Borisova. 2016. “Modulation of Biofilm Growth by Sub-Inhibitory Amounts of Antibacterial Substances.” *Microbial Biofilms - Importance and Applications* (July).

Strateva, Tanya, and Ivan Mitov. 2011. “Contribution of an Arsenal of Virulence Factors to Pathogenesis of Pseudomonas Aeruginosa Infections.” *Annals of Microbiology* 61(4): 717–32.

Sun, Evelyn, Sijie Liu, and Robert E.W. Hancock. 2018. “Surfing Motility : A Conserved yet Diverse Adaptation among Motile Bacteria.” *Journal of Bacteriology* 200(23): 1–13.

Tacconelli, Evelina et al. 2018. “Discovery, Research, and Development of New Antibiotics: The WHO Priority List of Antibiotic-Resistant Bacteria and Tuberculosis.” *The Lancet Infectious Diseases* 18(3): 318–27.

Thayer, M. M., K. M. Flaherty, and D. B. McKay. 1991. “Three-Dimensional Structure of the Elastase of Pseudomonas Aeruginosa at 1.5-Å Resolution.” *Journal of Biological Chemistry* 266(5): 2864–71.

Tsuji, Akiyoshi et al. 1982. “The Effects of Temperature and PH on the Growth of Eight Enteric and Nine Glucose Non-Fermenting Species of Gram-Negative Rods.” *Microbiology and Immunology* 26(1): 15–24.

Ueda, Akihiro, and Thomas K Wood. 2010. “Tyrosine Phosphatase TpbA of Pseudomonas Aeruginosa Controls Extracellular DNA via Cyclic Diguanylic Acid Concentrations.” 2: 449–55.

Valentini, Martina et al. 2016. “The Diguanylate Cyclase HsbD Intersects with the HptB Regulatory Cascade to Control Pseudomonas Aeruginosa Biofilm and Motility.” *PLoS Genetics* 12(10): 1–30.

Valverde, Claudio, Stephan Heeb, Christoph Keel, and Dieter Haas. 2003. “RsmY , a Small Regulatory RNA , Is Required in Concert with RsmZ for GacA-Dependent Expression of Biocontrol Traits in Pseudomonas Fluorescens CHA0.” 50: 1361–79.

Veening, Jan Willem, Wiep Klaas Smits, and Oscar P. Kuipers. 2008. “Bistability, Epigenetics, and Bet-Hedging in Bacteria.” *Annual Review of Microbiology* 62: 193–210.

Ventre, Isabelle et al. 2006. “Multiple Sensors Control Reciprocal Expression of Pseudomonas Aeruginosa Regulatory RNA and Virulence Genes.” *Proceedings of the National Academy of Sciences of the United States of America* 103(1): 171–76.

Wadhwa, Navish, and Howard C. Berg. 2021. “Bacterial Motility: Machinery and Mechanisms.” *Nature Reviews Microbiology* 0123456789. http://dx.doi.org/10.1038/s41579-021-00626-4.

Wang, Benjamin X. et al. 2021. “Mucin Glycans Signal through the Sensor Kinase RetS to Inhibit Virulence-Associated Traits in Pseudomonas Aeruginosa.” *Current Biology* 31(1): 90-102.e7. https://doi.org/10.1016/j.cub.2020.09.088.

Wang, Chao et al. 2014. “BswR Controls Bacterial Motility and Biofilm Formation in Pseudomonas Aeruginosa through Modulation of the Small RNA RsmZ.” *Nucleic Acids Research* 42(7): 4563–76.

Whitman, William B., David C. Coleman, and William J. Wiebe. 1998. “Prokaryotes: The Unseen Majority.” *Proceedings of the National Academy of Sciences of the United States of America* 95(12): 6578–83.

Wood, Lynn F., and Dennis E. Ohman. 2012. “Identification of Genes in the Σ22 Regulon of Pseudomonas Aeruginosa Required for Cell Envelope Homeostasis in Either the Planktonic or the Sessile Mode of Growth.” *mBio* 3(3): 1–11.

Wurtzel, Omri et al. 2012. “The Single-Nucleotide Resolution Transcriptome of Pseudomonas Aeruginosa Grown in Body Temperature.” 8(9).

Yang, Shuai et al. 2018. “Differential Production of Psl in Planktonic Cells Leads to Two Distinctive Attachment Phenotypes in Pseudomonas Aeruginosa.” *Applied and Environmental Microbiology* 84(14).

Zhu, Bin et al. 2016. “Membrane Association of SadC Enhances Its Diguanylate Cyclase Activity to Control Exopolysaccharides Synthesis and Biofilm Formation in Pseudomonas Aeruginosa.” *Environmental Microbiology* 18(10): 3440–52.